Microarray analysis of differentially regulated genes in human leukemia cells after expression of the inositol 5-phosphatase SHIP

Dissertation

zur Erlangung des naturwissenschaftlichen Doktorgrades
des Departments Biologie
der Fakultät für Mathematik, Informatik und Naturwissenschaften
an der Universität Hamburg

vorgelegt von

Lizet Elena García Palma

Hamburg 2006

Microarray analysis of differentially regulated genes in human leukemia cells after expression of the inositol 5-phosphatase SHIP

Doctoral Thesis

Submitted in partial fulfillment of the requirements
for the degree of Doctor of Philosophy
from the Department of Biology,
Faculty of Mathematics, Informatics und Natural Sciences,
University of Hamburg, Germany

By

Lizet Elena García Palma

Hamburg, Germany
2006

Genehmigt vom Department Biologie
der Fakultät für Mathematik, Informatik und Naturwissenschaften
an der Universität Hamburg
auf Antrag von Herrn Professor Dr. G. W. MAYR
Weiterer Gutachter der Dissertation:
Herr Professor Dr. U. WIENAND
Tag der Disputation: 19. Mai 2006

Hamburg, den 02. Mai 2006

Professor Dr. Arno Frühwald
Dekan

Die vorliegende Arbeit wurde in der Zeit von April 2002 bis März 2006 in der Abteilung für zelluläre Signaltransduktion am Zentrum für experimentelle Medizin, Institut für Biochemie und Molekularbiologie I, Universitäts-Klinikum Hamburg-Eppendorf angefertigt.

1. Gutachter: Prof. Dr. G. W. Mayr
Zentrum für Experimentelle Medizin
Institut für Biochemie und Molekularbiologie I:
Zelluläre Signaltransduktion
Universitäts-Klinikum Hamburg-Eppendorf

2. Gutachter: Prof. Dr. rer. nat. U. Wienand
Department für Biologie
Biozentrum Klein Flottbek
Molekularbiologie der Pflanzen
Universität Hamburg

Hiermit versichere ich, dass ich die vorliegende Arbeit selbstständig und ohne fremde Hilfe verfasst, keine anderen als die angegebenen Quellen und Hilsmittel benutzt und die aus Werken wörtlich oder inhaltlich entnommenen Stellen als solche kenntlich gemacht habe. Ferner versichere ich, dass ich diese Dissertation an keiner anderen Universität eingereicht habe, um ein Promotionsverfahren eröffnen zu lassen.

Hamburg, den 30.03.2006

Lizet Elena García Palma

HEINRICH-PETTE-INSTITUT FÜR EXPERIMENTELLE VIROLOGIE UND IMMUNOLOGIE
AN DER UNIVERSITÄT HAMBURG

HPI ▪ Postfach 20 16 52 ▪ 20206 Hamburg

Carol Stocking, Ph.D.
AG Molecular Pathology

Tel.: (+49)40-480-51-273
Fax.: (+49)40-480-51-187
e-mail: stocking@hpi.uni-hamburg.de

4. April 2006

Department Biologie
Universität Hamburg
Martin Luther King-Platz 2
D-20146 Hamburg

Sehr geehrte Damen und Herrn,

hiermit bestätige ich, dass die von Frau Lizet Elena Garciá Palma mit dem Titel "Microarray analysis of differentially regulated genes in human leukemia cells after the expression of the inositol-5'-phosphatase SHIP" vorgelegte Doktorarbeit in korrektem Englisch geschrieben ist.

Mit freundlichen Grüssen,

Carol Stocking

Dr. Carol Stocking

Table of Contents

List of Figures

List of Tables

1. Summary

The SH2-containing inositol 5-phosphatase SHIP-1 (SHIP) is a negative regulator of signal transduction in hematopoietic cells. Inactivation of SHIP may be involved in the pathogenesis of leukemia. In support of this hypothesis, it has been shown that the human T cell leukemia cell line Jurkat does not express SHIP. Restoration of SHIP expression leads to the inactivation of the phosphoinositide 3-kinase (PI3K)/AKT signal transduction pathway and the prolongation of the G1 phase of the cell cycle. Consequently, a partial inhibition of proliferation of these cells has been observed. The goal of this work was to identify the mechanism by which SHIP regulates cell cycle and proliferation. The first aim of this study was to investigate the differential expression of genes after restoration of SHIP expression in Jurkat cells. For this analysis, microarrays with approximately 39,000 transcripts of the human genome were used to determine the transcriptional expression pattern of Jurkat cells containing a doxycycline-inducible vector before and after induction of SHIP. Microarray analysis revealed that restoration of SHIP expression resulted in statistically significant changes (≥ 2.0-fold) in the expression levels of 37 unique mRNAs. SHIP induced the expression of 16 mRNAs, while it repressed 21 mRNAs. Analyses of functional annotations revealed that among the 37 mRNAs, 24 correspond to known genes. Of these, 11 genes (46%) had annotations found in the Gene Ontology data bank related to nucleus, transcription or cell cycle, 7 genes (29%) encode proteins associated with intracellular signaling cascades and/or localization in the plasma membrane, and 1 gene encodes an interleukin, IL26. The data show for the first time that SHIP regulates the expression of genes related to transcription and cell cycle.

The second aim of this study was the validation of the differentially expressed transcripts by quantitative real-time RT-PCR. Messenger-RNA sequences of 36 from the 37 transcripts were identified by searching different data banks. A primer software was used to assist in the design of the human gene-specific primers, and the 100% specificity of the primer sequences was verified. Of the 36 transcripts analyzed, 29 were validated by quantitative real-time PCR (81%). The analyses demonstrated a good correlation between quantitative real-time PCR and the Affymetrix platform, with a similar expression pattern of 90% (26 out of 29) of the transcripts being observed. Eleven of the genes showed statistically significant transcriptional regulation (≥ 2-fold) by SHIP. Of the three genes up-regulated by SHIP (*KLF2, CD62L* and *KCMF1*), two have been reported to be involved in regulation of transcription or quiescence. Of the 8 SHIP-repressed genes, three genes (*ATF5, ZNF75, DNAJB9*) are implicated in the regulation of transcription and cell cycle, whereas five are involved in signal transduction (*TRIB3, ARHGEF10, ARRDC3, PAG*, as well as the interleukin *IL26*).

For some of these genes, a role in T cell proliferation and survival has already been suggested or is implicated by their function in transcription, cell cycle, or apoptosis. CD62L (CD62 antigen ligand) is a L-selectin, integral to the plasma membrane. It has been reported that quiescent T cells are $CD62L^+$ and upon activation, expression is lost. The Krüppel-like transcription factor 2 (KLF2) is required to maintain $CD4^+$ or $CD8^+$ single-positive T cells in their quiescent state and has an inhibitory effect on their proliferation. Similarly to the expression of CD62L, KLF2 is also down-regulated after T cell activation. However, the signal transduction pathway mediating the regulation of KLF2 has not been elucidated. The genes coding for ATF5 (activating transcription factor 5) and ZNF75 (zinc finger protein 75 (D8C6)) were the most strongly SHIP-repressed genes. ZNF75 belongs to the Krüppel C2H2-type zinc finger protein family. The function of ZNF75 is largely unknown, but computational

analysis suggests that it could be involved in DNA-dependent regulation of transcription. ATF5 is an anti-apoptotic factor and its expression is down-regulated in a variety of cell lines undergoing apoptosis following growth factor deprivation. It has been reported that Akt mediates the down-regulation of one member of the ATF family, *ATF-6β*, simultaneously with an up-regulation of the SREBP (sterol-regulatory element binding proteins) genes, involved in fatty acid and cholesterol synthesis. Akt is also involved in the regulation of CREB and NF-κB. However, these factors were not differentially regulated at the mRNA level in this study, suggesting other mechanisms of regulation. IL26 was the only interleukin identified to be SHIP-regulated at the mRNA level. The presence of *IL26* transcripts in a series of leukemia T cell lines has been previously reported. IL26 is a novel cellular homolog of interleukin-10 and is produced by activated memory but not by naïve $CD4^+$ T cells, independently of costimulation. It has been described that the dimerization of the receptor units IL-20R1 and IL-10R2 generates a functional IL-26R complex, and the IL26-mediated signaling through this receptor complex induced activation of two members of the STAT family. It has been previously proposed that IL26 is a good candidate for autocrine growth stimulation, leading to spontaneous proliferation of T cells after (HVS) infection.

The third aim was to study the biological effect of the identified SHIP-regulated genes. Because KLF2 is involved in quiescence in naïve T-cells and in regulation of Jurkat T leukemia cell growth, and SHIP leads to an inhibition of proliferation in these cells, the SHIP-mediated regulation of *KLF2* in Jurkat T cells was of particular interest. Therefore, the biological function of KLF2 in Jurkat T cells was analyzed. *KLF2* mRNA was up-regulated two to threefold at the RNA and protein level after the induced expression of SHIP. Functional analysis of KLF2 expression in Jurkat cells was carried out to study the role of this protein in proliferation. hKLF2-expressing vectors or control EGFP (enhanced green fluorescent protein) vectors were introduced into Jurkat cells and proliferation was monitored by assessing the accumulation of newly synthesized DNA by BrdU incorporation (using anti-BrdU antibodies). A 45% reduction in proliferation was observed after KLF2 expression, as compared to a 60% reduction by SHIP expression. When expressed together, an 84% reduction in proliferation was observed, suggesting an additive effect on reduction of proliferation. SHIP induction up-regulates *KLF2* expression, implicating KLF2 in the SHIP-mediated growth inhibition of the human leukemic T-cell line Jurkat. Further analysis confirmed that the reduction of newly synthesized DNA correlated with increased KLF2 protein levels in Jurkat T-cells induced to express SHIP.

A fourth aim of this study was to determine if the regulation of KLF2 is directly regulated by the PI3K/Akt pathway, which is activated by the T cell receptor. Inhibition of PI3-kinase with wortmannin in Jurkat T-cells revealed a 2.4-fold increase in KLF2 protein levels. Furthermore, the silencing of Akt1 expression by RNAi led to a 2.5-fold increase in the expression of KLF2. In addition, expression of the inositol 5'-phosphatase SHIP reduced the activity of Akt, resulting in the up-regulation of KLF2.

A direct functional role for the SHIP-mediated reduction of cell proliferation has been confirmed for KLF2. Moreover, the data obtained by inactivation of the PI3K and silencing of the expression of Akt by RNAi confirmed the role of the PI3K/Akt signaling pathway in the up-regulation of KLF2 in Jurkat T cells. A model that summarizes the results obtained in this study including SHIP, KLF2, and the PI3K/Akt pathway, along with the events occurring downstream in the signal cascade is shown below.

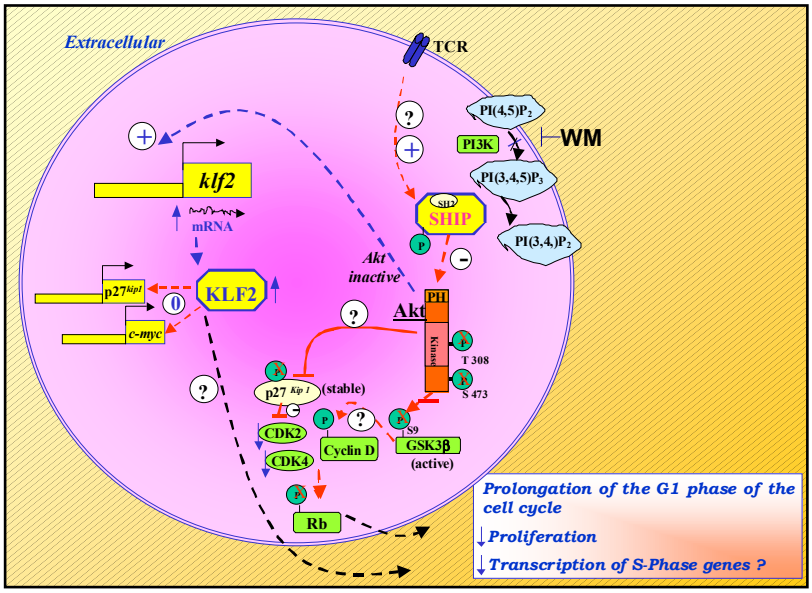

Up-regulation of the T cell quiescence factor KLF2 occurs via the Phosphatidylinositol 3-kinase/Akt signaling pathway. After expression of SHIP in Jurkat T cells, there is a reduction in the levels of PI(3,4,5)P_3 and inactivation of Akt by reduction of phosphorylation at residues Thr 308 and Ser 473. GSK3β is not phosphorylated at residue Ser 9, and becomes active; p27Kip1 is more stable and the phosphorylation of Rb at Ser780 is reduced. Consequently, there is prolongation of the G1 phase of the cell cycle and reduction of proliferation. This also may implicate a reduction in the transcription of S-phase genes. A second event comprises the fact that the expression of KLF2 increases by the activity of SHIP. Additionally, inhibition of PI3-kinase with wortmannin and knockdown of the expression of Akt1 by RNAi led to an increase in the expression of KLF2. This implicates SHIP and the PI3-kinase/Akt signaling pathway in the up-regulation of KLF2 in Jurkat T cells. **PI3K:** Phosphoinositide 3-kinase. **Akt (PKB):** Protein kinase B. **GSK3β:** Glycogen synthase kinase-3β. **CDK:** Cyclin-dependent kinase. **RB:** Retinoblastoma tumor suppressor protein. **p27Kip1**: Cyclin-dependent kinase inhibitor 1B. **KLF2:** Krüppel-like factor 2. **PI(3,4,5)P_3:** phosphatidylinositol 3,4,5-trisphosphate. **TCR:** T cell receptor. **WM:** Wortmannin.

This study contributes to the elucidation of novel factors and associations with the PI3K/Akt signaling pathway involved in the SHIP-mediated regulation of proliferation in Jurkat T cells. With respect to a possible function of SHIP in the development of leukemogenesis, the biological function of the SHIP-regulated genes identified in this study need to be further investigated in primary human leukemia.

2. Introduction

2.1. Hematopoiesis and Leukemogenesis

Hematopoietic stem cells (HSCs) are clonogenic cells that possess properties of both self-renewal and multilineage potential, giving rise to all types of mature blood cells (Spangrude *et al,* 1988). It has been assumed that each intermediate progenitor and each monopotent precursor has a distinct gene expression program that is established and maintained by specific combinations of transcription factors and chromatin remodeling components. There are numerous examples where seemingly committed hematopoietic cells can be induced to convert into cells of another lineage, showing the differentiation plasticity of hematopoietic cells (Figure 1). In a normal lineage, the stem cells differentiate into lymphoid and myeloid progenitors, which give rise to a variety of mature cells, including T cells and B cells, and monocytes and granulocytes, respectively. Leukemias represent abnormal and poorly regulated hematopoiesis, with leukemia stem cells (also) capable of self-renewal as well as the generation of multiple cell types (Passegue *et al,* 2003). Acquired mutations contributing to leukemogenesis, including chromosomal translocations that generate oncogenic fusion genes, may need to occur in hematopoietic stem cells (HSCs), as these cells have sufficient lifespan necessary for the acquisition of additional mutagenic hits. Alternatively, it is possible that oncogenic events happen in more committed progenitors, particularly if the mutation confers self-renewal to the cell or if the cell (such as a B cell progenitor) exhibits a sufficient life span (Jamieson *et al,* 2004; Passegue *et al,* 2003). As a result, the cancerous cells divide rapidly, replace the cells in the bone marrow and may invade other organs, such as liver, spleen, lymph nodes, kidneys and brain.

2.2. Major types of leukemia, prevalence and symptoms

There are four major types of leukemia. They are classified based on their progression as either acute (rapid) or chronic (slow), and the affected white blood cell type as either lymphocytic, or myelocytic (Table I).

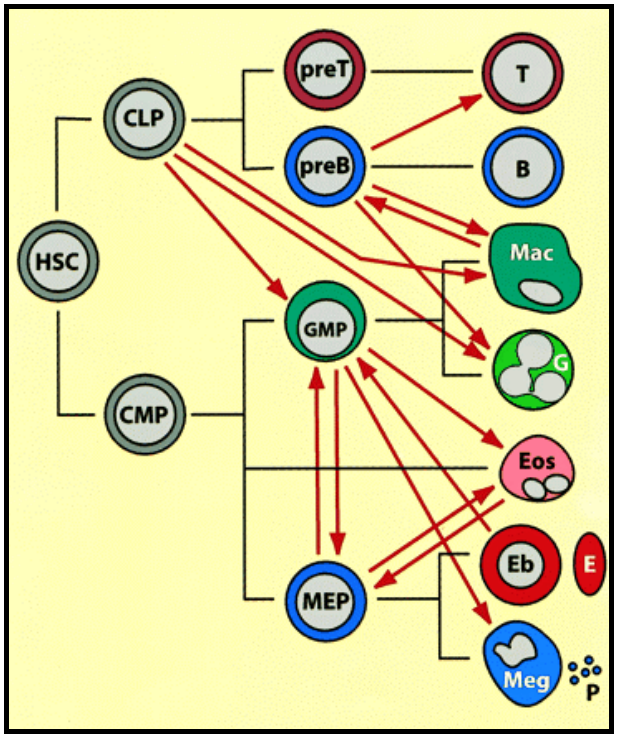

Figure 1. Summary of lineage switches observed between hematopoietic cells, placed in the context of normal hematopoietic differentiation (Akashi *et al,* 2000; Kondo *et al,* 1997)

The black lines indicate normal lineage relationships; the thick red arrows represent induced switches (these do not necessarily imply direct transitions). HSC indicates hematopoietic stem cell; CLP, common lymphoid progenitor; CMP, common multipotent progenitor; GMP, granulocyte/macrophage progenitor (also called "myeloblasts"); MEP, megakaryocyte erythrocyte progenitor; T, T lymphocyte; B, B lymphocyte; Mac, macrophage; G, neutrophil granulocyte; Eos, eosinophil, Eb, erythroblast; E, erythrocyte; Meg, megakaryocyte; P, platelet. Mast cells, NK cells, and dendritic cells have been omitted from the scheme and placement of eosinophils is speculative. Note that most of the switches were observed with transformed cell lines in culture and that the cell type designations (both before and after the switch) may not accurately reflect the phenotype of the normal counterparts. (Modified from Graf, 2002).

Table I. Major types of leukemia and annual prevalence

(Modified from Merck & Co. and contributors, 2002)

Type	Progression	White Blood Cell Affected	N° of Cases diagnosed yearly in the USA
Acute lymphocytic Leukemia (ALL)	Rapid	Lymphocytes	5,200
Acute myeloid leukemia (AML)	Rapid	Myelocytes	7,000
Chronic lymphocytic leukemia (CLL), including Sézary syndrome and hairy cell leukemia	Slow	Lymphocytes	8,500
Chronic myelocytic leukemia (CML)	Slow	Myelocytes	5,800

Acute lymphocytic leukemia (ALL) affects predominantly children and Acute myeloid leukemia (AML) is most likely to be found in adults. Particular subtypes of acute leukemia have been found to be associated with specific chromosomal translocations-for example, the t(12;21)(p13;q22) translocation occurs in 25% of patients with ALL, whereas the t(8;21)(q22;q22) occurs in 15% of patients with AML (Golub *et al,* 1995; McLean *et al,* 1996; Romana *et al,* 1995; Rowley, 1973; Shurtleff *et al,* 1995). According to the "Elimination of Leukemia Fund (ELF)" reports in 2002, leukemia killed more children between two and 15 years than any other disease in some developed countries. In Germany, it has been reported that every year 11,800 people come down with leukemia, including 600 children (*Deutsches Kinderkrebsregister*; Hellenbrecht *et al,* 2003). The most frequent first symptom of leukemia is anemia, because of the decreased number of red blood cells (RBCs), which are involved in the body tissue oxygenation process. Therefore, debility and shortness of breath also occur. The appearance of infections with subsequent fever is also frequent, since there are not enough normal white blood cells. Bleeding may occur in the form of nosebleeds, purple skin spots or easy bruising. Leukemia cells in the brain may cause headaches, vomiting and those in the bone marrow may cause bone and joint pain.

2.3. Pathways to leukemia

Tumors of T cells have been identified. However, unlike the malignancies of B cells, few that correspond to intermediate stages in T-cell development have been recognized in humans (Janeway *et al,* 1999). Instead, the tumors resemble either mature T cells or, in common acute lymphoblastic leukemia**,** the earliest type of lymphoid progenitor. It has been proposed that acute leukemias require at least two complementary mutations, one leading to enhanced proliferation and a second leading to a block in differentiation (Gilliland, 2002). A common cause of enhanced cell proliferation is inappropriate signal transduction.

2.3.1. T lymphocyte proliferation and apoptosis signaling pathways

Resting T lymphocytes are normally activated by antigen/MHC complexes through the TCR-CD3 complex (Weiss and Littman, 1994). The earliest signaling event following TCR

engagement is the sequential activation of the non-receptor protein tyrosine kinases (PTKs) of the Src and Syk families. Activated Src family PTKs, Lck and Fyn, subsequently phosphorylate tyrosine residues in T cells within a consensus sequence termed the immunoreceptor tyrosine-based activation motif (ITAM) in the cytosolic tails of the TCR subunits. Phosphorylated ITAMs promote the recruitment of the Syk family PTKs ZAP70 and Syk through their Src homology 2 (SH2) domains (Lin and Weiss, 2001; Straus and Weiss, 1993). Two known substrates of the activated ZAP70 are the adapter molecules LAT (linker for activation of T cells) and SLP-76 (SH2-containing leukocyte protein-76). Phosphorylation of tyrosine residues on LAT and SLP-76 leads to a recruitment of proteins involved in activation of the Ras pathway, calcium mobilization and cytoskeletal reorganization. One critical protein that is recruited to LAT upon TCR stimulation is the phospholipase-Cγ1 (PLCγ1) (Finco *et al,* 1998; Zhang *et al,* 1998). Phosphorylation of a tyrosine residue in PLC-γ activates the enzyme, which cleaves phosphatidylinositol 4,5-bisphosphate (PtdIns(4,5)P_2) into diacylglycerol (DAG) and inositol 1,4,5-triphosphate (Ins(1,4,5)P_3) (Berridge, 1987). DAG induces the activation of protein kinase C, which is an upstream regulator of the guanosine trisphosphate-binding RAS proteins (Nishizuka, 1988). RAS activates the MAPK cascade and cell proliferation (Davis, 1994; Kyriakis and Avruch, 2001). In theory, mutations at any point in this pathway could lead to constitutive activation of the MAPK cascade and uncontrolled cell proliferation (Lin and Aplan, 2004).

Mutations involving the apoptosis signaling pathway have been also associated with leukemogenesis. Patients with follicular lymphoma have a t(14;18)(q32;q21) that fuses the *IgH* gene with the *BCL-2* gene (Amakawa *et al,* 1991; Jäger *et al,* 2000). Consequently, the transcription of the anti-apoptotic *BCL-2* gene is enhanced, and cells escape from apoptosis. In addition, some T-ALL samples show inactivation of the pro-apoptotic *BAX* gene (Makover *et al,* 1991; Meijerink *et al,* 1998).

2.3.2. PI3K/Akt signaling pathway and leukemogenesis

The phosphoinositide 3-kinase (PI3K) family of lipid kinases phosphorylates the 3-hydroxyl group of the inositol ring of phosphoinositides in cellular membranes. 3-Phosphoinositides play integral roles in the assembly of membrane signaling complexes and in the intracellular trafficking of proteins (Katso *et al,* 2001; Vanhaesebroeck *et al,* 2001). Resting cells contain

substantial levels of PtdIns3*P*, but hardly any PtdIns(3,4)P_2 or PtdIns(3,4,5)P_3 (Vanhaesebroeck and Alessi, 2000). Stimuli that induce tyrosine (Tyr) kinase activity in cells almost invariably lead to the generation of PtdIns(3,4)P_2 and PtdIns(3,4,5)P_3 (Stephens *et al,* 1993). This Tyr kinase activity can be provided by receptors with intrinsic Tyr kinase activity or by non-receptor Tyr kinases.

PI3K-generated phosphatidylinositol 3,4,5-trisphosphate (PtdIns(3,4,5)P_3) can bind Akt (also known as protein kinase B (PKB)), which is subsequently activated by sequential phosphorylation on residues threonine 308 and serine 473 (Chan *et al,* 1999). Akt has been identified as the viral oncogene *v-akt*, and Akt activation is one of the crucial events involved in the transfer of the oncogenic signal initiated from a constitutively activated PI3K (Aoki *et al,* 1998). Three highly homologous isoforms of Akt are transcribed from independent genes and have overlapping but distinct functions (Bellacosa *et al,* 2004). In mice, PKBα, also known as Akt1, mediates signals downstream of PI3K activation that promote cell survival and proliferation. In contrast, PKBβ (also known as Akt2) activation is associated with insulin-mediated metabolic processes (Garofalo *et al,* 2003; Stiles *et al,* 2002). It has been reported that *Pkbγ*$^{-/-}$ (also known as *Akt3*) mice have reduced brain size and weight, which might be attributed to reduced cell size and cell number (Tschopp *et al,* 2005). The net result of the activation of all isoforms of Akt is protection from apoptosis and increased proliferation –events that favor tumorigenesis (Cully *et al,* 2006). The role of PI3K/Akt signaling in leukemogenesis has been demonstrated for the transformation of hematopoietic cells by *BCR/ABL* (Skorski *et al,* 1997). It has been reported that the activation of GAB2 is required for BCR-ABL-mediated leukemogenesis in mice, and *Gab2*$^{-/-}$ cells are resistant to BCR-ABL-induced transformation (Sattler *et al,* 2002). In addition, a mutated form of the p85 subunit of the PI3K has been identified in a human hematopoietic cell line (Jücker *et al,* 2002). Constitutive activation of PI3K/Akt signaling has been identified in approximately 70% of human leukemias (Min *et al,* 2003). However, mutations in the catalytic subunit of the PI3K, i.e. p110α seems to be a rare event in human acute leukemias (Lee *et al,* 2005).

2.4. Treatment of leukemia and gene technology

The common treatments for leukemia are chemotherapy, radiation therapy, biologic therapies and bone marrow transplantation. In the last years, an international group assessed a gene test

in order to identify which adult T-cell ALL patients could be successfully treated with chemotherapy only, avoiding whenever possible bone marrow transplantation (Ferrando and Look, 2002). The gene test used in this study is called "gene chip" or microarray. Gene expression patterns were found for each sample using this technique, and a correlation was made between these results, the specific treatment and the response of each patient. Bone marrow samples from two groups of adult T-cell ALL patients were analyzed. The total RNA from each sample was isolated and hybridized to probes in the microarray assay. The analysis revealed a differential *HOX11* gene expression in the population. The *HOX11* (*homeo box 11*) gene controls the genesis of a single organ (Roberts *et al*., 1994) and is involved in the tumorigenesis of T-cell ALL. However, it does not occur very frequently, up to 7% of childhood T-cell ALL is accompanied by a translocation of chromosome 10 and a subsequent *HOX11* gene expression (OMIM, 1998). As the authors reported, their results demonstrate that the patients with high *HOX11* gene activity have an excellent prognosis after treatment with chemotherapy. In addition, they proposed that bone marrow transplantation should be avoided with these patients, owing to the risks of early death. Cully *et al.* (2006) have considered that the identification of the multiple mechanisms than can activate PI3K signaling might be of significant therapeutic value. They proposed, for example, that the inhibition of the Gab family proteins could be a therapeutic target in the treatment of leukemia. Additionally, Leung and Whittaker (2005) have proposed that although protein-protein interactions are complex to disrupt through chemical inhibition, the *in vivo* delivery of inhibitory RNA molecules could be a feasible approach to inhibiting the PI3K signaling pathway.

2.5. Reduction of leukemia cell proliferation

It has been shown that the molecular analysis applied to leukemia has an advantage in the identification and targeting of some genes involved in leukemogenesis. Leukemia cell reduction through antileukemic therapy may be caused by the inhibition of proliferation or direct induction of cell death. *In vitro* studies with tumor and leukemia cell lines have shown that cytotoxic drugs in anticancer chemotherapy induce cell death by the activation of diverse apoptosis signaling pathways (Dive *et al,* 1992; Hannun, 1997). It has been suggested that

functional defects in apoptosis signaling molecules or deficient activation of apoptosis pathways are responsible for chemotherapy resistance and treatment failure in acute leukemia.

2.5.1. The SHIP protein, role in cellular regulation and human leukemia

The SH2-containing Inositol 5-Phosphatase 1 (SHIP-1/SHIP) is a negative regulator of signal transduction in hematopoietic cells. SHIP was originally identified as a 145 kDa protein that was phosphorylated on tyrosine following stimulation by a wide range of cytokines and growth factors (Rohrschneider *et al,* 2000). Subsequent cloning of the molecule revealed a 1190 amino acid protein that contains several motifs important for protein-protein interactions. Full-length SHIP (1190 amino acid residues) is the product of a 3570-nucleotide open reading frame (ORF). SHIP proteins exhibit frequently discrete size variability (e.g. 145, 135, 125, and 119 kDa), as described by some laboratories (Lioubin *et al,* 1996; Lucas and Rohrschneider, 1999; Ono *et al,* 1996). Bone marrow or immature hematopoietic cell lines express increasingly larger SHIP proteins as differentiation proceeds to mature blood cells (Geier *et al,* 1997). It has been shown that during the preparation of protein extracts under non-denaturing conditions from hematopoietic cell lines and in primary leukemia samples, an artificial cleavage of SHIP proteins can occur (Horn *et al,* 2001).

The domain and motif structure of p145 SHIP is shown in Figure 2. The amino-terminal Src homology 2 (SH2) domain (Schaffhausen, 1995) is crucial in the interactions of SHIP with signaling molecules, including cell surface receptors and cytoplasmic proteins (e.g. Shc, $p62^{dok}$) (March and Ravichandran, 2002; Rohrschneider *et al,* 2000). The central 400-500 amino acid region of SHIP encodes an enzymatic activity for removal of phosphate from the 5' position of inositol polyphosphate (Rohrschneider *et al,* 2000). SHIP recruitment to the plasma membrane via interactions of its SH2 domain brings SHIP in proximity to its enzymatic substrate phosphatidylinositol 3,4,5-trisphosphate (PtdIns(3,4,5)P_3), which is hydrolyzed by SHIP to produce phosphatidylinositol 3,4-bisphosphate (PtdIns(3,4)P_2). There are some signaling molecules that contain plekstrin homology (PH) domains, which by binding to PtdIns(3,4,5)P_3, mediate recruitment to the plasma membrane and activation. Because of its enzymatic activity, SHIP inhibits the activation of those molecules (e.g. PLCγ, Btk, Akt). Taking into consideration the carboxy-terminal region of SHIP, the two tyrosine residues contained within the sequence NPXY, when phosphorylated bind to phosphotyrosine

binding (PTB) domain-containing signaling molecules (e.g. Shc, p62^{dok}). The proline-rich regions bind to molecules containing SH3 domains (e.g. Grb2).

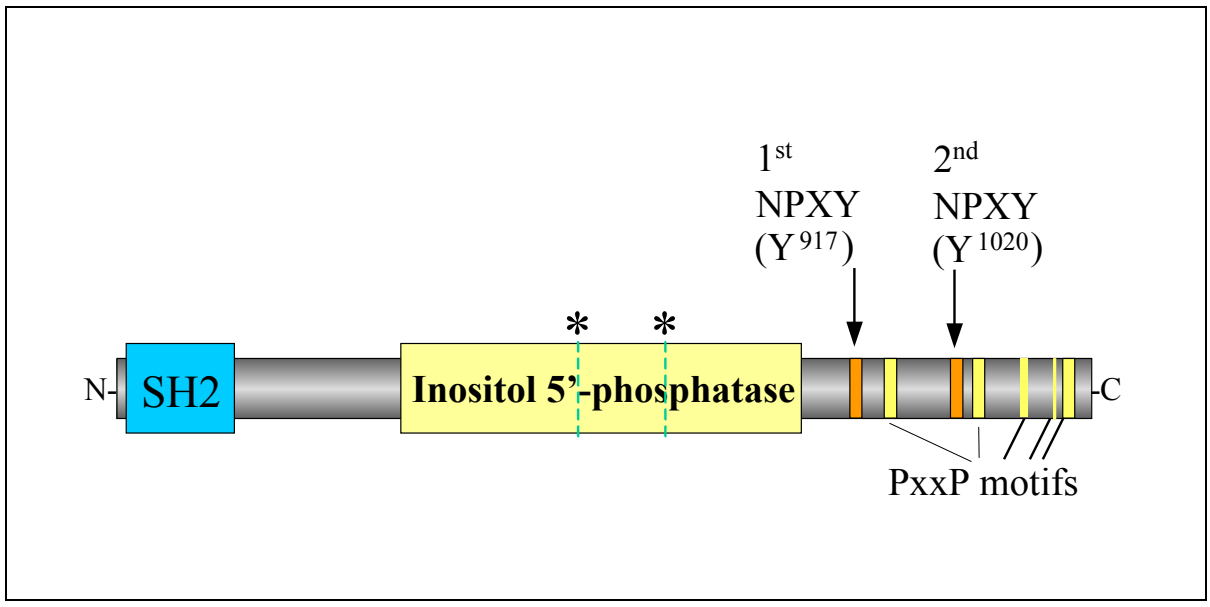

Figure 2. The domain structure of p145 SHIP.

The SH2, inositol 5'-phosphatase and carboxy-terminal domains are shown. The region between the SH2 and inositol 5'-phosphatase domains is of unknown function. Two asterisks above the central enzymatic domain mark the location of homology regions with all inositol 5'-phosphatases; and two NPXY motifs, when tyrosine phosphorylated, have potential for binding PTB or possibly SH2 domains. These are designated with orange in the carboxy–terminal region. The remainder of the carboxy-terminal domain has several potential polyproline motifs (PxxP) for binding SH3 domains. These polyproline motifs are shown in yellow. Three of the motifs show very good consensus for SH3 domain binding; two others have weaker homology, and are shown with narrower yellow bands. **SH2:** Src homology 2. **PTB:** phosphotyrosine binding domain. (Modified from Rohschneider *et al,* 2000).

SHIP is expressed in all hematopoietic cells analyzed to this point, including CD34^{+} cells derived from human bone marrow (Geier *et al,* 1997; Horn *et al,* 2001; Liu *et al,* 1998). In humans, a reduced SHIP expression in primary myeloid leukemia cells from patients with chronic myelogenous leukemia (CML) has been observed, as a result of direct inhibition by the *BCR/ABL* oncogene, which causes CML (Sattler *et al,* 1999). Additionally, a dominant-negative mutation of the *SHIP* gene was identified in primary leukemia cells from a patient with acute myeloid leukemia (AML) (Luo *et al,* 2003). Further analyses revealed mutations in the *SHIP* gene in 7 out of 32 AML patients (22%) and one out of nine ALL patients (12%) (Luo *et al,* 2004). The differential expression of various SHIP isoforms during differentiation of the human ML-1 myeloid leukemia cell line from an immature myeloid state to mature

macrophages or granulocytes has been also demonstrated (Geier *et al,* 1997). The immature cells expressed a p110 SHIP isoform primarily, whereas the mature cells expressed mostly SHIPα (145 kDa product) and SHIPβ (p135, product of the Δ183 deletion). These results indicate complex splicing events for SHIP expression during hematopoietic cell development, with potentially different functions.

2.5.2. SHIP is a negative regulator of the PI3K/Akt signaling pathway in the human leukemia cell line Jurkat.

Recently, it has been demonstrated that restoration of SHIP activity in Jurkat T cells, which have lost the expression of SHIP, down-regulates constitutively activated PI3K/Akt/GSK-3β signaling (Horn *et al,* 2004). The inducible expression of SHIP in these cells led to a reduction of the steady-state levels of PtdIns(3,4,5)P_3, associated with a reduced phosphorylation (Thr 308/Ser 473) and activity of Akt (Figure 3).

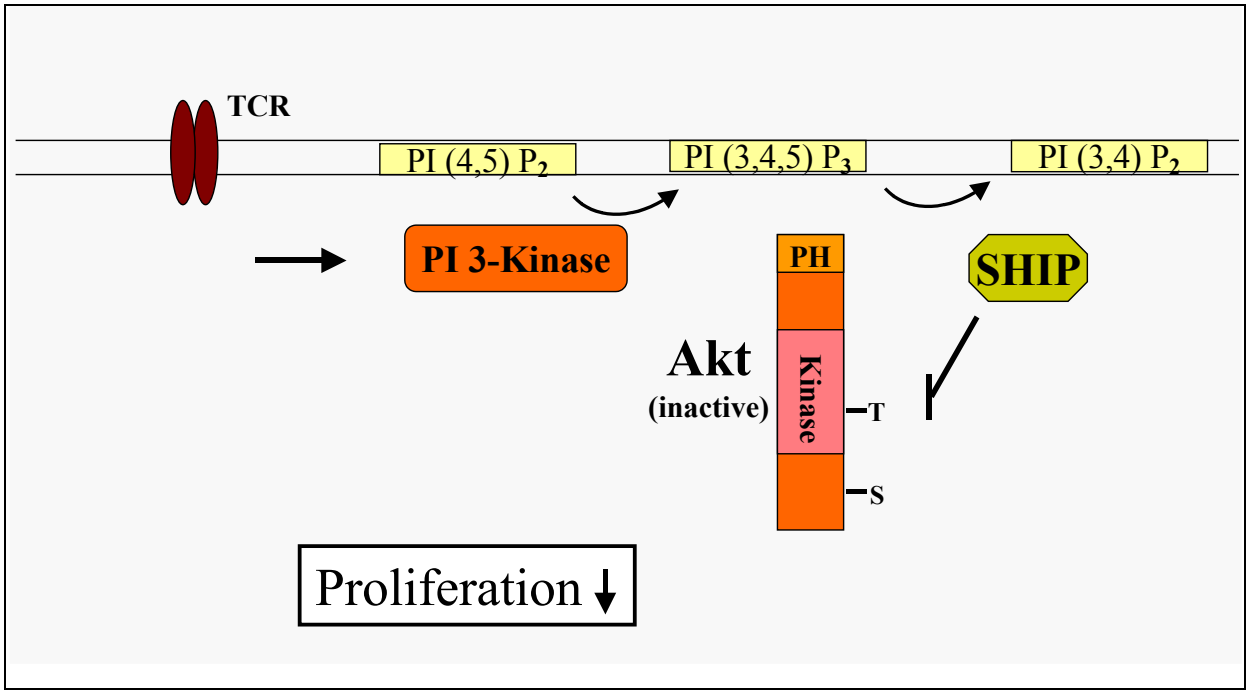

Figure 3. SHIP is a negative regulator of the PI3K/AKT pathway.

After expression of SHIP in hematopoietic cells, there is a reduction in the phosphorylation of AKT at residues Thr 308 and Ser 473. Consequently, proliferation is diminished. PI3-Kinase: Phosphoinositide 3-kinase. Akt (PKB): Protein kinase B. PI: Phosphatidylinositol. PH: plekstrin homology domain. TCR: T cell receptor.

In addition, the reduced proliferation of Jurkat T cells after the induced expression of SHIP was associated with an increased transit time through the G1 phase of the cell cycle, but no increased number of quiescent cells (G0) was detected. A stabilization of the cell cycle inhibitor $p27^{Kip1}$ was also shown, as well as reduced phosphorylation of the retinoblastoma protein Rb (Horn *et al,* 2004). These data suggest a possible function of SHIP in the pathogenesis of human leukemia.

2.6. Regulation of T cell quiescence

Circulating $CD4^+$ and $CD8^+$ T lymphocytes are found primarily in a quiescent state that is characterized by small cell size, lack of proliferation low cellular metabolism, and resistance to apoptosis. Upon antigenic stimulation, these cells are induced to express large numbers of activation-specific genes and undergo rapid entry into the cell cycle. Studies of lymphocyte activation have identified gene products involved in maintaining quiescence, suggesting that T cell quiescence is an active process rather than a default state resulting from a lack of activation signals (Yusuf and Fruman, 2003). Two transcription factors which are down-regulated following T cell activation have been demonstrated to play important roles in quiescence, LKLF (KLF2) and Tob (Kuo *et al,* 1997; Tzachanis *et al,* 2001).

2.6.1. The family of mammalian Sp/XKLF transcription factors

G-rich elements, such as GC (GGGGCGGGG) and GT/CACC boxes (GGTGTGGGG) are important *cis*-acting elements required for the appropriate expression of housekeeping as well as many tissue-specific and viral genes. These motifs have been found and analyzed in promoters, enhancers and locus control regions (LCRs) of genes that are under different ways of control, such as cell cycle regulation, hormonal activation and developmental patterning. Furthermore, GC/GT boxes are commonly found in promoters embedded in CpG-rich methylation-free islands (Philipsen and Suske, 1999). The maintenance of the proper methylation patterns is essential for normal development (Li *et al,* 1992). The general transcription factor Sp1 (name according to the original purification scheme including Sephacryl and phosphocellulose columns) (Kadonaga *et al,* 1987) can bind and act through

GC/GT boxes. Sp1 represents the first identified and cloned member of a family of transcription factors, which contain a highly conserved DNA-binding domain consisting of three zinc fingers. Figure 4 shows the family of these transcription factors.

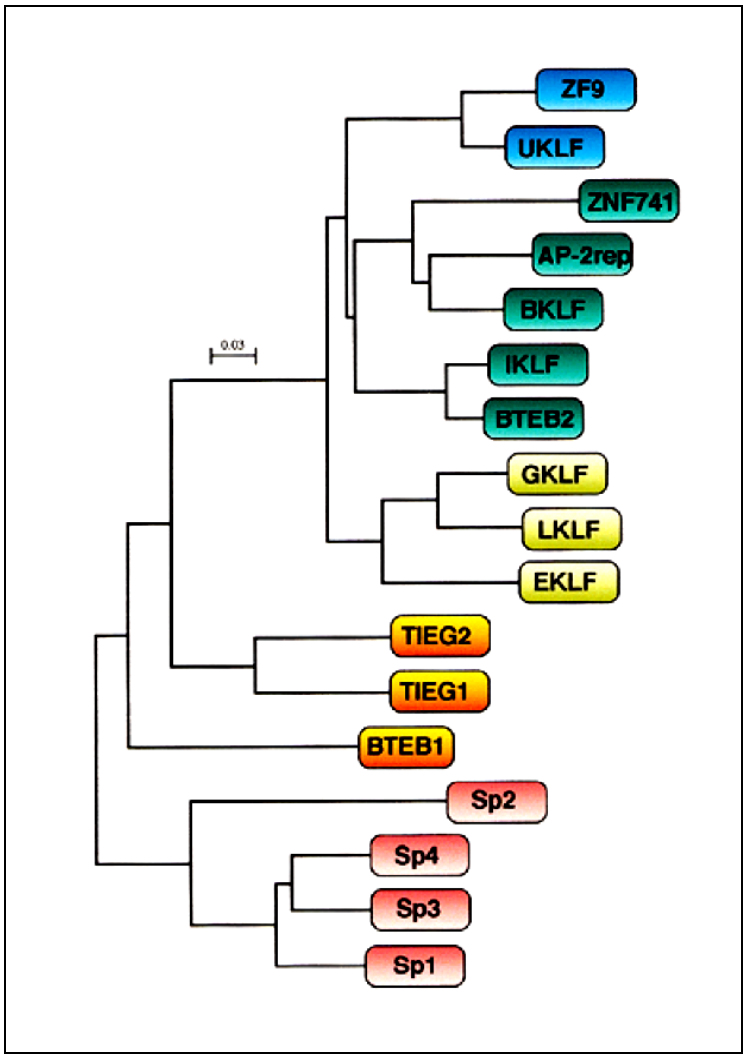

Figure 4. Phylogenetic tree of the Sp/XKLF transcription factors.

The tree was generated with the CLUSTALW Multiple Sequence Alignment Program v.1.7 (June 1997) (Thompson *et al,* 1994) using the amino acid sequences of the DNA-binding domains of the Sp/XKLF proteins. (From Philipsen and Suske, 1999).

The 81 amino acid DNA-binding domain found close to the C-termini of all members essentially defines the Sp/XKLF family of transcription factors. It consists of three C2H2-type zinc fingers, arranged similar to those found in the *Drosophila melanogaster* regulator protein Krüppel. Therefore, some of the proteins have been named Krüppel-like factors

(Philipsen and Suske, 1999). The remarkable similarity of the linker amino acids between the individual fingers, in addition to the identical length of the DNA-binding domain strongly suggest that the higher order structure of the three fingers is crucial for the biological function of the proteins (Figure 5). The amino acids of the Sp1 that are most likely to make specific contacts with the DNA are the amino acids KHA within the first, RER within the second, and RHK within the third zinc finger domain (Figure 5). These amino acids are conserved in Sp3, Sp4, BTEB1, TIEG1 and TIEG2 proteins (Figure 5). Consistent with this conservation, Sp3, Sp4, BTEB1, and TIEG2 recognize classical Sp1-binding sites (Cook *et al,* 1998; Hagen *et al,* 1992; Sogawa *et al,* 1993).

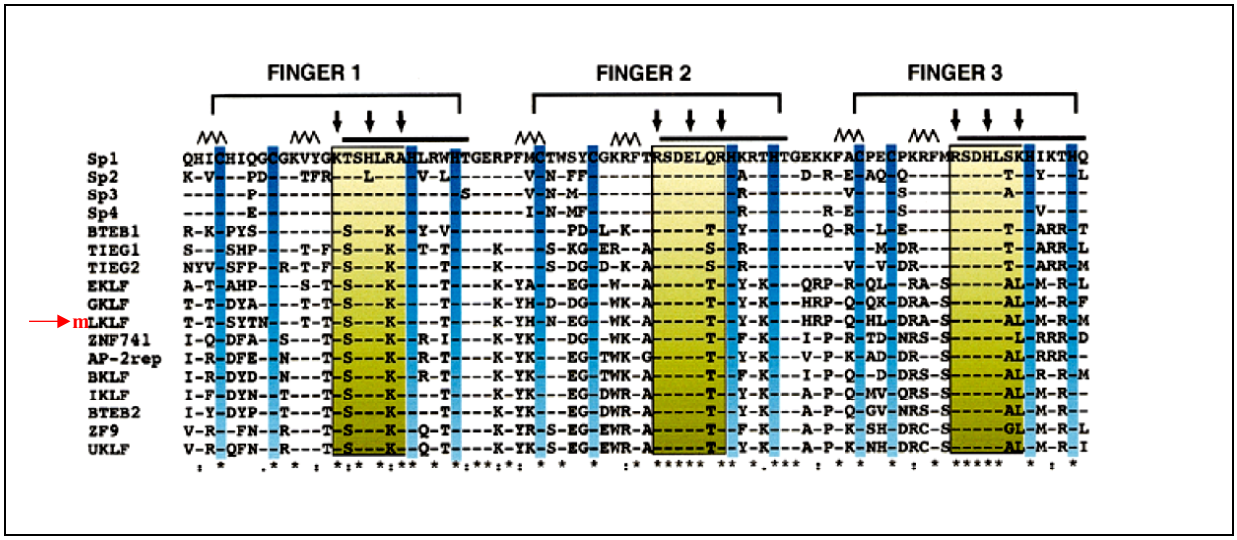

Figure 5. Protein sequence alignment of the zinc finger domains of mammalian Sp/XKLF family members.

All sequences are human sequences with the exception of LKLF, AP-2rep, BKLF and IKLF, which are of mouse origin. The cysteine and histidine residues that are involved in zinc coordination are in blue. Black arrows point to the amino acid positions that probably determine the recognition specificity of the fingers by contacting specific bases of the DNA. Black lines indicate α-helices; β-sheets are shown as zigzag lines. The amino acids that are thought to make base contacts are boxed (adapted from (Pavletich and Pabo, 1991). Residues conserved between all family members are indicated (*). The red arrow points the LKLF mouse sequence (mLKLF). (Modified from Philipsen and Suske, 1999).

Based on the structural relationships of the proteins (Figures 4 and 5), it has been suggested to divide the Sp/XKLF family into three subgroups: i) the four Sp transcription factors; ii) the close relatives, BTEB1, TIEG1 and TIEG2; iii) the Krüppel-like factors (XKLFs). The latter also includes BTEB2, GBF/ZF9, ZNF741 and AP-2rep (Philipsen and Suske, 1999). Although all proteins recognize very similar DNA target sites, the relative affinities for

specific sequences differ. Sp factors bind more strongly to GC boxes than to GT boxes (Thiesen and Bach, 1990), while XKLF bind preferentially to GT boxes (Crossley *et al,* 1996; Feng *et al,* 1994; Matsumoto *et al,* 1998; Shields and Yang, 1998).

As convention, the "X" by XKLFs usually indicates the major expression site of the factor, i.e. erythroid cells (EKLF) (Miller and Bieker, 1993; Southwood *et al,* 1996) or lung (LKLF) (Anderson *et al,* 1995). However, their expression is not always restricted to these tissues. An inverse correlation exists between cell proliferation and expression of KLF transcription factors: the latter are up-regulated under conditions associated with growth arrest, whereas they are suppressed in actively proliferating and neoplastic cells.

2.6.2. The human Krüppel-like factor 2 (KLF2/LKLF)

The Krüppel-like factor 2 (lung) or Lung Krüppel-like transcription factor (KLF2/LKLF) is a member of the Krüppel-like factor (KLF) family of transcription factors that contains zinc-finger binding domains and bind to GC-rich sequences in mammalian promoters (Kaczynski *et al,* 2003). The Krüppel-like factor family members typically function as transcriptional switches in differentiation/activation processes in many cell types (Philipsen and Suske, 1999). Kozyrev *et al.* (1999) isolated a cDNA encoding KLF2, which they termed LKLF. Sequence analysis predicted that the 355-amino acid LKLF/KLF2 protein, which is 87% identical to the mouse protein, and shares 90.2% amino acid similarity, has N-terminal proline-rich repeats, a putative activation domain, a potential nuclear localization signal (KPKRGRRSWPRKRTAT), and a C-terminal zinc finger domain (Figure 6). The three zinc fingers are similar to the zinc finger consensus sequence Cys-X_{2-4}-Cys-X_{12}-His-X_{3-4}-His (Miller *et al,* 1985), while only the first inter-finger spacer, called H/C link, consisting of seven amino acids, has the conservation sequence TGEKPYH (Kozyrev *et al,* 1999). Thus, human KLF2 is divided into two domains, the Pro-rich transactivating N-terminal domain and the C-terminal zinc finger-containing domain. By PCR and genome sequencing analysis, it was determined that the KLF2 gene spans more than 3 Kb and contains three exons, having sizes of 174 bp, 817 bp and 680 bp, respectively, interrupted by two introns (Kozyrev *et al,* 1999; Wani *et al,* 1999a) (Figure 7). The 5-prime flanking region has features of a GC-rich promoter with multiple SP1-binding sites, but it also has two putative TATA boxes. From the proximal promoter to the end of the second exon, it has been found that the CpG island has a

76% GC content in average, and two regions of unusually high GC density (Kozyrev *et al,* 1999).

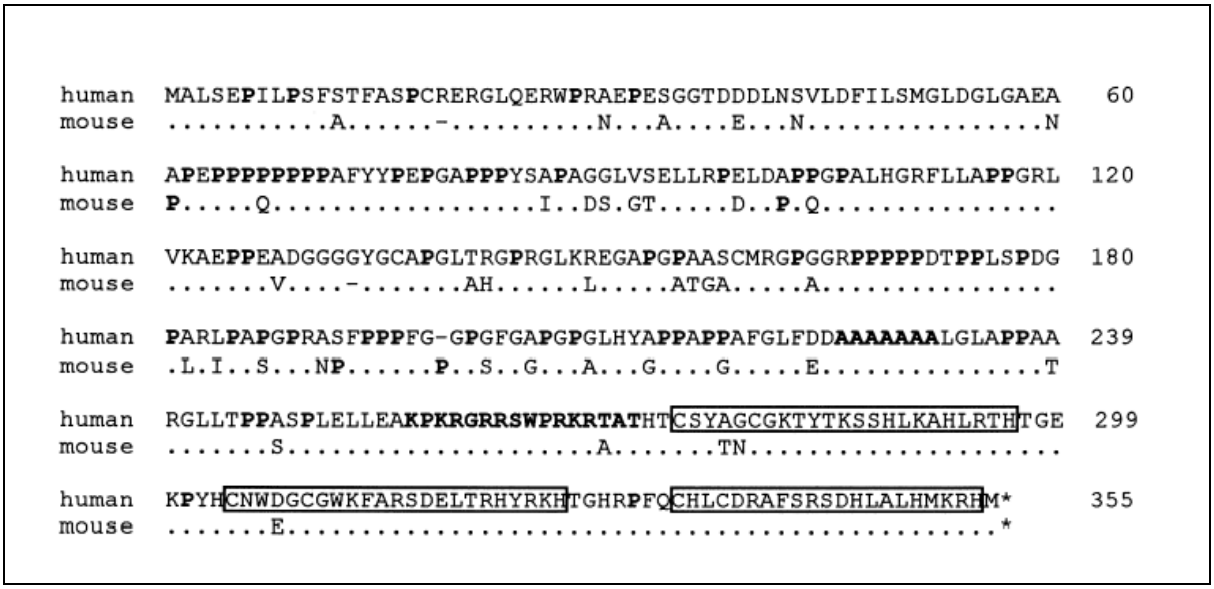

Figure 6. Alignment of the human and mouse LKLF protein sequences.

Amino acids are shown in standard one-letter code. Dots represent identical amino acids, and dashes indicate gaps. The three zinc fingers are boxed. Proline residues, alanine stretch and nuclear localization signal are in bold letters. (From Kozyrev *et al.,* 1999).

Additionally, it has been reported that the human *KLF2* gene is located on chromosome 19p13.11-13 (Kozyrev *et al,* 1999). There are a number of zinc finger genes mapped on human chromosome 19 (Lichter *et al,* 1992). One of them is the human erythroid Krüppel-like factor (*EKLF*) gene, reported to map in 19p13.12-p13.13 (van Ree *et al,* 1997), the same locus where the human *KLF2* gene is located.

2.6.3. KLF2 and T-cell quiescence

Naive T lymphocytes circulate in the peripheral blood and lymphoid organs in a quiescent state, characterized by small cell size, low metabolic rate, and a distinctive cell-surface phenotype ($CD69^{-}CD25^{-}CD44^{-}CD62L^{+}$) (Abbas *et al,* 1994; Freitas and Rocha, 2000). The proliferation of naive T cells is regulated by homeostatic mechanisms that maintain the total number of circulating T cells, whereas the survival of naïve T cells appears to require

signaling through the T cell antigen receptor (TCR), as well as tonic stimulation by specific lymphokines (Freitas and Rocha, 2000). It has been suggested that T cell quiescence is actively regulated and that KLF2 plays an important role in programming and maintaining naïve T cell quiescence (Buckley *et al,* 2001).

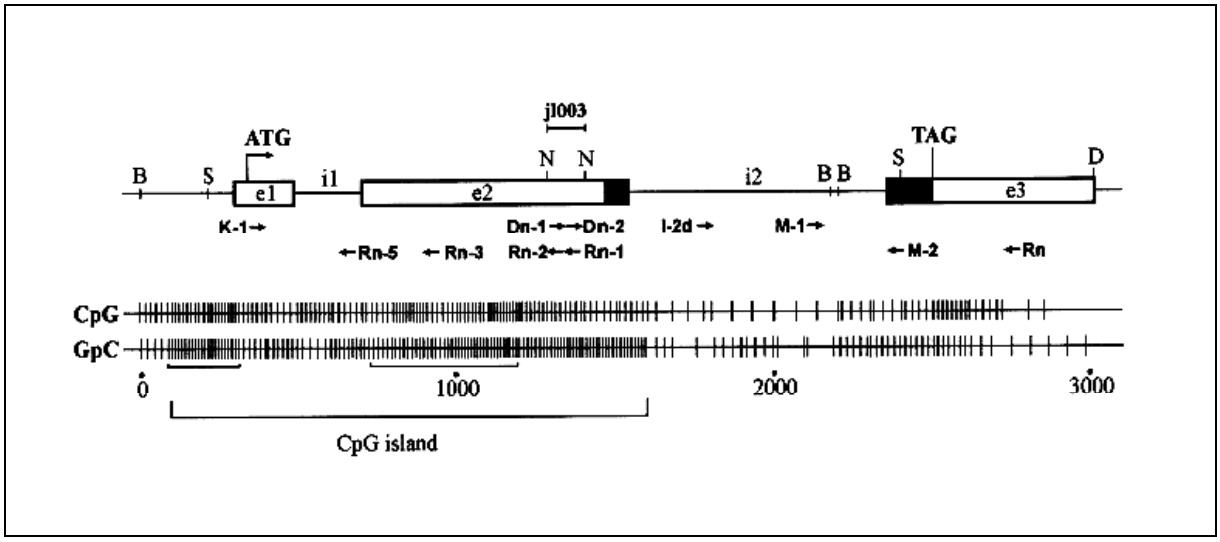

Figure 7. Genomic organization of the human KLF2/LKLF gene.

Exons (e1, e2, e3) are shown as boxes separated by intronic sequences (i1, i2). Zinc finger region is shaded. The letters B, N, S and D indicate the restriction sites for *Bam*HI, *Not*I, *Sac*I and *Dra*I, respectively. The jl003 *Not*I clone and PCR primers are shown above and below the gene structure. A map plot of CpG and GpC distribution through the gene is represented by the short vertical lines. CpG island and two regions of increased CpG/GpC density are marked by horizontal brackets. (Modified from Kozyrev *et al.,* 1999).

Targeted disruption of KLF2/lung KLF revealed an essential role in programming the quiescent phenotype of single-positive T cells and lung development (Kuo *et al,* 1997; Wani *et al,* 1999b). The expression of KLF2 mRNA and protein is induced during single positive thymocyte development and are maintained at a high level in quiescent lymphocytes. Upon lymphocyte activation through the T cell receptor, both KLF2 mRNA and protein are down-regulated (Kuo *et al,* 1997). It has been demonstrated that T cell attachment and rolling was markedly attenuated in KLF2-overexpressing cells. The data demonstrated that KLF2 can inhibit adhesion molecule expression, and T cell attachment and rolling to activated endothelial cells (SenBanerjee *et al,* 2004). Expression of KLF2/LKLF in $CD4^+$ or $CD8^+$ T lymphocytes correlates with quiescence, as KLF2/LKLF expression is high in quiescent lymphocytes, and is down-regulated following T cell activation (Kuo *et al,* 1997). KLF2

expression is reinduced in $CD8^+$ memory (small $CD44^-CD69^-CD25^-$) T cells (Schober *et al,* 1999), which are considered to be relatively quiescent (Sprent and Surh, 2001). KLF2-deficient T cells produced by gene targeting showed a spontaneously activated cell-surface phenotype ($CD69^+CD44^-CD62L^-FasL^+$) and died in the periphery from an apoptotic process that resembled activation-induced cell death (Kuo *et al,* 1997).

The induction of KLF2/LKLF in Jurkat T cell lines expressing KLF2 under control of a tetracycline-inducible promoter results in inhibition of cell proliferation and protein synthesis, a decrease in cell size, and reduction of expression of the cell surface markers CD30, CD71 and CD1a (Buckley *et al,* 2001). Conversely, KLF2-deficient T cells produced by gene targeting spontaneously entered the S phase of the cell cycle and showed increased cell size and CD71 (the transferring receptor) expression *in vivo*. Inducible expression of KLF2 also resulted in a rapid and marked down-regulation of c-Myc expression in Jurkat cells. Buckley *et al.* (2001) concluded that KLF2 functions, in part, by negatively regulating a MYC-dependent pathway. Myc family members in general function to control cell division, differentiation and apoptosis, and are commonly deregulated in diverse tumors (Mateyak *et al,* 1999). Quiescent cells lack c-Myc, and its expression is rapidly induced after proliferative stimuli. However, the definitive targets of c-Myc remain elusive.

While actively induced expression of Bcl-2 family members (Bcl-2 and Bcl-x_L) and the phosphoinositide 3-kinase (PI3K)/protein kinase B (PKB) pathways likely provide the signals that are essential for naïve T cells survival, the molecular events leading to cellular quiescence are less well defined (Di Santo, 2001). Additionally, because the DNA binding sequence of KLF2 has not been definitively established, and KLFs likely bind to DNA in association with other factors (Turner and Crossley, 1999), the effect of KLF2 on target genes remains also to a certain extent elusive.

3. Objectives

The first aim of this study is to investigate the transcriptional regulation of genes after the restoration of the inositol 5-Phosphatase SHIP in the human leukemic cell line Jurkat. It has been shown in our laboratory that the restoration of SHIP in Jurkat T cells leads to a reduction of constitutively phosphorylated Akt (Horn *et al,* 2004), and that SHIP is a negative regulator of the PI3K/Akt pathway, with an effect on reduction of proliferation. Therefore, microarray analysis by the use of the Human U133 GeneChips A and B (Affymetrix, Santa Clara, USA) should be carried out, in order to identify the genes that are differentially regulated at the transcriptional level after the restoration of SHIP in Jurkat T cells. Accordingly, this should allow the elucidation of genes that are likely involved in the SHIP-mediated reduction of proliferation of these cells.

The second aim of this study is the validation of the results obtained by microarray analysis. With this purpose, quantitative real-time RT-PCR analysis will be assessed for those genes that are identified to be at least 2-fold significantly up- or down-regulated after the restoration of SHIP in Jurkat T cells. Furthermore, analyses of the ontology of the validated genes, verified to be significantly regulated by microarray analysis and quantitative real-time RT-PCR, should be performed. According to their function, localization, and possible relationship to proliferation of T cells, and with respect to their expression in leukemia T cell lines, one candidate gene should be chosen for further analyses. Western blotting analyses of the protein expression of the SHIP-regulated candidate gene should be carried out, with the purpose to verify the differential expression at the protein level.

As the third aim of this study, after validation of differential expression of mRNA and protein levels, biological analysis of a SHIP-regulated gene should be carried out, with focus on cell proliferation. In order to achieve that, ectopic expression of the target gene by transient transfection in Jurkat-SHIP cells should be performed. The effect of the protein expression of the SHIP-regulated gene on proliferation of Jurkat cells should be assessed by FACS analysis of BrdU incorporation.

Since the activation of the T cell receptor results in stimulation of PI3-kinase, a fourth aim of this study is to determine whether the PI3K/Akt pathway is involved in the regulation of the expression of the SHIP-regulated gene. Analysis of changes in protein expression after pharmacological inhibition of PI3K with wortmannin in Jurkat T cells should be performed. Moreover, the silencing of Akt1 expression by knockdown using RNAi and the effect on the expression of the target protein should be investigated.

4. Materials and Methods

4.1. Reagents, Enzymes and Materials

Cell culture media and supplements were purchased from Invitrogen (Karlsruhe, Germany). Restriction enzymes were supplied from MBI Fermentas (St. Leon-Rot, Germany) and used according to the recommendations of the manufacturer. Doxycycline, a tetracycline analog, was acquired from ICN Biomedicals (Aurora, Ohio, USA) and used for the induction of the expression of SHIP in Jurkat cells. The pharmacological inhibitor wortmannin was supplied by Calbiochem-Novabiochem (Schwalbach, Germany). The oligonucleotides used in conventional PCR and quantitative real-time RT-PCR were synthesized by MWG Biotech (Ebersberg, Germany). The RNA isolation was carried out by performing CsCl gradients in a Beckman L-60 ultracentrifuge (rotor SW40 Ti) (Beckman Instruments, München, Germany). The high purity and special reagents used for the RNA isolation, including the diethylpyrocarbonate (DEPC) were provided by BioMol (Hamburg, Germany) and Sigma-Aldrich (Germany). The determination of concentration of the nucleic acids was performed in a BioPhotometer, Model 6131 (Eppendorf, Hamburg, Germany).

The oligonucleotides arrays U133A and U133B were obtained from Affymetrix, Santa Clara, CA, USA) and used according to the manufacturer's protocol, in collaboration with the Institute of Clinical Chemistry (UKE, Hamburg, Germany). The validated Stealth™ RNAi duplex sequences used for silencing the Akt1 expression, in addition to the Block-iT™ fluorescent oligo for electroporation were obtained from Invitrogen (Paisley, UK). The Gene Pulser used for electroporation of Jurkat cells was provided by Bio-Rad (München, Germany). The analyses by inverse fluorescence microscopy were performed in an Axiovert 25 CFL microscope (Zeiss). The reagents for cDNA synthesis were purchased from Invitrogen (Karlsruhe, Germany). The reagents for quantitative real-time RT-PCR were supplied by Roche (Mannheim, Germany); the reactions and the data analysis were performed on a LightCycler system, Version 3.5 and LightCycler detection software, according to the instructions of the manufacturer (Roche, Mannheim, Germany). *Taq* Polymerases used in conventional PCR reactions were acquired from Qiagen (Hilden, Germany) and Invitrogen (Karlsruhe). Antibodies were supplied by Santa Cruz Biotechnology (Heidelberg, Germany),

Cell Signaling Technology (Beverly, MA, USA), Upstate Biotechnology (Lake Placid, NY, USA), BD Pharmingen (San Diego, CA, USA) and Molecular Probes (Leiden, the Netherlands). The Bromodeoxyuridine (BrdU), the anti-BrdU-antibodies coupled to the fluorochrome allophycocyanine (APC), fixation and permeabilization reagents, and DNase used in the immunofluorescent staining of incorporated BrdU were supplied by BD Pharmingen™ (San Diego, CA, USA). Reagents for protein biochemical analyses were obtained from Bio-Rad (München), Merck (Darmstadt, Germany) and Roth (Karlsruhe). The ECL™ detection system was supplied by Amersham Biosciences (Heidelberg). Chemiluminescence signals were measured with a LAS3000 Imager, using the AIDA software (Raytest/Fuji, Straubenhardt, Germany). FACS (fluorescence-activated cell sorter) analyses were performed by the use of a BD FACSCalibur™ (BD, Heidelberg).

4.2. Cells

Jurkat is a human T-cell line established from a patient with acute lymphocytic leukemia (Schneider *et al.,* 1977). Jurkat Tet-On cells carrying the reverse transactivator (BD Clontech, Heidelberg, Germany) were cultured in Roswell Park Memorial Institute (RPMI) 1640 Medium, supplemented with GlutaMAX™ I, 25 mM HEPES (Invitrogen, Karlsruhe, Germany), 10% v/v fetal calf serum (FCS), 1% penicillin-streptomycin solution and 1 mM sodium pyruvate at 37°C in a humidified atmosphere in the presence of 5% CO_2. The infection of Jurkat Tet-On cells with pseudotyped retroviruses carrying the human *SHIP* cDNA under the control of a tetracycline inducible response element (TRE) (Figure 8), the selection of individual clones in hygromycine and cloning by limiting dilution has been already performed in our laboratory by Dr. Horn (2003). The resulting Jurkat-SHIP cells (clone no. 51) and a vector transduced control clone were used in this study. Jurkat-SHIP cells (clone no. 51) were maintained in culture, grown in supplemented RPMI, before an experiment was performed. The medium was changed every 48 h. Independent replicates were used in the course of the study.

4.3. Induction of SHIP expression

For transcriptional regulation analyses by the use of microarrays and western blot verification of protein expression after the restoration of SHIP in Jurkat T cells, sister cultures of Jurkat-SHIP cells (clone no. 51), from at least two independent replicas were cultured for 82 hours

either in fresh supplemented RPMI medium, containing 0.8 µg/ml doxycycline (Dox) to induce the expression of SHIP (+Dox), or in the same medium containing a corresponding volume of 70% ethanol (- Dox). The supplemented medium (including doxycycline or ethanol) was changed every 48 hours. The cell density was calculated in each case by manual counting using a Neubauer Cell Chamber. The percentage of death cells was estimated by staining with 0.1% trypan blue solution (Sigma-Aldrich). Differences in the cell number between the cells induced and not induced were estimated, as indicator of proliferation of the populations. $5x10^7$ -$1x10^8$ cells were harvested for further RNA isolation, and $5x10^6$ -$5x10^7$ cells for protein lysates. For transcriptional regulation analyses by quantitative real-time RT-PCR and western blot analyses of protein expression after the restoration of SHIP in Jurkat T cells, sister cultures of Jurkat SHIP cells (clone no. 51) from at least two independent biological replicas were cultured for 72 hours, following the protocol described above.

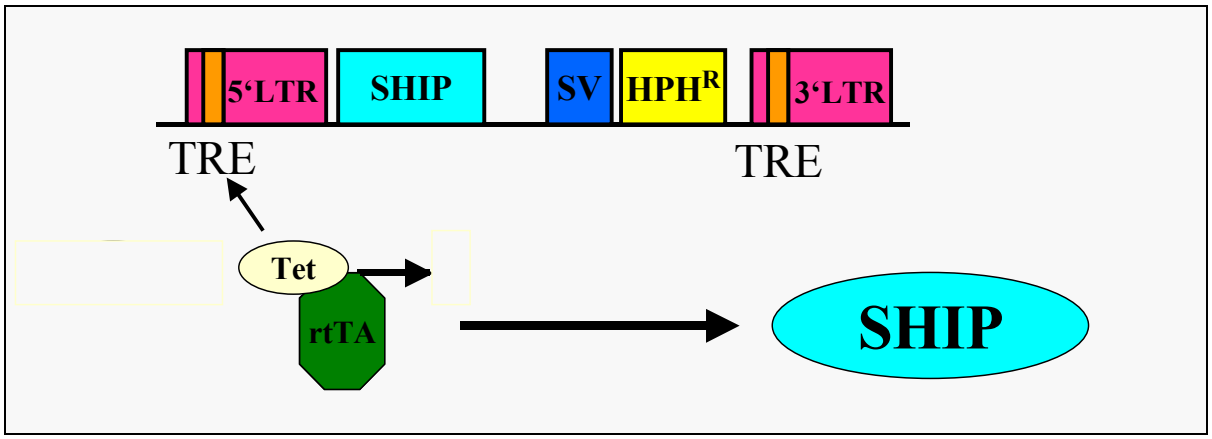

Figure 8. Infection of Jurkat Tet-On cells with retroviruses carrying tetracycline inducible *SHIP*.

SHIP transcription is induced by the addition of doxycycline (a tetracycline analog) to the culture medium. LTR: long terminal repeat; SV: SV40-promoter; HPHR: hygromycine resistance-gene; TRE: Tetracycline-response–element; rtTA: reverse tetracycline transactivator. SHIP: SH2-containing Inositol-5'-Phosphatase. (Modified from Horn, 2003).

For cell proliferation analyses, sister cultures of Jurkat SHIP cells (clone no. 51), corresponding to at least three biological independent replicas were seeded at a density of ~$2.5x10^5$ cells/ml in fresh RPMI supplemented medium and grown for 48 h in the absence (-Dox) or presence (+ Dox) of 0.8 µg/ml doxycycline. Control cells (-Dox) were incubated with

70% ethanol, as described before. The cells were harvested by centrifugation and resuspended in fresh medium at a density of ~$7x10^6$ cells/700 µl for subsequent electroporation.

4.4. Inhibition with wortmannin

For experiments using the pharmacological inhibitor of the PI3-kinase wortmannin, sister cultures of Jurkat SHIP cells (clone no. 51) from at least two independent experiments were cultured for 75 h either in fresh supplemented RPMI medium, containing 100 nM wortmannin (+ WM), freshly diluted in DMSO, with (+Dox) or without (-Dox) induction of the expression of SHIP, as described previously. Cell culture controls for wortmannin were grown in the same medium containing a corresponding volume of DMSO. Since wortmannin is not so stable for long periods in cell culture, the supplemented mediums containing wortmannin, doxycycline or both, and the corresponding control reagents were changed twice a day during the assay. The cell density was calculated in each case by manual counting using a Neubauer Cell Chamber every day and differences in the cell number corresponding to each population were evaluated. After 75 h inhibition with wortmannin, the cells were harvested for protein analyses, as described in 4.8.

4.5. Cell proliferation analyses

4.5.1. Vectors and plasmid preparation

The vector pKLF2-EGFP was kindly provided by Prof. Dr. Haag, Institute of Immunology (UKE, Hamburg). After validation of the cloning orientation by sequencing and the size of the cloned region by restriction analysis, the pKLF2-EGFP and the plasmid control (pEGFP-N1) without insert were amplified in *E. coli* host strains. Plasmid DNAs were isolated from the transformed cells by the use of a plasmid purification kit (Maxi kit, Qiagen), following the instructions of the manufacturer. Validation control experiments by restriction analysis were performed to confirm the positive clones. Restriction analysis was performed by specific restriction enzyme cleavage of DNA that allowed detection of differences in size, by comparing digestion patterns of the recombinant plasmid to that of the vector. The fragments were separated by agarose gel electrophoresis, stained with EtBr (ethidium bromide) and visualized by exposure to ultraviolet (UV) light.

4.5.2. Transfection of Jurkat-SHIP cells

For cell proliferation analysis, $7x10^6$ cells/700µl were transferred to 0.4 cm sterile Gene Pulser™ cuvettes for mammalian cells (Bio-Rad) and transfected by electroporation (Gene Pulser® Transfection Apparatus, Bio-Rad, Munich, Germany) with 10 µg of the pKLF2-EGFP vector and plasmid control (pEGFP-N1) without insert. The electroporation conditions were set as followed, after standardization with pEGFP-N1: 330 V, 960 µF. The cells from each population were transferred to pre-warmed fresh medium in 10-ml culture flasks and grown for 24 h before determination of transfection efficiencies and subsequently labeling with bromodeoxyuridine (BrdU). Additional controls without vectors were included.

4.5.3. Bromodeoxyuridine (BrdU) labeling

For the standardization of the suitable pulse time of BrdU, sister cultures of Jurkat-SHIP cells (clone no. 51) were grown in the presence or absence of Doxycycline for 72h, changing the medium each 48h. As a first measurement of cell proliferation, the cell density was determined by manual counting using a Neubauer Cell Chamber. The percentage of death cells was estimated by staining with 0.1% trypan blue solution (Sigma-Aldrich). Subsequently, cell culture densities of $1.5x10^6$ cells/ml from each population and their controls were incubated with fresh RPMI medium containing 0.8 µg/ml doxycycline or 70% ethanol, respectively, in sterile polystyrene non-tissue culture treated 6 well plates (BD, NJ, USA), and labeled with 10 µM BrdU at different time points. Cells from the same population were not BrdU-labeled and used as negative staining control for the assay.

The cells were washed and stained with anti-BrdU-antibodies coupled to the fluorochrome allophycocyanine (APC), according to the protocol of the manufacturer (BD Pharmingen™, San Diego, CA, USA). The BrdU-pulsed cells corresponding to each population and respective controls were transferred to flow cytometry tubes, washed 1X by adding 1 ml of staining buffer (1x DPBS, 3% Fetal Bovine Serum (heat inactivated), 0.09% sodium azide) per tube, and centrifuged 5 min at 200-300 *g*. The supernatant was discarded, and the cells were fixed and permeabilized by resuspension with 100 µl of BD Cytofix/Cytoperm™ Buffer (BD Pharmigen™) per tube and incubation for 30 minutes on ice. The cells were washed 1x with 1 ml of 1x BD Perm/Wash Buffer (BD Pharmigen™) (diluted 1:10 with deionized ultra pure H_20), centrifuged as described before and the supernatant was discarded. The cells were

resuspended with 100 µl of BD Cytoperm™ Plus Buffer (BD Pharmigen™) per tube, incubated 10 minutes on ice, and washed 1x with 1 ml of 1x BD Perm/Wash Buffer as described before. The cells were re-fixated by resuspension with 100 µl of BD Cytofix/Cytoperm™ Buffer per tube, incubation for 5 minutes on ice and washing with 1 ml of 1x BD Perm/Wash Buffer as described before. The cells were treated with DNase to expose incorporated BrdU by resuspension with 100 µl of diluted DNase (300µg/ml in DPBS) per tube and incubation for 1 hour at 37°C. The cells were washed with 1 ml of 1x BD Perm/Wash Buffer as described before. The cells were stained by resuspension with anti-BrdU-antibodies coupled to the fluorochrome allophycocyanine (APC), contained in 50 µl of BD Perm/Wash Buffer and incubation for 20 minutes at room temperature and protected from the exposure to light. The cells were washed as described before, resuspended in 1.5 ml of staining buffer and chilled on ice, protected from exposure to light prior to Flow Cytometric Analysis.

4.6. Flow Cytometry Analyses

For determination of transfection efficiencies in cells transfected with pKLF2-EGFP vector and the plasmid control (pEGFP-N1) were analyzed 24 h post-transfection by flow cytometry, using a BD FACSCalibur™ (BD, Heidelberg, Germany), in collaboration with Prof. Dr. Haag, at the Institute of Immunology (UKE, Hamburg). $5x10^5$ cells from each population and their controls were harvested, washed with 1X PBS buffer, centrifuged for 5 min at 4°C, and resuspended in 500 µl 1X PBS. The fluorescence was analyzed by flow cytometry and transfection efficiencies were determined by FACS analysis of the EGFP positive population. For determination of transfection efficiencies after transfection with the *Block-iT™ Fluorescent Oligo for Electroporation,* the cells were harvested and washed for FACS analysis, as described previously. The efficiency of transfection was determined by measuring the fluorescence intensity of the positive transfected population of cells.

For single BrdU incorporation analyses, the percentage of BrdU-APC positive cells was measured by FACS. The percentage of reduction of BrdU incorporation after the expression of SHIP in comparison to the control (-SHIP) was calculated in each case, and the effect of SHIP expression on proliferation was expressed as percentage of reduction of newly synthesized DNA in each population. Additionally, the optimal BrdU pulse time was

determined. For analysis of BrdU incorporation in the population of cells transfected with the pKLF2-EGFP and EGFP-N1 vectors, the BrdU-APC positive cells in the EGFP-gated population were measured. The percentage of BrdU-APC positive cells was determined by setting a gate (M1) on cells with higher fluorescence intensities relative to the negative control, in which the cells were not labeled with BrdU before the addition of the anti-BrdU-APC monoclonal antibody. The percentage of incorporation of BrdU into newly synthesized DNA by cells entering and progressing through the S (DNA synthesis) phase of the cell cycle was calculated for each population. The correlation between fluorescence intensities and BrdU incorporation was also determined.

4.7. siRNA transfection

Inhibition of the *Homo sapiens v-akt murine thymoma viral oncogene homolog 1* (Akt1; NM_005163.1) gene expression was achieved by the use of double stranded RNA, known as "AKT1 Validated Stealth™ RNAi DuoPak" (Invitrogen™). They consist of two non-overlapping duplexes per gene, consistent with the guidelines for publication –quality data.

4.7.1. Control and optimization of RNAi transfection conditions

Jurkat-SHIP cells (clone no. 51) were seeded at a density of $2.5x10^5$ cells/ml and grown for 48 h, induced or not with Doxycycline. The cells were electroporated with the Block-iT™ Fluorescent Oligo for Electroporation, according to the basic protocol from the manufacturer for *Delivering Stealth™ RNAi or siRNA to Jurkat Cells by electroporation* (Invitrogen™). In the optimization procedure were tested some different parameters, such as Fluorescent Oligo concentration, electroporation conditions, transfection solutions and incubation times before fluorescence microscopy and FACS analyses. After 24 h, the cells were analyzed by inverse fluorescence microscopy, in order to assess the oligo uptake and its stabilization. The signal from the *Block-iT™ Fluorescent Oligo for Electroporation* was detected by the use of a standard FITC filter set. The cells were grown for additional 24h, washed and harvested for FACS analysis, as described in section 4.5.4, in order to quantify the efficiency of transfection with the different parameters used in the optimization of transfection of Jurkat-SHIP cells (clone no. 51) with the *Block-iT™ Fluorescent Oligo for Electroporation*. Furthermore, the stabilization of the Oligo 48h post-transfection was evaluated.

4.7.2. Silencing of *Akt1* expression by RNAi and data analyses

Jurkat-SHIP cells (clone no. 51) were grown as described previously. $4x10^6$ cells were resuspended in 200 µl of sterile phosphate-buffered sucrose (PB-Sucrose) (prepared with endotoxin-free stock solutions). The cells were added to 0.4 cm Cuvettes (Bio-Rad) and transfected by electroporation with the *Block-iT™ Fluorescent Oligo for Electroporation* ([Fluor. Oligo]= 25 µM) or Validated Stealth™ RNAi Duplexes against *Akt1,* at the same concentration, respectively. The parameters set in the optimization procedures (330 V / 960 µF) were used for the electroporation. The corresponding negative controls were included. The cells were grown for additionally 24h in non-tissue culture 6-well plates before FACS analysis. The efficiency of transfection was determined by measuring the fluorescence intensity of the positive transfected population of cells, as described in section 4.5.4. After determination of efficiency of transfection, cell lysates were prepared for western blotting analyses, in order to verify the silencing of Akt1 expression by Validated Stealth™ RNAi Duplexes, relative to the controls, and relative to MAPK. The levels of KLF2 protein expression were also measured, and relative protein expression was quantified by comparison to MAPK expression, for Akt1 and KLF2 .

4.8. Transcriptional analyses

4.8.1. RNA Preparation

Total RNA was isolated from Jurkat cells by using Guanidine thiocyanate lysis and ultracentrifugation in CsCl (cesium chloride) density gradients, according to modifications to the protocol reported by Chirgwin *et al.* (1979). The solutions were prepared in 0.1% DEPC-treated water, if suitable. $5x10^7$-$1x10^8$ cells from each sample were collected in a new 50 ml-tube (820 *g*, 7 min, 4°C). The supernatants were discarded and the tubes were put upside down on a paper, in order to remove the residual solution from the wall inside the tube. 7 ml of fresh and cold GCN-Solution (4M Guanidine thiocyanate, 25 mM sodium citrate pH 7.0, 0.5% N-Lauroylsarcosine, 100 mM β-mercaptoethanol), were added and immediately vortexed, followed by freezing of the lysates at –20°C. After thawing the lysates on ice, the DNA was shorn by vortexing for 3 min.

Each preparation was added in SW-40 tubes (Beckman) pre-washed with cold GCN-solution. 3.5 ml of 5.7 M CsCl-Solution was added to each tube. The samples were centrifuged using a Beckman L-60 ultracentrifuge (rotor SW40 Ti) at 180,000 *g* for 20 h at 20 °C. After ultracentrifugation, the supernatants were carefully discarded. The RNA pellets were resuspended in 1000 µl of DEPC-treated water, pre-warmed at 65°C, and transferred to a new tube. 1 volume of Phenol/Chloroform/Isoamylalcohol (25:24:1) was added to each sample, followed by vortexing (10 sec) and harvesting by centrifugation (4100 g, 5 min, room Temperature). The aqueous phase from each sample was transferred to a 10 ml tube, and precipitated with 2.5 volumes of absolute Ethanol and 1/10 volume of 2 M sodium acetate (pH 5.5) (o/n, -20°C). The samples were transferred to 2 ml Eppendorf tubes and recovered by centrifugation for 30 min, at 4°C in a Eppendorf microcentrifuge (14,000 *g*). The supernatants were discarded, and the pellets were dried 10-20 minutes in a lyophilizer. The samples were resuspended in pre-warmed DEPC-treated water, and incubated 10 min at 65°C in a water bath, followed by precipitation with 1/10 volume of 2 M sodium acetate (pH 5.5), 2.5 volumes of absolute Ethanol and storage at -20°C. To determine the RNA concentrations, 25 µl of each sample were transferred to a new tube, centrifuged at 14,000 *g* for 30 min at 4°C, dried as described previously and resuspended in 100-µl of 0.1% DEPC-treated water. Measurements of the optic densities and purity were performed in a BioPhotometer (Eppendorf), and the concentrations were calculated. For further analyses, aliquots of the samples stored at –20°C were collected as described before, and resuspended in appropriate volumes of DEPC-treated water.

4.8.2. Microarray analysis

As an initial screening, oligonucleotide arrays (Affymetrix, U133A and B) were used for expression analysis according to the manufacturer's protocol (Affymetrix, Santa Clara, CA, USA). Concisely: Jurkat-SHIP cells (clone no. 51) were treated either with or without 0.8 µg/ml doxycycline for 82 h and total RNA was prepared by the guanidinium thiocyanate method, as described previously. 15 µg of each RNA sample were used to synthesize cDNAs, which were further used as templates to prepare biotinylated RNAs by *in vitro* transcription according to the protocol of the manufacturer (Affymetrix), and in collaboration with Dr. T. Streichert, from Institute of Clinical Chemistry, UKE, Hamburg. The human U133A and U133B microarrays containing 39,000 transcripts corresponding to approximately 33,000 genes and ESTs in 45,000 probe sets from Affymetrix were hybridized with the biotinylated

RNA probes for 16 h at 45°C, washed and stained using the Affymetrix Fluidics Station according to the GeneChip Expression Analysis Technical Manual. Microarrays were scanned with the Hewlett-Packard-Agilent GeneChip scanner, and the signals were processed using the GeneChip expression analysis algorithm (v.2; Affymetrix). To compare samples and experiments, the trimmed mean signal of each array was scaled to a target intensity of 100 (A-Array) and 80 (B-Array). Absolute and comparison analyses were performed with Affymetrix MAS 5.0 and DMT software using default parameters.

To assist in the identification of genes that were positively or negatively regulated in the experiment, genes that were at least two-fold increased or decreased significantly after the expression of SHIP ($p< 0.05$) were selected. To overcome the limitations of a single microarray analysis, biological independent replicates ($n\geq2$) were further analyzed using quantitative real-time polymerase chain reaction (RT-PCR) (see 4.7.5).

4.8.3. cDNA Synthesis

Total RNA was used for first-strand cDNA synthesis with SuperScript II Reverse Transcriptase for RT-PCR and Oligo-(dT)12-18 primer (Invitrogen), following the instructions of the manufacturer. The total RNA (3 µg), resuspended in 11 µl of DEPC-treated water, was incubated with 1 µl of Oligo-(dT)12-18 (500 µg/ml) 10 min at 70°C, and quick chilled on ice. The contents of the tube were collected by brief centrifugation, and 4 µl of 5X First Strand Buffer (Invitrogen), 2 µl of 0.1 M DTT, 1 µl of 10 mM dNTP Mix (10 mM each dATP, dGTP, dCTP and dTTP at neutral pH) were added. The preparation was incubated at 42°C for 2 min and 200 Units of SuperScript II were added, followed by 50 min incubation at 42°C. The reaction was inactivated by incubation at 70°C for 15 min. The RNA complementary to the cDNA was removed by incubation with 2 Units of *E. coli* RNase H (Invitrogen) at 37°C for 20 min. The cDNAs were stored at –20°C for further analyses.

4.8.4. Conventional PCR

2 µl of a five-fold dilution of each cDNA were used for conventional PCR reactions, in order to verify purity of the RNA isolated, efficiency of the cDNA synthesis, and specificity of the primers designed for quantitative real-time RT-PCR. PCR reactions were performed using 2 µl of the diluted cDNA in a 20 µl reaction containing 1X PCR buffer (Qiagen), 4 mM $MgCl_2$, 0.2 mM dNTP Mix (Invitrogen), 1 Unit of *Taq* Polymerase from QIAGEN, 0.5 µM of each

primer (forward and reverse). Alternatively, the PCR reactions were performed using 1X PCR buffer (Invitrogen), and 2 Units of the *Taq* Recombinant Polymerase (Invitrogen). PCR reactions to analyze purity of RNA by use of primers specific for the exons 7 and 8 of the regulatory subunit of the *PI3K* gene sequence, and amplification of the β-actin house keeping gene sequence, were carried out in 0.5 ml microcentrifuge tubes using a Mastercycler® gradient, model 5331 (Eppendorf, Hamburg). Primers used were (5' to 3'): β-actin (forward): ACCTCTATGCCAACACAGTGC, β-actin (reverse): CTCATCGTACTCCTGCTTGC, *PI3K(p85)(*exon7) (forward): CATGAATTCGAGAAGACATGGAATGTTGGAAGCAGC, *PI3K(p85)(*exon 8) (reverse): TGTGAATTCCAAGGGAGGTGTGTTGGTAATGTAGC. The program consists of a 2 min initial denaturation at 95°C, followed by thirty cycles of 1 min denaturation at 95°C, 1 min annealing at 55°C, 1 min 30 sec elongation at 72°C. After 5 min of final elongation at 72°C, the reactions were hold at 4°C. The amplification products were electrophoresed in agarose gels, using 1X Tris-Borate (TBE) buffer (89 mM Tris-borate, 89 mM boric acid, 2 mM EDTA) as gel and tank buffer. The amplified products were stained with EtBr and visualized by the use of a UV detection system. PCR reactions were carried out as described before, in order to verify the specificity of the primers designed for quantitative real-time RT-PCR and standardize the reaction conditions. The basic programs consists of a 10 min initial denaturation at 95°C, followed by 55 cycles of 15 sec denaturation at 95°C, 5 sec annealing at different Temperatures (in order to standardize), 20 sec elongation at 72°C. Additional steps consists of 1 sec at 95°C, followed by 15 sec at 65°C, 1 sec at 95°C, 30 sec at 40°C, and finally the reactions were hold at 4°C. The amplification products were electrophoresed in agarose gels and visualized by staining with EtBr and using a UV detection system. Once the specificity of the primers was verified, the quantitative real-time RT-PCR analyses for each target sequence were performed.

4.8.5. Quantitative real-time RT-PCR and data analyses

Total RNA was isolated from Jurkat-SHIP cells (clone no. 51) treated with or without 0.8 µg/ml doxycycline for 72 h, corresponding to biological independent replicates ($n \geq 2$). The cDNA was prepared by reverse transcription of 3 µg total RNA as described previously (4.7.3). Once the representative mRNA sequence for each gene was selected by searching in data banks, specific forward and reverse primers used for real-time PCR were designed using the Primer 3 Software (v. 0.2) from the Whitehead Institute for Biomedical Research (http://frodo.wi.mit.edu/cgi-bin/primer3/primer3_www.cgi), and one human Mispriming

library. All the primers were designed based on the corresponding human mRNA sequences. For further details about primer design and the sequences corresponding to the genes analyzed see section (5.3.1). The specificity in the amplification was verified and standardized for each pair of primers by conventional PCR. LightCycler quantitative real-time RT-PCR reactions and data analysis were performed on a LightCycler system, Version 3.5 and LightCycler detection software, according to the instructions of the manufacturer (Roche, Mannheim, Germany). RNAs from at least two independent experiments were used for quantitative real-time RT-PCR. All samples were run in duplicate in glass capillaries. The samples were analyzed at least two times in a LightCycler by using 2 µl cDNA (1:5 diluted) or no-template negative control, 2 µl of LightCycler-FastStart DNA Master SYBR Green I, 0.5 µM specific primers, 4 mM Mg^{2+} in a final volume of 20 µl. Cycling conditions included one cycle of 95°C for 10 min, followed by 45 cycles, consisting of denaturation by heating to 95°C, annealing for 5 seconds at the corresponding standardized temperature for each pair of primers (Table VI), and elongation for 20 seconds at 72°C. Then, the melting curve program was performed by a denaturing step from 65°C to 95°C, in order to determine product specificity. After the final cycle, the capillaries were cooled for 30 s at 40°C. Fluorescence curves were analyzed with the LC software (Version 3.5.). The calculation of crossing points was automatically done by the second derivative maximum method of the LC software. The PCR efficiency (*E*) of each primer for each individual sample and its respective duplicate was determined by linear regression analysis from the raw quantitative real-time RT-PCR data, using the LinRegPCR program (Ramakers *et al,* 2003). Only the efficiencies of each PCR amplification for each gene-specific product that were similar among them ($E \geq 1.5$, SD $\leq$ 0.05) and additionally similar to that for the housekeeping gene *GAPDH* ($E \geq 1.5$, SD ≤ 0.05) were chosen for further analyses, setting the best fitting line through 4-6 points, $R \geq 0.999$). The $2^{-\Delta\Delta C}{}_T$ method (Livak and Schmittgen, 2001) was used to analyze the relative changes in gene expression from the quantitative real-time RT-PCR experiments. For the $\Delta\Delta C_T$ calculation to be valid, the amplification efficiencies of the target and reference must be approximately equal (Livak and Schmittgen, 2001). Using the $2^{-\Delta\Delta C}{}_T$ method, the data are presented as the fold change in gene expression normalized to an endogenous reference gene and relative to the untreated control (Livak and Schmittgen, 2001). The relative amounts of all mRNAs analyzed in this study with induction of SHIP expression were calculated after normalization to *GAPDH* and expressed as fold changes, relative to the untreated control, without induction. For analyses of transcriptional expression of *Akt1*, the same procedure was performed.

4.9. Protein biochemical analyses

4.9.1. Preparation of cell lysates

Cells grown in the conditions specified en each case were harvested by centrifugation, and cell lysates were prepared for protein analyses in ice-cold Nonidet® P40 (NP40)-containing lysis buffer, as described previously (Jücker *et al,* 1997). The buffer contains 50 mM HEPES (pH 7.5), 150 mM NaCl, 1% (v/v) NP40, 2 mM EDTA, 10% (v/v) glycerol, 50 mM NaF, 10 mM sodium pyrophosphate, 1 mM sodium orthovanadate and 2% (v/v) Trasylol®. The lysates were transferred to 1.5 ml microcentrifuge tubes and centrifuged at 14,000 *g* for 10 min at 4°C, in a cold room. The supernatants were transferred to cryotubes. 10 µl aliquots were transferred to 0.5 ml microcentrifuge tubes and stored at -20°C for protein quantification. The cell lysates were frozen in liquid nitrogen and stored at –80°C. The protein concentrations of the extracts were measured by the use of the *DC* (detergent compatible)-Protein assays system (Bio-Rad), according to the recommendations of the manufacturer.

4.9.2. Western blotting and protein quantification analyses

Western blot analyses for protein expression after restoration of SHIP expression in Jurkat T cells were performed as described previously (Horn *et al*., 2004). Total cell lysates were analyzed by sodium dodecyl sulfate (SDS) polyacrylamide gel electrophoresis (PAGE), by loading equal amounts of protein lysates (100 µg total protein) in each lane. Protein electrophoreses were carried out in 8.5% polyacrylamide gels. Alternatively, and for protein expression analyses after inhibition of PI3K with wortmannin and silencing of the expression of Akt1 by RNAi, the cell lysates were analyzed by 4-12% Bis-Tris gradient mini-gels (Invitrogen), using the NuPAGE® Novex Bis-Tris Gels (Invitrogen), with the XCell *SureLock*™ Mini-Cell (Invitrogen), according to the instructions of the manufacturer. This system offers the advantage of loading low amounts of protein samples, providing a high resolution in the electrophoresis and subsequently high intensities in the signal measurements.

After electrophoresis, the proteins were transferred to 0.45 µm nitrocellulose membranes (Protran® BA 45, Schleicher & Schuell, Dassel), using the transfer Trans-Blot™-Cell system (Bio-Rad), following the instructions of the provider. As control of the transfer, the gels were stained subsequently using the SimplyBlue™ Safe Stain (Invitrogen). Duplicate membranes

were blocked, cut and incubated with either antibodies specific for SHIP (SHIP, P1C1, Santa Cruz Biotechnology, Heidelberg, Germany), Akt phosphorylated at serine residue 473 (Ser473, 587F11, mouse monoclonal antibody; Cell Signaling Technology, Beverly, MA, USA) or KLF2 (N-13, Santa Cruz Biotechnology, Heidelberg, Germany), followed by incubation with GAPDH antibodies (6C5, Santa Cruz Biotechnology, Heidelberg, Germany), or MAPK antibodies (K-23, Santa Cruz Biotechnology, Heidelberg, Germany). The phosphorylation on GSK-3β at serine 9 was analyzed with specific antibodies (Ser^9, #9336) (Cell Signaling Technology, Beverly, MA, USA). The western blot analyses of expression of Akt1 after silencing with RNAi, and expression of KLF2 were performed by incubation of duplicate membranes with antibodies specific for Akt1 (B-1, sc-5298, mouse monoclonal IgG1, Santa Cruz Biotechnology, Heidelberg, Germany) and KLF2, followed by incubation with the MAPK antibodies (K-23, Santa Cruz Biotechnology, Heidelberg, Germany). Signals were detected by incubation of the membranes with HRP-conjugated secondary antibodies (Santa Cruz Biotechnologies), followed by chemiluminescent detection, using the ECL™ detection system (Amersham Biosciences), according to the instructions of the manufacturer. The chemiluminescence signals were measured with an LAS3000 Imager (Raytest/Fuji, Straubenhardt, Germany), and the protein quantification was performed by the use of the AIDA software (Raytest/Fuji). Protein expression and phosphorylation values were calculated by relative quantification to GAPDH and MAPK expressions. If necessary, the membranes were stripped later by incubation at 70°C in a buffer containing 62.5 mM Tris-HCl (pH 6.7), 2% (w/v) SDS and 100 mM β-mercaptoethanol, in order to remove the antibodies and reuse the membrane with new antibodies.

5. Results

5.1. The human leukemia cell line Jurkat as model system for SHIP expression profiles

The first objective of this study was the identification of differentially regulated genes after the expression of the inositol-5-phosphatase SHIP-1 (SHIP) in hematopoietic cells, specifically leukemia cells. In addition, the elucidation of signal transduction pathways involved was considered. For that purpose, the human leukemia T cell line Jurkat, carrying a Doxycycline inducible *SHIP* expression vector was used as model system (referred also as Jurkat-SHIP cells (clone no. 51)). It has been shown that SHIP is a negative regulator of the constituvely activated PI3K/Akt pathway in the human Jurkat-T cell clone SHIP no.51 (Horn, 2003), causing a reduction of proliferation. The inducible expression system Jurkat Tet-On, carrying the reverse Transactivator (rtTA) (Clontech, Palo Alto, CA, USA), was used to express the SHIP gene. Before induction, there is almost no SHIP protein detectable, similar to the phenotype of Jurkat T-cells. After addition of Doxycycline (Dox) to the culture media, the expression of the SHIP gene was induced, which has been confirmed by western blot analysis (Figure 9). In addition, downstream signaling of the PI3K/Akt pathway was inhibited, as demonstrated by the reduction of phosphorylation of Akt at serine residue 473 (Figure 9). Two independent experiments were carried out at different time-points. Figure 9 shows the inducible expression of SHIP after addition of Doxycycline in Jurkat-SHIP cells (clone no. 51). SHIP is highly expressed, in comparison to the controls without induction (-Dox). Additionally, the effect on the reduction of phosphorylation of Akt at residue serine 473 after the expression of SHIP was reproducible. The verification by western blotting analysis was performed on every occasion.

5.1.1. Inhibitory effects of SHIP on the PI3K/Akt signaling pathway downstream of Akt in Jurkat T cells

It is known that the protein *glycogen synthase kinase-3 beta* (GSK3β) is downstream of Akt in the PI3K/Akt pathway. It has been demonstrated that the phosphorylation of GSK3β at residue serine 9 is reduced after the restoration of SHIP, as a consequence of the reduction in the phosphorylation of AKT at residues Thr 308 and Ser 473. GSK3β is not phosphorylated at

residue Ser 9, and becomes active, p27Kip1 is more stable, and the phosphorylation of Rb is reduced (Horn, 2003). Consequently, there is prolongation of the G1 phase of the cell cycle and reduction of proliferation.

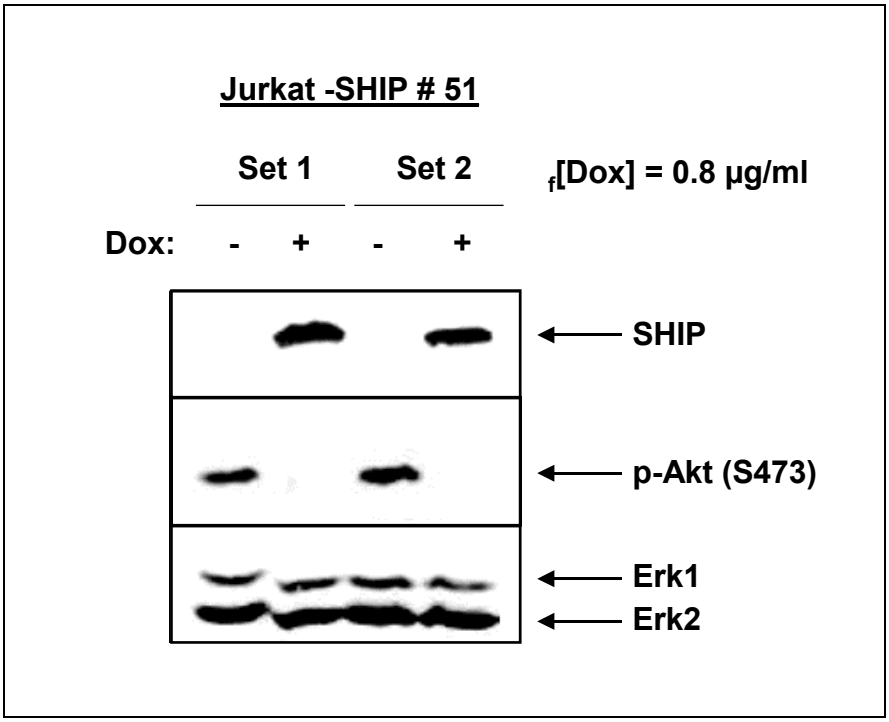

Figure 9. Western Blot Analysis of the expression of SHIP and phosphorylation of Akt (S473) in Jurkat-SHIP cells.

Cell lysates from Jurkat-SHIP cells (clone no.51) were prepared in NP40 Buffer, corresponding to two independent experiments: Set 1 and 2, after 72h and 82h induction with Doxycycline (Dox), respectively. Cell lysates containing 100 µg of protein were separated in SDS-polyacrylamide gels and western blot analyses were performed with antibodies specific for SHIP, phosphorylated Akt (serine residue 473) and MAPK (Erk1 and Erk2). The signals obtained with the antibodies specific for MAPK showed the comparable loaded protein quantities. $_f$[Dox]: final concentration of Doxycycline.

Two independent experiments were carried out to verify the effect of SHIP on the PI3K/Akt signaling pathway downstream of Akt in Jurkat T-cells, as described in 5.1. Figure 10 shows with one representative experiment the inducible expression of SHIP after addition of Doxycycline in Jurkat-SHIP cells (clone no. 51). SHIP is highly expressed, in comparison to the controls without induction (-Dox). Additionally, the effect on the reduction of both phosphorylation of Akt at residue serine 473 and GSK3β at residue Serine 9 after the expression of SHIP was reproducible. After verification of the inducible system and the signal

transduction pathway, the identification of genes that were regulated after the induction of expression of SHIP was carried out by microarray analysis.

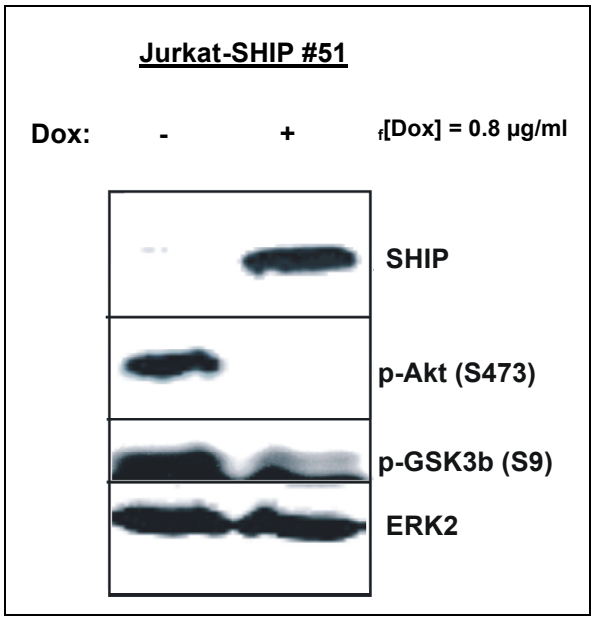

Figure 10. Western Blot Analyses of the expression of SHIP, phosphorylation of Akt (S473) and GSK3β in Jurkat-SHIP cells.

Cell lysates from Jurkat-SHIP cells (clone no. 51) were prepared in NP40 Buffer, as described in Fig. 9. Cell lysates containing 100 µg of protein were separated in SDS-polyacrylamide gels and western blot analyses were performed with antibodies specific for SHIP, phosphorylated Akt (serine residue 473), phosphorylated GSK3β (serine residue 9) and MAPK (Erk1 and Erk2). The signals obtained with the antibodies specific for ERK2 showed the comparable loaded protein quantities. Dox: Doxycycline. Akt: Protein kinase B. GSK3β: glycogen synthase kinase-3 beta.

5.2. Microarray analysis revealed the presence of 37 differentially SHIP-regulated mRNAs in Jurkat T cells.

The mRNAs from Jurkat-SHIP cells (clone no. 51) with or without induction of SHIP expression were used to perform the Microarray analysis. The DNA-Microarrays ***Human Genome U133*** (HG-U133A und HG-U133B) from the company Affymetrix (Santa Clara, CA, USA) were used to perform an initial screening for expression analysis, according to the manufacturer's protocol. The advantage of this technology is the performance of a global view of gene expression in one specific system. The human Chip U133A and Chip U133B sets contain together about 1,000,000 oligonucleotides, which correspond to about 39,000

transcripts that together represent approximately 33,000 genes and expressed sequence tags (ESTs) in 45,000 probe sets from Affymetrix. The probe pairs synthesized on GeneChip® Expression Analysis arrays are all *a priori* selected based on sequence information derived from public sequence databases available at the time of the array design (Affymetrix). For each probe set Identity (ID) there are 11 oligonucleotides that perfect match and 11 that mismatch, as they contain one mutated nucleotide in the sequence. The microarray experiments were carried out to identify differentially expressed genes in Jurkat-SHIP cells (clone no. 51) after induction (+Dox) or before induction (-Dox) of the expression of SHIP, respectively. The signals were processed using the GeneChip® Expression Analysis algorithm (v.2; Affymetrix) at the Institute of Clinical Chemistry, University Hospital Hamburg-Eppendorf, in collaboration with Dr. Thomas Streichert. The use of the Microarray human U133 sets allowed the screening from the human genes in the leukemic cell line that identified differentially expressed genes after the restoration of SHIP.

Double-stranded cDNAs were synthesized from total RNA isolated from Jurkat-SHIP cells (clone no. 51) with and without induction of expression of SHIP. An *in vitro* transcription (IVT) reaction was then done to produce biotin-labeled cRNAs. The cRNAs were fragmented (ca. 100 bp) before hybridization to the probe arrays and their quality was verified by carrying out a Test-DNA-Microarray (Affymetrix®) (data not shown). The cRNAs hybridized to their complementary oligonucleotides present in each array, U133A or U133B, respectively. After washing and incubation with streptavidin phycoerythrin conjugate, the fluorescent signals corresponding to the cRNAs that hybridized to their complementary oligonucleotides on each array were processed using the GeneChip® Expression Analysis algorithm (v.2; Affymetrix). To compare samples and experiments, the trimmed mean signal of each array was scaled to a target intensity of 100 (A-Array) and 80 (B-Array). Absolute and comparison analyses were performed with Affymetrix MAS 5.0 (v.2; Affymetrix) and DMT software using default parameters. The raw data from the Chips A and B contained values corresponding to the analysis of 22,283 and 22,645 probe set IDs, respectively, which assembles 44,928 probe set IDs in total (data not shown).

Figure 11 shows representative images obtained from two probe set ID array analysis. Comparisons between perfect match (PM) and mismatch (MM) intensity levels for each probe set confirmed the present calls (P) or the absent calls (A) for a specific target.

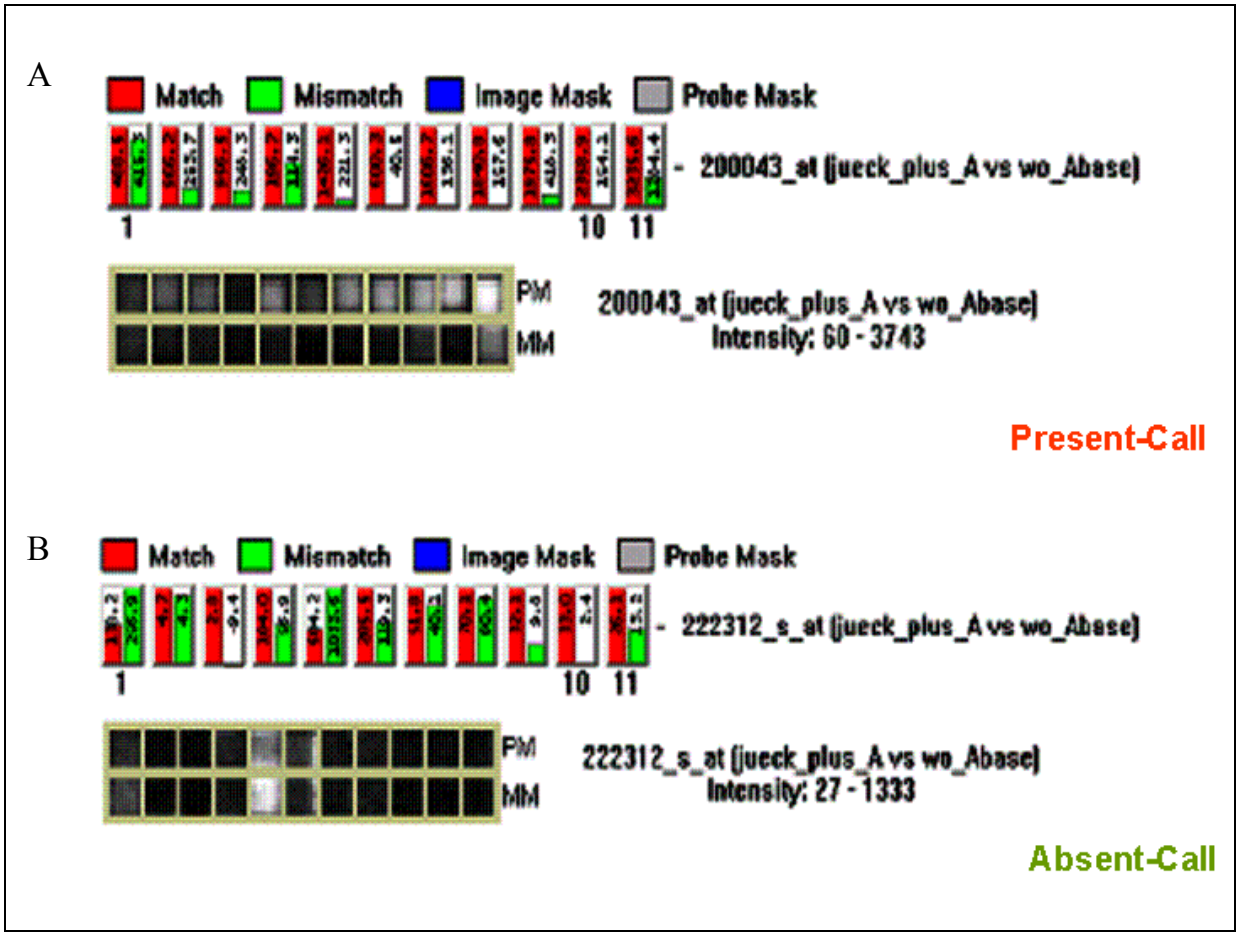

Figure 11. Intensity patterns for each probe pair in the Array Analysis of Jurkat-SHIP cells.

Two representative arrays corresponding to Present-Call and Absent-Call showed the intensity patterns from each probe pair of the eleven designs for a single probe set identity. The Array analyses were performed by comparison of the results obtained on Chip U133A (_A) with induction of the expression of SHIP (plus) versus the base lane without induction (wo). A) Present call, determined for the probe set identity 200043_at. The Perfect Match (PM) intensity values are larger than the Mismatch (MM) intensity values. B) Absent Call, determined for the probe set identity 222312_s_at. As the intensity of the MM increases, the ability to discriminate between the PM and MM decreases.

Microarray analysis of the probe sets that exceeded the probe pair threshold and are not called "No Call" was performed. The data revealed a total of 15,704 probe sets identified as "present" in Jurkat-SHIP cells (clone no.51), which represents a 35.0% of the total population analyzed in the human Chip Arrays HG-U133A and B (data nor shown). Similarly, 28,441 probe sets were identified as "absent", and 783 probe sets were identified as "marginal", representing 63.3% and 1.7% of the population analyzed in Chip Arrays HG-U133A and B, respectively (data not shown).

After evaluation of significant differences in expression, the analysis revealed the presence of 180 and 11 probe set IDs in the experiment arrays from Chip A and B that were increased with the expression of SHIP (+Dox), in comparison to the basal array, without expression of SHIP (-Dox), on the basis of the lowest *p*-values (Table II). Similarly, the analysis showed the presence of 183 and 157 probe set IDs that were decreased on Chip A and B, after the expression of SHIP, respectively (Table II). The differentially expressed probe set IDs represent together 0.4% (191 out of 44,928) significantly increased and 0.8% (340 out of 44,928) significantly decreased probe set IDs from the total probe set IDs analyzed. Thus, the microarray analysis of differential expression in Jurkat-SHIP cells (clone no. 51) shown the presence of 531 probe set IDs that were significantly regulated, representing 1.2% of the total population studied.

Table II. Number of Affymetrix Probe Set Identities differentially expressed in Jurkat-SHIP cells after the restoration of SHIP, identified by analysis on U133 microarrays.

Number of probe set IDs significantly increased or decreased after the expression of SHIP (experiment array), compared to untreated controls (baseline array) following doxycycline treatment for 82 h. The probe set IDs significantly regulated at least 2-fold were chosen for further analyses.

Increased				
	Number of probe set IDs	N° of probe set IDs (Fold change ≥ 2)	N° of unique mRNAs (Fold change ≥ 2)	Percentage in the sub-population (Fold change ≥ 2)
Chip A	180	13		
Chip B	11	3		
	191	**16**	**16**	**43%**
Decreased				
	Number of probe set IDs	N° of probe set IDs (Fold change ≥ 2)	N° of unique mRNAs (Fold change ≥ 2)	Percentage in the sub-population (Fold change ≥ 2)
Chip A	183	8		
Chip B	157	16		
	340	**24**	**21**	**57%**
Total	***531***	***40***	***37***	***100%***

Genes that were at least two-fold increased or decreased in their expression after the restoration of SHIP were further analyzed, and only the values that were statistically significant ($P<0.05$) were included. To overcome the limitations of a single microarray

analysis, independent replicates (n ≥2) were analyzed using quantitative real-time RT-PCR (see Section 5.3).

The analysis revealed the presence of 41 probe set IDs out of 44,928 that were at least two-fold statistically significant regulated (0.1%). That represents 7.7% from the probe set IDs identified as regulated (41/531). The data were grouped according to the fold change values from high to low, obtained from the both human probe arrays HG_U133A and HG_U133B. After analysis of the targets using different platforms, including NetAffx™ (Affymetrix), HUGO, UniGene (NCBI), BLAST (NCBI), GeneTide V0.6, GeneCards®, the genes or ESTs that correspond to the transcripts identified were recognized and confirmed (if the information was available). Microarray analysis verified the induction of transcription of the *SHIP* gene cloned in Jurkat cells, expressed from the retroviral vector, since further experiments confirmed that the endogenous *SHIP* mRNA expression is not regulated in Jurkat-SHIP cells (see 5.3.3). Accordingly, microarray analysis allowed the identification of 40 probe set IDs significantly SHIP-regulated (≥ 2-fold) in Jurkat cells. Of these, 16 were SHIP-induced (13 on Chip A and 3 on Chip B, respectively) (40%) and 24 were SHIP-repressed (8 on Chip A and 16 on Chip B, respectively) (60%). Detailed information about the signals and fold changes obtained by microarray analysis from the 16 SHIP-induced and 24 SHIP-repressed probe set IDs (in addition of *SHIP* itself), are shown on Tables III and IV, respectively.

The 40 SHIP-regulated probe set IDs identified by microarray analysis represented together 37 known genes, ESTs and sequences that code for hypothetical proteins, since some of the transcripts match to the same reported gene. In Table IV was shown that the *PAG* gene was represented by two probe set IDs on Chip B, and both were at least two-fold repressed. Similarly, the *ATF* gene was represented by two independent probe set IDs on Chip A, and were equally repressed. Finally, two probe set IDs with the same fold-change for differential expression corresponding to the sequence that codes for the hypothetical protein LOC284801 on Chip B were found. These results provided to a certain extent a good quality control check. Thus, of the 37 unique, significantly SHIP-regulated transcripts, 16 genes, ESTs and sequences that coded for hypothetical proteins were induced (43%) and 21 repressed (57 %) after SHIP expression in Jurkat cells (clone no. 51). In Tables II, III and IV the results obtained after analysis of the Microarray data after the restoration of SHIP expression in Jurkat-SHIP cells (clone no. 51) are shown.

Table III. Probe sets induced (≥ 2.0-fold) identified on U133 microarrays after the expression of SHIP in Jurkat-SHIP cells [a].

Affymetrix Probe Set ID [b]	Gene Symbol [*Homo sapiens*]	Title [*Homo sapiens*]	RefSeq Transcript ID (GenBank Source)	Signal (-/+ Dox) [c]	Fold change (+/- Dox)
203331_s_at HG-U133A	*SHIP1* [e]	SH2 containing inositol 5'-phosphatase	U57650.1	5.7A-118.4P [e]	18.4 [e]
241674_s_at HG-U133B	*AI820854* [d]	AI820854 (Homo sapiens transcribed sequences), cDNA Clone ID: IMAGE:1983167	AI820854 (Resource:dbEST); (GenBank Acc.)	1.2A-14.4P	10.6
220149_at HG-U133A	*FLJ22671*	Hypothetical protein FLJ22671	NM_024861.1 (predicted)	3.7A-32.6P	6.1
220460_at HG-U133A	*SLC01C1*	Solute carrier organic anion transporter family, member 1C1	AF260704.1/ NM_017435.2 (provisional)	3.4A-22.8P	6.1
234136_at HG-U133B	*VPS54*	Vacuolar protein sorting 54 (yeast)	AK023632.1	9.2A-39.9P	4.6
209419_at HG-U133A	*C22ORF19*	Chromosome 22 open reading frame 19/ Fmip, PK1.3, KIAA0983	AB023200.1 (provisional)	5.1A-12.0P	3.3
219371_s_at HG-U133A	*KLF2*	Krüppel-like factor 2 (lung)	NM_016270.1	102.0P-321.3P	3.0
214942_at HG-U133A	*KIAA0117*	KIAA0117 protein	D38491.1 (partial cds)	9.1A-32.8P	2.8
204563_at HG-U133A	*SELL/CD62L*	Selectin L, lymphocyte adhesion molecule 1/ CD62 antigen ligand	NM_000655.2	70.6P-195.0P	2.6
214439_x_at HG-U133A	*BIN1*	Bridging integrator 1	AF068917.1	33.3A-110.1P	2.3

Affymetrix Probe Set ID [b]	Gene Symbol [*Homo sapiens*]	Title [*Homo sapiens*]	RefSeq Transcript ID (GenBank Source)	Signal (-/+ Dox) [c]	Fold change (+/- Dox)
218600_at_HG-U133A	*MGC10986*	Hypothetical protein MGC10986	NM_030576.2	19.9P-56.5P	2.3
237329_at_HG-U133B	*LOC389100*	Hypothetical LOC389100 (*Homo sapiens transcribed sequences*)	XM_374035.1 (predicted)/ AW102716 (EST)	27.1A-58.6P	2.1
209738_x_at_HG-U133A	*PSG6*	Pregnancy specific beta-1-glycoprotein 6	NM_002782.3	17.4A-39.9P	2.1
220729_at_HG-U133A	*RBM15*	RNA binding motif protein 15	NM_022768.4	9.8A-16.7P	2.0
220167_s_at_HG-U133A	*TP53TG3*	TP53TG3 protein	NM_015369.1	31.1A-62.0P	2.0
216437_at_HG-U133A	*EPC1*	Enhancer of polycomb homolog 1	NM_025209.2	16.4P-21.4P	2.0
205949_at_HG-U133A	*CA1*	Carbonic anhydrase I	NM_001738.1	13.6A-34.2P	2.0

[a] Induced transcripts (≥ 2.0-fold) compared to untreated controls following doxycycline treatment for 82 h.
[b] Affymetrix GeneChip Human Genome U133 Array Set HG-U133A and HG-U133B Targets. ID: Identity.
[c] A: Absent; P: Present.
[d] No gene annotations available for this transcript; no mRNA sequences currently available (GenBank Source). Original annotation of the probe set, as provided by Affymetrix (Annotation quality (GeneAnnot) (http://genecards.weizmann.ac.il/geneannot/).
[e] Positive control. Increased expression of *SHIP* from the inducible expression vector. The endogenous *SHIP* expression did not change after the ectopic expression of SHIP from the vector. (see 5.3.3)

Table IV. Probe sets repressed (≥ 2.0-fold) identified on U133 microarrays after the expression of SHIP in Jurkat-SHIP cells [a].

Affymetrix Probe Set ID [b]	Gene Symbol [*Homo sapiens*]	Title [*Homo sapiens*]	RefSeq Transcript ID (GenBank Source)	Signal (-/+ Dox) [c]	Fold change (+/- Dox)
238525_at_HG-U133B	*DDX56*	DEAD (Asp-Glu-Ala-Asp) box polypeptide 56	NM_019082.1	125.3P-11.9A	-9.9
225626_at_HG-U133B	*PAG*	Phosphoprotein associated with glycosphingolipid-enriched microdomains	NM_018440	98.4P-7.4A	-5.3
230265_at_HG-U133B	*SEL1L*	Sel-1 suppressor of lin-12-like *(C. elegans)*	NM_005065.3	62.1P-9.3A	-4.9
218145_at_HG-U133A	*TRIB3*	Tribbles homolog 3 (*Drosophila*)	AY247738.1	1270.7P-344.8P	-3.7
204999_s_at_HG-U133A	*ATF5*	Activating transcription factor 5	NM_012068	147.7P-51.5P	-3.7
224797_at_HG-U133B	*ARRDC3*	Arresting domain containing 3	NM_020801	40.0P-19.6A	-3.5
237745_at_HG-U133B	*TSC22*	Transforming growth factor-beta-stimulated protein TSC22	NM_006022.2	51.6P-17.6A	-3.3
202843_at_HG-U133A	*DNAJB9*	DnaJ (Hsp40) homolog, subfamily B, member 9	NM_012328 (provisional)	22.6P-6.2A	-3.3
204998_s_at_HG-U133A	*ATF5*	Activating transcription factor 5	NM_012068	235.3P-103.8P	-3.0
242887_at_HG-U133B	*KCMF1*	Potassium channel modulatory factor 1	NM_020122.3	14.5P-3.5A	-2.6
227301_at_HG-U133B	*LOC441241*	Chaperonin containing TCP1, subunit 6A (zeta 1)-like	BX649060.1/ XM_496886 (predicted)	193.8P-62.9A	-2.5

Affymetrix Probe Set ID [b]	Gene Symbol [*Homo sapiens*]	Title [*Homo sapiens*]	RefSeq Transcript ID (GenBank Source)	Signal (-/+ Dox) [c]	Fold change (+/- Dox)
221111_at_HG-U133A	*IL26*	Interleukin 26	NM_018402	82.3P-29.1P	-2.3
207076_s_at_HG-U133A	*ASS*	Argininosuccinate synthetase	NM_000050.2	520.6P-232.8P	-2.1
216620_s_at_HG-U133A	*ARHGEF10*	Rho guanine nucleotide exchange factor (GEF) 10	NM_014629.1	210.8P-122.2P	-2.1
232489_at_HG-U133B	*FLJ10287*	Hypothetical protein FLJ10287	NM_019083.1	93.3P-50.8P	-2.1
235900_at_HG-U133B	*MGC29671*	Hypothetical protein MGC29671	NM_182538.3	191.4P-81.1A	-2.1
223261_at_HG-U133B	*POLK*	Polymerase (DNA directed) kappa	NM_016218.1	39.2P-18.8A	-2.0
225284_at_HG-U133B	*LOC144871*	Hypothetical protein LOC144871	AK024941.1	227.7P-97.7P	-2.0
213659_at_HG-U133A	*ZNF75*	Zinc finger protein 75 (D8C6)	NM_007131.1	38.2P-17.9M	-2.0
227354_at_HG-U133B	*PAG*	PAG1 (phosphoprotein associated with glycosphingolipid microdomains 1)	NM_018440.3	83.4P-52.3A	-2.0
225762_x_at_HG-U133B	*LOC284801*	Hypothetical protein LOC284801	XM_378973.2 (predicted)	171.5P-98.9A	-2.0
225767_at_HG-U133B	*LOC284801*	Hypothetical protein LOC284801	XM_378973.2 (predicted)	218.9P-78.8P	-2.0
228176_at_HG-U133B	*EDG3*	Endothelial differentiation, sphingolipid G-protein-coupled receptor, 3	NM_005226.2	198.3P-84.3P	-2.0
244669_at_HG-U133B	*C6ORF160 (LOC441164)*	Chromosome 6 open reading frame 160/ (LOC441164)	BC009220.2	44.0P-22.6A	-2.0

[a] Repressed genes (≥ 2.0-fold) compared to untreated controls following doxycycline treatment for 82 h.
[b] Affymetrix GeneChip Human Genome U133 Array Set HG-U133A and HG-U133B Targets. ID: Identity
[c] A: Absent; P: Present; M: Marginal.

Table III shows that the gene for *SHIP* itself was the most strongly up-regulated, expressed from the retroviral vector. From those 16 that were induced, 9 corresponded to genes coding for known proteins, with known mRNA sequences, except for one, the *SLC01C1* gene, whose mRNA sequence was provisional at the time of analysis. Five (5) from the additional seven (7) transcripts corresponded to hypothetical proteins and novel genes, and two (2) represented ESTs. Of the known genes shown on Table III, with revised mRNA sequences, the gene for *VPS54* was the most strongly up-regulated (+360%), followed by the genes for *KLF2* (+200%), *SELL/CD62L* (+160%), and *BIN1* (+130%) respectively. Considering the high magnitude of the Signal, it was shown that from the leading genes, those for *KLF2*, *SELL/CD62L*, and *BIN1* were at the top of the up-regulated genes. Similarly, by analysis of the 21 transcripts identified as reduced, it is shown on Table IV the presence of 15 reduced genes coding for known proteins with known mRNA sequences, except for one, the *DNAJB9* gene, whose mRNA sequence was provisional at the time of analysis. The additional six (6) transcripts corresponded to sequences that code for hypothetical proteins. Of the known genes with revised mRNA sequences, the gene for *DDX56* was the most strongly down-regulated (-90%), followed by the genes for *PAG* (-81%), *SELL1L* (-80%), *TRIB3* (-73%), *ATF5* (-73%), *ARRDC3* (-71%), and *TSC22* (-70%), respectively. All of these genes showed high magnitude of the signal and were at the top of the down-regulated genes.

Table V shows the percentage of transcripts that correspond to known genes, ESTs, and sequences that coded for hypothetical proteins, after the evaluation of the results obtained by microarray analysis. Accordingly to the results, from the 37 genes that were at least two-fold significantly regulated after the expression of SHIP in Jurkat-SHIP cells (clone no. 51), 24 were identified as known genes (65%) with revised mRNA sequences, except two of them, with provisional mRNA sequences, 11 coded for hypothetical proteins and novel genes (30%) and 2 represented ESTs (5%). Based upon Gene Ontology (GO) annotations (Gene Ontology), of the 24 genes, 11 genes (46%) had GO annotations relating to nucleus, transcription or cell cycle, 7 genes (29%) encode proteins associated with intracellular signaling cascades and/or localization in the plasma membrane, and 1 gene (4%) codes for one interleukin, IL26 (Tables VII and VIII).

The top 37 transcripts identified as significantly regulated by SHIP in Jurkat T cells (≥ 2-fold) were chosen for confirmation by quantitative real-time RT-PCR. In view of the fact that for one of the two ESTs, *AI820854,* no mRNA sequence was available at the time of analysis

(Table III), 36 transcripts could be analyzed by quantitative real-time RT-PCR, in addition to *SHIP* itself.

Table V. Classification of the differentially expressed transcripts identified by microarray analysis on U133 Chips in Jurkat-SHIP cells (clone no. 51) after the restoration of SHIP.

Transcripts significantly increased or decreased (fold change ≥ 2) after the expression of SHIP (experiment array), compared to untreated controls (baseline array) following doxycycline treatment for 82 h.

U133 Chip A and B	*Known genes*	*Hypothetical proteins/novel genes*	*ESTs*	*Total*
N° Increased	9[a]	5[a]	2[b]	16
N° Decreased	15 [a]	6	0	21
Sub-total	**24**	**11**	**2**	**37**
Percentage	***65%***	***30%***	***5%***	***100%***

[a] One of them represented by a provisional mRNA sequence.
[b] No mRNA sequence was available for one of them (*AI820854*).

5.3. Validation of the SHIP-regulated mRNAs by quantitative real-time RT-PCR

Once the induced or reduced genes, ESTs and sequences that coded for hypothetical proteins after the expression of SHIP in Jurkat-SHIP cells (clone no. 51) were identified by Microarray analysis, the validation of the results obtained by quantitative real-time PCR was performed for each transcript identified, if the mRNA sequence information was available. It has been shown that quantitative real-time RT-PCR is more accurate than microarray analysis, and should be used only to investigate a few genes at a time (Etienne *et al,* 2004). In this study, all the genes, ESTs and sequences that coded for hypothetical proteins with available sequences were analyzed by quantitative real-time RT-PCR for the validation of the microarray results. Firstly, the known genes with high levels of expression were analyzed, and secondly the ESTs and sequences that coded for hypothetical proteins.

5.3.1 Primer design for the selection of the oligonucleotides used in the validation by quantitative real-time RT-PCR and standardization

An extended research of information was done for the corresponding genes, ESTs and sequences that coded for hypothetical proteins identified from microarray analysis, with the

purpose to confirm or update the data available on NetAffx™ analysis center (Affymetrix). In order to achieve that, different data banks were used to select the representative mRNA sequence for each gene, as mentioned before (5.2). All the primers were designed based on the corresponding human mRNA sequences. Once each public representative mRNA sequence was identified, it was used to design the oligonucleotides that were subsequently used in the validation by quantitative real-time RT-PCR. For the primer design, approximately the last 600 nt near the 3'end of the specific mRNA sequence were chosen.

The Primer 3 Software (v. 0.2) from the Whitehead Institute for Biomedical Research (http://frodo.wi.mit.edu/cgi-bin/primer3/primer3_www.cgi) was used to assist in the design of the gene-specific primers, using a human Mispriming Library for the search. Following the setting of the parameters in the design, such as primer length, melting Temperature, GC content and product size, the best forward- and reverse-primers for each target sequence were obtained. The specificity of the primer sequences was verified using BLAST nucleotide-nucleotide search analysis function from NCBI (http://www.ncbi.nlm.nih.gov/BLAST/). Only 100% complementarities between each primers and the target mRNA sequences were taken into consideration. Additionally, aligments to other mRNA sequences corresponding to other targets were avoided.

Table VI shows the primer sequences obtained and used in the verification by quantitative real-time RT-PCR. A total of 41 PCR primer pairs were designed and tested. In addition, one pair was used for the coding region of the *SHIP* gene. All the transcripts identified were tested by RT-PCR, except that for *AI820854,* because no mRNA sequence was available at the time of analysis (see Table III). All the primers shown on Table VI were tested at least once by conventional PCR and quantitative real-time RT-PCR. Intended for high specificity in the amplification reactions, it was necessary in some cases to design additional pairs of primers for the transcripts analyzed in the optimization process. For instance, three different pair of primers were tested, specific for the *SLC01C1* gene, which was represented by a provisional mRNA sequence. Furthermore, different amplification conditions were set for each pair of primers in the standardization process.

Table VI. Sequences of primers for the amplification of the selected human genes evaluated by quantitative real-time RT-PCR.

Gene Symbol [*Homo sapiens*]	RefSeq Transcript ID (GenBank Source)	Primer sequences (5'→3') (Forward and Reverse)	Primer Length	Primer Start	Primer Tm (°C)	Primer GC (%)	Product size (bp)	a.T[j] (°C)
Known genes								
ARRDC3	NM_020801.1	CTGATAATTGGCACTGGATCAC GCCTACAAGGACATATTCAGCAC	22 23	3698 4031	59.46 60.04	45.45 47.83	334	60
ARHGEF10	NM_014629.1	CTGTTGACGTGGAATGCTGT CCGTCCAGTAAGTGAAACACTG	20 22	7973 8267	59.75 59.70	50.00 50.00	295	57
ASS	NM_000050.2	TATACCGGTTTACGGCCTAGC CTCCTCATTGTACACGGGTCT	21 21	1039 1333	60.35 59.08	52.38 52.38	295	57
ATF5	NM_012068.2	TGCTTATCACCTCTCTTGCGTA CTAGCCTGCTTTTTGCCTGTAG	22 22	1452 1757	60.04 60.55	45.45 50.00	306	60
BIN1	AF068917.1	GTCTTCCCCGAGAACTTCACT ACTAGAGGACACAGCAGCTTCA	21 22	1474 1743	59.73 59.31	52.38 50.00	270	59
CA1	NM_001738.1	GCTCTCTGACTCATCCTCCTCTT GATTATGTCAGAAGCAGGGCTGT	23 23	736 990	60.53 61.86	52.17 47.83	255	55-66[h]
DDX56	NM_019082.1	ACTACCTGGTTCCTCCTGCTCT GAAGTGCCAAGGAGCTAAAGG	22 21	1548 1858	60.67 60.38	54.55 52.38	311	60
EDG3	NM_005226.2 [d]	TAACTCTACTAGGGAGCCCACAG CAGCATAGAAGACCACCTGTTTC	23 23	3820 4098	58.99 60.18	52.17 47.83	279	55-69[h]
EPC1	NM_025209.2	ACACAGACTTCAAGTTCCCACAG CGCTACTGTGTTGTCTGCTATGT	23 23	2446 2766	60.62 59.52	47.83 47.83	321	60
GAPDH [a]	NM_002046	GATGACATCAAGAAGGTGGTGA CTTACTCCTTGGAGGCCATGT	22 21	841 1084	59.97 60.50	45.45 52.38	244	55-75[i]
IL26	NM_018402.1	GGCAGAAATTGAGCCACTGT GAATCACCTAACATGCCGTCAG	20 22	379 679	60.26 61.80	50.00 50.00	301	59
KCMF1	NM_020122.3	GCGTGCATGAGTTTTAGTGACC CACAGGCAAGATGACTAACAGG	22 22	1860 2129	61.96 59.80	50.00 50.00	270	57

Gene Symbol [*Homo sapiens*]	RefSeq Transcript ID (GenBank Source)	Primer sequences (5'→3') (Forward and Reverse)	Primer Length	Primer Start	Primer Tm (°C)	Primer GC (%)	Product size (bp)	a.T[j] (°C)
Known genes								
KLF2	**NM_016270.1**	GGAAAAGACCACGATCCTCCTT [e] GAACCAGGTAGCCCAAAAATG	**22** **21**	**1349** **1588**	**62.86** **60.71**	**50.00** **47.62**	**240**	**57**
PAG	**NM_018440.2**	TGCAGAGTGAGCTATGTTGAGG GCTAGGTGTGTAAGATGACATGG	**22** **23**	**3364** **3660**	**60.59** **58.67**	**50.00** **47.83**	**297**	**60**
POLK	**NM_016218.1**	ATTAGTTAGGCCAGGCACAATG CTTTGACCTCCCAGGTTCAAGTAG	**22** **24**	**3718** **3954**	**60.38** **62.48**	**45.45** **50.00**	**237**	**60**
PSG6	**NM_002782.3**	GAGAAAACCTCGACTTGTCCTG ATAGGTAACCTGGGGAGATGCT	**22** **22**	**1089** **1318**	**60.28** **60.22**	**50.00** **50.00**	**230**	**55-62 [h]**
RBM15	**NM_022768.4**	GAGTTTACATGGGCCTCTGATG GCACGTTTGAGAGACAGCTACT	**22** **22**	**3139** **3370**	**60.88** **58.82**	**50.00** **50.00**	**232**	**60**
SEL1L	**NM_005065.3**	TGATGAGCTACAGCCTCTTTCC GATGGCGAAGTAGTGACGTAAG	**22** **22**	**7324** **7617**	**60.89** **58.93**	**50.00** **50.00**	**294**	**59**
SELL/ CD62L	**NM_000655.2**	GAGAGAAATAGCCTGCGCTGT AAAAGAAGTGGTGGGGTTGAG	**21** **21**	**1897** **2206**	**61.04** **60.38**	**52.38** **47.62**	**310**	**57**
SHIP1	**U57650.1**	ATGGGGATCCGCTGGAACCATGGCAACATCACCCGCTCC [b] CTCTGTCGACAGCGGCACAGGGTATTGCAGATGGGTC [b]	**39** **37**	**523** **820**	**>75** **>75**	**61.50** **59.50**	**298**	**57**
		AAAGGGCCTAGCTTCTGTGTG [e,f] CTCTCGAGGTCATCCTGATATG [f]	**21** **22**	**4206** **4525**	**60.80** **58.77**	**52.38** **50.00**	**320**	**57**
		GGAAATCAGCTCCTATTCTCCA [f] CACACACCACTGGATTTAGCTC [f]	**22** **22**	**4810** **5196**	**58.40** **60.30**	**45.50** **50.00**	**387**	**57**
TRIB3	**AY247738.1**	GCTGACAACACTTTTCCATGAC [e] CAGAGATGCTGGGAACACAGT	**22** **21**	**1905** **2161**	**59.64** **60.31**	**45.45** **52.38**	**257**	**57**
TSC22	**NM_006022.2**	TGTCTGAGGAGGTGTGGACTT GGTGATATGCAGAAACCCCTAC	**21** **22**	**1388** **1638**	**59.74** **59.73**	**52.38** **50.00**	**251**	**60**

Gene Symbol [*Homo sapiens*]	RefSeq Transcript ID (GenBank Source)	Primer sequences (5'→3') (Forward and Reverse)	Primer Length	Primer Start	Primer Tm (°C)	Primer GC (%)	Product size (bp)	a.T[j] (°C)
Known genes								
VPS54	AK023632.1	ACCCTTCAAAGGGCCATAGTA ATACAGGTATGCACCACCACAC	21 22	2024 2256	59.84 59.67	47.62 50.00	233	59
ZNF75	NM_007131.1	TGTGACAGGAGGTTTAGATGGA AGAAGGCTCGATCGCCTACTA	22 21	965 1251	59.59 60.50	45.45 52.38	287	55
Known genes (provisional mRNA sequences)								
DNAJB9	NM_012328.1 (provisional)	GGGACATATGCTGATCACAGG ACCACGCCTAAAGAGGAAAGA	21 21	1993 2211	60.36 60.25	52.38 47.62	219	57
SLC01C1[d]	AF260704.1	GTTTTGGTCCTAGGCATTAGGT CTTGAAGGAACCCAAGGTATGA	22 22	2627 2921	58.59 60.34	45.45 45.45	295	55-66[h]
	NM_017435.2 (provisional)	TCTCCCATAGCTGTCTTCATCTG CCATAGTCACTTATAGCGCCACAC	23 24	2941 3163	60.77 62.05	47.83 50.00	223	55-57[h]
		GTTTTGGTCCTAGGCATTAGGT TGAAGGAACCCAAGGTATGAGT	22 22	2627 2919	58.59 59.86	45.45 45.45	293	55-66[h]
Sequences that code for hypothetical proteins/novel genes								
C6ORF160 (LOC441164)	BC009220.2	ACAGTGGAGCAGCTCTGAAGAT CCAAGACAATCTGGCCTCTATC	22 22	540 771	60.59 60.10	50.00 50.00	232	59
C22ORF19	AB023200.1 (provisional)	ACCCGGCCTGAGTAGAGTCTTT CCAGCCTCCCAAAGTACTGAT	22 21	4166 4456	62.68 60.50	54.55 52.38	291	59
FLJ10287	NM_019083.1	TGGGCATGCTACCTAATCTCTT TTGGGGACATGGGTAACTAACT	22 22	2669 2988	60.12 59.63	45.45 45.45	320	57
FLJ22671[d]	NM_024861.1 (predicted)	GTATGCCATTCCTTGGTGATG GAAGCAGATGGGAGTAGTCCTG	21 22	1265 1564	60.21 60.27	47.62 54.55	300	55-64[h]
KIAA0117	D38491.1 (partial cds)	CAGAAACAAGGGCAGAAAAGG GCTTCACCATCTCACTAACAGC	21 22	415 754	61.12 59.01	47.62 50.00	340	57

Gene Symbol [*Homo sapiens*]	RefSeq Transcript ID (GenBank Source)	Primer sequences (5'→3') (Forward and Reverse)	Primer Length	Primer Start	Primer Tm (°C)	Primer GC (%)	Product size (bp)	a.T[j] (°C)
Sequences that code for hypothetical proteins/novel genes								
LOC144871	**AK024941.1**	CTGAGCACACAGCAATGGTATC GCCACGCAGTGGCTAATTTTAC	**22** **22**	**1779** **2061**	**60.72** **62.98**	**50.00** **50.00**	**283**	**59**
LOC284801	**XM_378973.2 (predicted)** [d]	GAGTACAAGCTGATCCACCTACG TCTCTCTCCTCAGTAGTCCATCG	**23** **23**	**1718** **1917**	**60.20** **60.02**	**52.17** **52.17**	**200**	**55-66**
LOC441241	**BX649060.1**	GGAGTAAACTAGAGGCAAGGGAGT CCAAAACCCACAGCCTAGTAAC	**24** **22**	**3399** **3659**	**60.51** **59.93**	**50.00** **50.00**	**261**	**75**
MGC10986	**NM_030576.2**	CTTGGAGTCAAGTTCTCTTCTGC CCCAGCTCTATGTCTGTGTCTG	**23** **22**	**2648** **2937**	**59.69** **59.93**	**47.83** **54.55**	**290**	**59**
MGC29671	**NM_182538.3**	CTGTACCTGGAGAGAGACGAGAC GGGAATTCAAAAGTGGCAGATG	**23** **22**	**1449** **1708**	**59.56** **62.90**	**56.52** **45.45**	**260**	**60**
TP53TG3 [k]	**NM_015369.1**	CACAGGTCTGTAAGGCTCTGTTC GTCCAAGATGTAAACGGCAGAC	**23** **22**	**1484** **1745**	**60.35** **60.91**	**52.17** **50.00**	**262**	**55-61** [h]
ESTs								
AI820854 [c]	**AI820854 (Resource:dbEST)**	[c]						
LOC389100 [g]	**XM_374035.1 (predicted)**	CAGCAGTTTCAGCCATGTTATC GGCTCAGGAGTGGTGAATCTTA	**22** **22**	**572** **803**	**59.77** **60.63**	**45.45** **50.00**	**232**	**60**

[a] Housekeeping gene transcript serving as the normalization control for quantitative real-time RT-PCR.
[b] It was validated the up-regulation of *SHIP* itself (expression of the cloned sequence) by quantitative real-time RT-PCR. The primers used were already in the laboratory.
[c] No mRNA sequences currently available.
[d] Not good; experimental evidence, after testing the primer pairs described here.
[e] Source primer sequence: The best probe of intensity patterns evaluation, obtained from Affymetrix analysis.
[f] The forward and reverse primers are complementary to the region near of the 3'end of the *SHIP* mRNA sequence, downstream of the end of the open reading frame. This pair of primers was used as control for the detection of the endogenous *SHIP* mRNA transcripts.
[g] The primers are in addition complementary to the EST sequence (AW102716).
[h] The primers were tested with different annealing Temperatures, elongation times, cycle numbers, and cDNA dilutions.
[i] The primers were suitable for different annealing Temperatures.
[j] Annealing Temperature.
[k] Novel gene.

It was confirmed by microarray analysis that the expression of *GAPDH* and *ß-actin* were not regulated after the induction of SHIP in Jurkat-SHIP cells (clone no. 51) (data not shown). Consequently, both, the *GAPDH* and *ß-actin* gene transcript sequences were used as positive control for conventional PCR reactions (Figure 12). Furthermore, the sequence from the housekeeping gene glyceraldehyde-3-phosphate-dehydrogenase (*GAPDH)* was used as normalization control for quantitative real-time RT-PCR analysis (section 5.3.3, Figure 13 and section 5.4.1, Figure 15). Despite the fact that in the primer design was attempted to enclose the minimum of variability in the parameters, the *GAPDH* primers were tested at different Temperatures and elongation times to verify if they were suitable for the amplification of specific products under diverse conditions, because of the large number of particular targets.

5.3.2 Verification of the template purity for the validation analyses by quantitative real-time RT-PCR

The RNA isolation procedure by CsCl gradient centrifugation is a method that guarantees in some extent the purity of the RNA and provides high concentrations of total high quality RNA. In optimal conditions, the probability that contaminating DNA is present is very low. Nevertheless, the purity of the RNA isolated was verified, in each case. The possible presence of contaminating genomic DNA in the RNA preparation was analyzed using primers specific for the regions corresponding to the exons 7 and 8 of the regulatory 85 kDa subunit of the *PI3K* target gene, which spanned extron-intron junctions. In the case that only the exons were present in the RNA preparation, that means no DNA contamination, a PCR product of approximately 300 base pairs (bp) was obtained, as shown in Figure 12. In the case of DNA contamination, the intron is supposed to be present, resulting in an approximately expected 1.4 Kb PCR product. The 300 bp-amplified products shown on Figure 12 (absence of introns) confirmed the purity of the templates used subsequently in mRNA analysis. Additionally, specific primers targeting the *ß-actin* sequences were used in the PCR analysis as control of cDNA templates in the samples. The verification of purity was on every occasion performed after RNA isolation and cDNA synthesis.

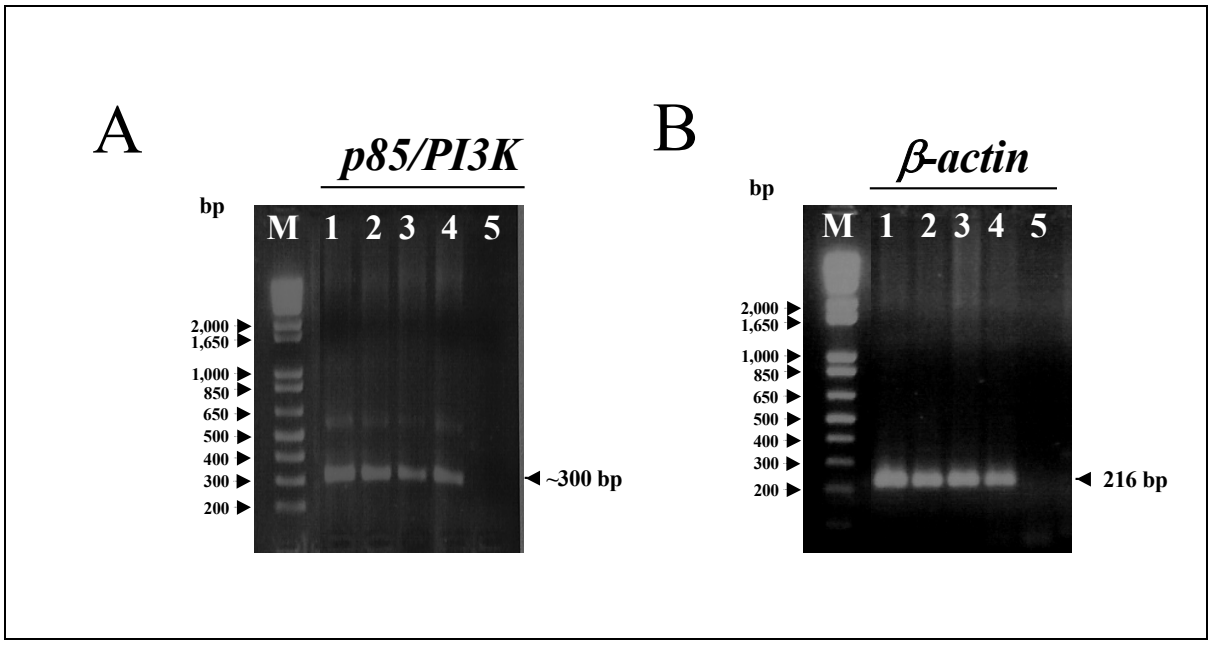

Figure 12. PCR analyses of the templates used in quantitative real-time PCR, corresponding to samples isolated from Jurkat-SHIP cells.

Sister cells from Jurkat-SHIP clone no. 51 were harvested and prepared in GCN-solution, corresponding to two independent experiments, Set 1 and 2, after 72h and 82h induction with Doxycycline (Dox), respectively. The total RNA isolation was carried out by CsCl gradient centrifugation. 3 µg from the total RNA were used for cDNA synthesis. The cDNAs were used as templates for conventional PCR analyses, in order to verify the purity of the RNA isolated. PCR reactions were performed with primers specific for the exons 7 and 8 of the regulatory 85 kD subunit of *PI3K* gene sequence (A), and the *β-actin* sequence (B), respectively. The products were loaded and electrophoresed on 2% agarose gels, stained with EtBr and visualized with an UV-documentation system. Lane M shows the DNA ladder markers (1 Kb Plus DNA Ladder™, Invitrogen). **A:** The ~ 300-bp amplified target fragments, corresponding to pure RNA, without DNA contamination obtained with primers specific for the exons 7 and 8 of the regulatory 85 kD subunit of *PI3K* gene sequence are shown. An additional slight 500-600 bp band was present, corresponding likely to an alternatively spliced transcript or an unspecific product, because of the low stringency used in the purity-PCR verification assay. It was no ~1.4 Kb amplified target, which confirmed absence of DNA contamination. **B:** The 216-bp target fragments of the *β-actin* housekeeping gene transcript served as control of cDNA templates in the samples. **1**: Jurkat-SHIP cells (clone no. 51) Set 1, 72h (-Dox); **2**: Jurkat-SHIP cells (clone no. 51) Set 1, 72h (+Dox); **3:** Jurkat-SHIP cells (clone no. 51) Set 2, 82h (-Dox); **4**: Jurkat-SHIP cells (clone no. 51) Set 2, 82h (+Dox); **5:** negative PCR control. +: with induction; - : without induction. Dox: Doxycycline.

5.3.3 Endogenous *SHIP* mRNA expression is not regulated after the restoration of SHIP in Jurkat T cells

In this study, the expression of the endogenous *SHIP* mRNA levels in Jurkat-SHIP cells (clone no. 51) was confirmed by quantitative real-time RT-PCR. Additionally, the data revealed that there is no regulation of the endogenous *SHIP* transcription after restoration of

SHIP in Jurkat T cells (clone no.51) (Figure 13). The expression of the endogenous *SHIP* mRNA levels in Jurkat T-cells was also confirmed (data not shown). The specific primers chosen for *SHIP* mRNA expression analysis by quantitative real-time RT-PCR were already designed and used in the laboratory before. In Jurkat-SHIP cells (clone no.51), the cloned sequence does not contain the 3'-end of *SHIP* mRNA, downstream of the open reading frame (ORF). Therefore, the identification and analysis of the endogenous expression of *SHIP* mRNA was performed by quantitative real-time RT-PCR analysis, targeting its 3'-region downstream of the ORF.

The design and test of the primers complementary to the 3'-end region of *SHIP* mRNA sequence, downstream of the open reading frame (ORF) allowed the confirmation that *SHIP* is endogenously expressed on the mRNA level in Jurkat-SHIP cells (clone no. 51) (Figure 13) and Jurkat T cells (data not shown). In Figure 13 the expression of the 3'-end target sequence of the *SHIP* mRNA in Jurkat-SHIP cells (clone no. 51), corresponding only to the expression of the endogenous *SHIP,* is shown. After verification on agarose gels, quantitative real-time RT-PCR analyses from two independent experiments run in duplicates were performed (see 5.3.4). The data revealed that the transcripts corresponding to endogenous *SHIP* in these cells were not regulated after the induction with Doxycycline (fold-change: 1.0 ± 0.28). It was confirmed by further analysis targeting the expression of *SHIP* in Jurkat-SHIP cells (clone no. 51) that the up-regulation of *SHIP* after induction with Doxycycline corresponds to the transcription of the cloned region (section 5.3.4, Table VII). That means, the differential expression of *SHIP* mRNA obtained after SHIP restoration was due to the induction of transcription of the *SHIP* gene from the retroviral vector, cloned in Jurkat T cells, and this has no effect on the regulation of the endogenous *SHIP* expression. Very interestingly is the fact that although Jurkat T-cells do not express SHIP at the protein level, they *do* express *SHIP* at the messenger RNA level. It suggests the presence of specific posttranscriptional processing events involved in the regulation of expression of SHIP in Jurkat cells.

5.3.4 Validation by quantitative real-time RT-PCR confirmed the effect of SHIP on differential gene expression in Jurkat T cells

In order to achieve the validation assays, the relative increase or decrease in mRNA was measured by quantitative real-time polymerase chain reaction (RT-PCR), using SYBR Green-

based detection with a LightCycler analysis system, Version 3.5 and the LightCycler detection software, according of the instructions of the manufacturer (Roche, Mannheim, Germany).

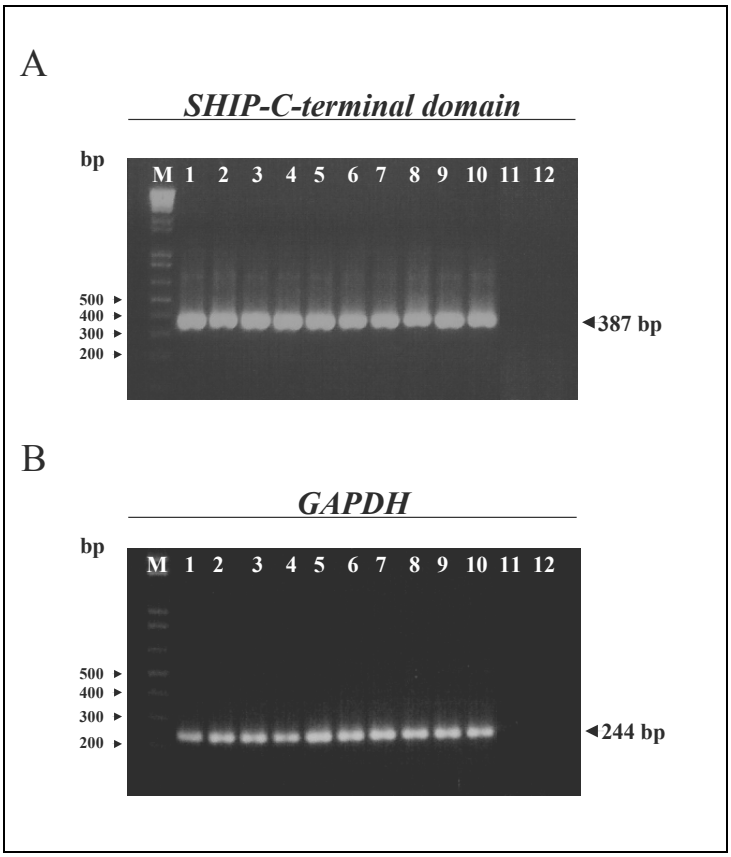

Figure 13. Quantitative real-time RT-PCR analysis of expression of endogenous *SHIP* in Jurkat-SHIP cells.

Sister cells from Jurkat-SHIP clone no. 51 were harvested and prepared in GCN-solution, corresponding to two independent experiments, Set 1 and 2, after 72h and 82h induction with Doxycycline (Dox), respectively. Additionally, TF-1 cells were used in the analysis. The total RNA isolation was carried out by CsCl gradient centrifugation. 3 µg from the total RNA were used for cDNA synthesis. After verification of purity (section 5.3.2), conventional PCR and quantitative real-time PCR analyses were run two times, performed in duplicates, with primers specific for the 3'-end region of the *SHIP* mRNA sequence*, downstream* of the ORF. The products were loaded and electrophoresed on 2% agarose gels, stained with EtBr and visualized with an UV-documentation system. Lane M shows the DNA ladder markers (1 Kb Plus DNA Ladder™, Invitrogen). **A:** The 387-bp amplified target fragments obtained with primers specific for the 3'-end of the *SHIP* mRNA sequence are shown, from one representative experiment, in duplicates, in each case. **B:** The 244-bp target fragments of the *GAPDH* housekeeping gene transcript served as a normalization control to ensure equal amounts of starting cDNA template in samples. **1-2**: TF-1 cells; **3-4**: Jurkat-SHIP cells (clone no. 51) Set 1, 72h (-Dox); **5-6**: Jurkat-SHIP cells (clone no. 51) Set 1, 72h (+Dox); **7-8**: Jurkat-SHIP cells (clone no. 51) Set 2, 82h (-Dox); **9-10**: Jurkat-SHIP cells (clone no. 51) Set 2, 82h (+Dox); **11-12**: negative PCR control. +: with induction; - : without induction. Dox: Doxycycline.

The calculation of crossing points was automatically done by the second derivative maximum method of the LightCycler software. Amplified products were also analyzed for specificity by agarose gel electrophoresis (Figure 14). The *GAPDH* gene was selected as the house keeping gene transcript to normalize the samples, as its expression level was previously confirmed to be reliably constant by the microarray analysis done in this study for Jurkat-SHIP cells (clone no.51) (data not shown), and preliminary quantitative real-time RT-PCR results (Figure 14). Figure 14 shows a representative example from agarose gel electrophoresis analysis of amplified products after quantitative real-time RT-PCR, corresponding to the target sequences of the transcription factors *KLF2* and *ATF5*, and the housekeeping gene *GAPDH*. The Figure shows one specific product for each target sequence analyzed, corresponding to the expected size, in each case. The *Krüppel-like factor 2* **(***KLF2*) gene was identified by microarray analysis as up-regulated at the mRNA level after the restoration of SHIP expression in Jurkat T-cells (clone no.51). In contrast, the *activating transcription factor 5* (*ATF5*) gene was identified to be down-regulated at the mRNA level in the same analysis. Preliminary quantitative real-time RT-PCR analyses revealed the presence of both transcripts, *KLF2* and *ATF5*, and confirmed the amplification of only one specific product, for all the samples, in each independent experiment.

After verification of the specificity in the amplification by quantitative real-time RT-PCR and agarose gel electrophoresis, analyses of the differential mRNA expression for each target sequence were carried out. The PCR efficiency of each primer for each individual sample (*E*) and its corresponding duplicate was determined by linear regression analysis from the raw real-time PCR data, using the LinRegPCR program (Ramakers *et al,* 2003), adjusting the parameters to the best fitting line through 4-6 points and $R \geq 0.999$. Only the data whose efficiencies (*E*) obtained from each sample for each gene specific product were similar among them and between those obtained from the housekeeping gene *GAPDH* were selected, as described in Materials and Methods. Finally, the $2^{-\Delta\Delta C}{}_T$ method (Livak and Schmittgen, 2001) was used to analyze the relative changes in mRNA expression.

With the *GAPDH* gene serving as a normalization control, the changes in expression, efficiencies, and significances analyzed by quantitative real-time RT-PCR, compared to the

microarray data are listed in Tables VII and VIII, corresponding to the SHIP-induced and SHIP-repressed genes in Jurkat cells, respectively.

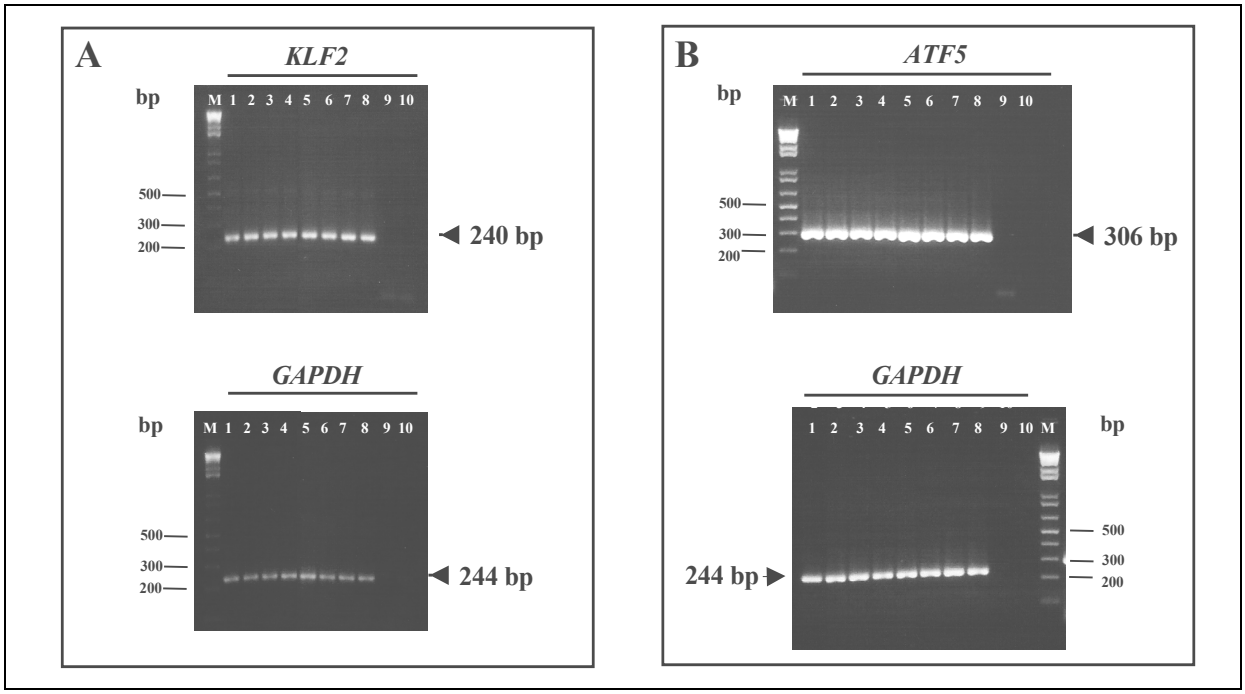

Figure 14. Agarose gel electrophoresis analysis from the products amplified for *KLF2* and *ATF5* target sequences by quantitative real-time RT-PCR from samples isolated from Jurkat-SHIP cells.

Sister cells from Jurkat-SHIP cells (clone no. 51) were harvested and prepared in GCN-solution, corresponding to two independent experiments, Set 1 and 2, after 72h and 82h induction with Doxycycline (Dox), respectively, as described in Figure 12. After cDNA synthesis and verification of purity, PCR analyses were performed with primers specific for the target gene sequences. After standardization, quantitative real-time RT-PCR analyses were carried out for the quantification of mRNA differential expression after the induction of SHIP in Jurkat-SHIP cells (clone no.51). Agarose gel electrophoresis analyses were performed to verifiy the specificity in the amplification. The products were loaded and electrophoresed on 2% agarose gels, stained with EtBr and visualized with an UV-documentation system. Lane M shows the DNA ladder markers (1 Kb Plus DNA Ladder™, Invitrogen). The products corresponding to target sequence and *GAPDH* amplification are shown. **A:** The 240-bp amplified target fragments obtained with primers specific for the *KLF2* mRNA sequence are shown in duplicates, in each case (top). The 244-bp target fragments of the *GAPDH* housekeeping gene transcript served as a normalization control to ensure equal amounts of starting cDNA template in samples (bottom). **B:** The 306-bp amplified target fragments of the *ATF5* gene transcript are shown. Primers specific for the *GAPDH* transcript sequence were used for the normalization control (bottom). **1-2**: Jurkat-SHIP cells (clone no. 51) Set 1, 72h (-Dox); **3-4**: Jurkat-SHIP cells (clone no. 51) Set 1, 72h (+Dox); **5-6**: Jurkat-SHIP cells (clone no. 51) Set 2, 82h (-Dox); **7-8**: Jurkat-SHIP cells (clone no. 51) Set 2, 82h (+Dox); **9-10**: negative PCR control. +: with induction; - : without induction. Dox: Doxycycline.

In Tables VII and VIII the 24 known genes mentioned previously are grouped, based upon gene annotations (Gene Ontology) (5.2. Table V). Of the 24 known genes, 11 genes (46%) had GO annotations relating to nucleus, transcription or cell cycle, 7 genes (29%) encode proteins associated with intracellular signaling cascades and/or localization in the plasma membrane, and 1 gene (4%) codes for an interleukin, IL26. In detail, of the 7 genes associated with intracellular signaling cascades and/or localized in the plasma membrane, 6 were identified and analyzed by quantitative real-time RT-PCR (86%), in addition to *SHIP* itself. This group includes *SELL/CD62L*, *PAG, SEL1L, TRIB3, ARRDC3,* and *ARHGEF10* (Tables VII and VIII).

The eleven genes reported to be involved in the translation of proteins that have a function in the transcription process, in the cell cycle and/or are localized in the nucleus were identified and analyzed by quantitative real time RT-PCR. This group includes *KLF2, BIN1, RBM15, EPC1, DDX56, ATF5, TSC22, POLK, ZNF75, DNAJB9* and *KCMF1*. In search of interleukines, only one transcript was identified to be significantly regulated, the gene that codes for IL26, which was transcriptionally SHIP-repressed. The SHIP-mediated repression of *IL26* mRNA was identified, analyzed and validated by quantitative real-time RT-PCR (Table VIII). The remaining genes code for proteins reported to be involved in other functions, grouped as miscellaneous, proteins with unknown function and the TP53TG3 protein, whose gene was identified as a novel gene. TP53TG3 is supposed to be involved in the TP53-mediated signaling pathway (Ng *et al,* 1999). However, the available sequence chosen for the novel *TP53TG3* gene at the time of analysis was recently permanent suppressed (2006), because it is a non-sense mediated mRNA decay (NMD) candidate (Entrez Gene), and has been replaced for another one, which is additionally a provisional sequence. This could explain the absence of detection of the transcript by quantitative real-time RT-PCR in this study (Table VII).

Of the 5 genes grouped in miscellaneous, 2 were identified and analyzed by quantitative real-time RT-PCR: *VPS54* and *ASS* (Tables VII and VIII). From the group of unknown function/novel genes, 9 out of 13 were identified and analyzed by quantitative real-time RT-PCR. This group includes: *C22orf19, KIAA0117, MGC10986, LOC389100, LOC441241, FLJ10287, MGC29671, LOC144871* and *C6orf160 (LOC441164).*

Table VII. SHIP-induced changes of gene expression obtained from quantitative real-time RT-PCR analyses.

Comparison of the data obtained using the Affymetrix platform (GeneChip Human Genome U133 Array Set HG-U133A and HG-U133B Targets) with the results from quantitative real-time RT-PCR experiments for genes that were induced after the expression of SHIP in Jurkat T-cells (clone no.51). Affymetrix and quantitative real-time RT-PCR are shown as a fold change of the level of mRNA from Jurkat T-cells (clone no.51) with the induction of SHIP expression with Doxycycline, relative to the level of that transcript in the same cell line without induction of SHIP expression.

Gene Symbol [*Homo sapiens*]	Title [*Homo sapiens*]	Fold change Affymetrix (+/-)	Fold change LightCycler (+/-) [a]	Statistical significance [b]	Efficiency (*E*) [c]
Signal Transduction/Plasma membrane					
SHIP1 [g]	SH2 containing inositol 5'-phosphatase	18.4 [g]	3.5 [g]	(**)	1.6
SELL / CD62L	Selectin L, lymphocyte adhesion molecule 1/ CD62 antigen ligand	2.6	2.8	(***)	1.7
Transcription/Cell cycle/Nucleus					
KLF2	Krüppel-like factor 2 (lung)	3.0	3.2	(***)	1.6
BIN1	Bridging integrator 1	2.3	1.3	(*)	1.7
RBM15	RNA binding motif protein 15	2.0	-1.3	(NS)	1.7
EPC1	Enhancer of polycomb homolog 1	2.0	1.1	(NS)	1.6
Miscellaneous					
SLC01C1	Solute carrier organic anion transporter family, member 1C1	6.1	ND		
VPS54	Vacuolar protein sorting 54 (yeast)	4.6	1.1	(NS)	1.6
PSG6	Pregnancy specific beta-1-glycoprotein 6	2.1	ND		
CA1	Carbonic anhydrase I	2.0	ND		
Unknown function/Novel genes					
AI820854 [d]	AI820854 (EST)	10.6	NA [e]		
FLJ22671	Hypothetical protein FLJ22671	6.1	ND		
C22ORF19	Chromosome 22 open reading frame 19/ Fmip, PK1.3, KIAA0983	3.3	1.0	(NS)	1.6
KIAA0117	KIAA0117 protein	2.8	1.2	(*)	1.6
MGC10986	Hypothetical protein MGC10986	2.3	1.5	(NS)	1.6
LOC389100	Hypothetical LOC389100 (EST)	2.1	1.9	(NS)	1.6
TP53TG3	TP53TG3 protein	2.0	ND [f]		

[a] ND: not detectable.
[b] Statistical analysis was performed with a Student's t-test and the P-value is indicated by asterisks. (*): $P < 0.05$; (**): $P < 0.01$; (***): $P < 0.001$; NS: not significant.
[c] GAPDH-Target gene.
[d] No gene annotations available for this transcript; no mRNA sequences currently available (GenBank Source). Original annotation of the probe set, as provided by Affymetrix. Annotation quality (GeneAnnot) (http://genecards.weizmann.ac.il/geneannot/).
[e] NA: not applicable.
[f] According to UniGene ID information (Entrez Gene) (March 2006), the sequence NM_015369.1 was permanently suppressed, because is a non-sense mediated decay (NMD) candidate. It has been substituted for NM_016212 (provisional).
[g] Positive control. Increased expression of *SHIP* from the inducible expression vector. The endogenous *SHIP* expression did not change after the ectopic expression of SHIP from the vector (see 5.3.3)

Table VIII. SHIP-reduced changes of gene expression obtained from quantitative real-time RT-PCR analyses.

Comparison of the data obtained using the Affymetrix platform (GeneChip Human Genome U133 Array Set HG-U133A and HG-U133B Targets) with the results from quantitative real-time RT-PCR experiments for genes that were induced after the expression of SHIP in Jurkat T-cells (clone no.51). Affymetrix and quantitative real-time RT-PCR are shown as a fold change of the level of mRNA from Jurkat-SHIP cells (clone no.51) with the induction of SHIP expression with Doxycycline, relative to the level of that transcript in the same cell line without induction of SHIP expression.

Gene Symbol [*Homo sapiens*]	Title [*Homo sapiens*]	Fold change Affymetrix (+/-)	Fold change LightCycler (+/-) [a]	Statistical significance [b]	Efficiency (*E*) [c]
Signal transduction/Plasma membrane					
PAG	Phosphoprotein associated with glycosphingolipid-enriched microdomains	-5.3	-2.0	(***)	1.6
SEL1L	Sel-1 suppressor of lin-12-like *(C. elegans)*	-4.9	-1.1	(NS)	1.7
TRIB3	Tribbles homolog 3 (*Drosophila*)	-3.7	-4.5	(*)	1.7
ARRDC3	Arresting domain containing 3	-3.5	-2.2	(***)	1.6
ARHGEF10	Rho guanine nucleotide exchange factor (GEF) 10	-2.1	-2.9	(*)	1.5
EDG3	Endothelial differentiation, sphingolipid G-protein-coupled receptor, 3	-2.0	ND		
Transcription/Cell cycle/Nucleus					
DDX56	DEAD (Asp-Glu-Ala-Asp) box polypeptide 56	-9.9	1.1	(NS)	1.5
ATF5	Activating transcription factor 5	-3.7	-4.8	(*)	1.6
TSC22	Transforming growth factor-beta-stimulated protein TSC22	-3.3	-1.3	(*)	1.5
POLK	Polymerase (DNA directed) kappa	-2.0	-1.7	(*)	1.6
ZNF75	Zinc finger protein 75 (D8C6)	-2.0	-4.7	(**)	1.7
DNAJB9	DnaJ (Hsp40) homolog, subfamily B, member 9/Microvascular endothelial differentiation gene 1	-3.3	-2.8	(**)	1.7
KCMF1	Potassium channel modulatory factor 1	-2.6	3.6	(*)	1.6
Cell-cell signaling					
IL26	Interleukin 26	-2.3	-4.1	(*)	1.7
Miscellaneous					
ASS	Argininosuccinate synthetase	-2.1	-1.7	(NS)	1.6

Gene Symbol [*Homo sapiens*]	Title [*Homo sapiens*]	Fold change Affymetrix (+/-)	Fold change LightCycler (+/-) [a]	Statistical significance [b]	Efficiency (*E*) [c]
Unknown function					
LOC441241	**Chaperonin containing TCP1, subunit 6A (zeta 1)-like**	**-2.5**	**-1.0**	**(NS)**	**1.5**
FLJ10287	**Hypothetical protein FLJ10287**	**-2.1**	**-1.2**	**(NS)**	**1.6**
MGC29671	**Hypothetical protein MGC29671 /ESTs, Weakly similar to spinster-like protein *(H. sapiens)***	**-2.1**	**-1.3**	**(NS)**	**1.6**
LOC144871	**Hypothetical protein LOC144871**	**-2.0**	**-1.4**	**(NS)**	**1.6**
LOC284801	**Hypothetical protein LOC284801**	**-2.0**	**ND**		
C6ORF160 (LOC441164)	**Chromosome 6 open reading frame 160/ (LOC441164)**	**-2.0**	**-1.7**	**(*)**	**1.6**

[a] ND: not detectable.

[b] Statistical analysis was performed with a Student's t-test and the P-value is indicated by asterisks. (*): $P < 0.05$; (**): $P < 0.01$; (***): $P < 0.001$; NS: not significant.

[c] *GAPDH*-Target gene.

In summary, of the 36 transcripts analyzed by quantitative real-time RT-PCR, it was possible to validate 29 transcripts (81%), in addition to *SHIP* itself. In detail, of the 16 significant SHIP-induced transcripts (≥2-fold) identified by microarray analysis, 15 were analyzed by quantitative real-time RT-PCR (no gene annotations were available for *AI820854,* see Table VII). Of these 15, 10 were validated by quantitative real-time RT-PCR and the data from the direction of change of nine (9) of them agree with those obtained by microarray analysis, in addition to *SHIP* itself, except one, the *RBM15* gene (Table VII), which was confirmed as repressed. The 9 genes are *SELL/CD62L, KLF2, BIN1, EPC1, VPS54, C22orf19, KIAA0117, MGC10986,* and *LOC389100.* Similarly, of the 21 SHIP-repressed transcripts analyzed, 19 were identified and validated by quantitative real-time RT-PCR and the data from the direction of change of 17 of them agree with the results obtained by microarray analysis, except two, the *DDX56* and *KCMF1* genes (Table VIII), confirmed as increased. The 17 genes are: *PAG, SEL1L, TRIB3, ARRDC3, ARHGEF10, ATF5, TSC22, POLK, ZNF75, DNAJB9, IL26, ASS, LOC441241, FLJ10287, MGC29671, LOC144871* and *C6orf160 (LOC441164).* Accordingly, of the 29 transcripts validated by quantitative real-time RT-PCR, 11 transcripts were identified as SHIP-increased (38%) and 18 as SHIP-repressed (62%) in Jurkat T cells.

To sum up to this point, the validation by quantitative real-time RT-PCR revealed the presence of 29 genes, ESTs and sequences that code for hypothetical proteins out of 36 identified by microarray analysis (81%). Of the 29, 26 coincided with the change direction obtained by microarray analysis. The analysis demonstrated a good correlation between quantitative real-time PCR and the Affymetrix platform, with 90% of the probes changing in the same direction by both methods.

Concerning to statistical significance analyses, of the 29 transcripts validated by quantitative real-time RT-PCR, 16 were significantly regulated ($P< 0.05$) after the expression of SHIP in Jurkat cells (clone no. 51) (55%) (Tables IX and X). In detail, five (5) out of the 11 transcripts confirmed as SHIP-induced were significantly increased: *SELL/CD62L, KLF2, BIN1, KCMF1,* and *KIAA0117.* Similarly, 11 out of the 18 genes confirmed as SHIP-repressed were significantly decreased: *PAG, TRIB3, ARRDC3, ARHGEF10, ATF5, TSC22, POLK, ZNF75, DNAJB9, IL26* and *C6orf160 (LOC441164).* Accordingly, of the 16 significantly SHIP-regulated genes, 5 genes were SHIP-induced (31%) and 11 genes SHIP-repressed (69%) at the transcriptional level. The genes were grouped according to function and/or localization

descriptions, as described before. Additionally, they were listed from top to bottom, according to the results obtained previously by microarray analysis.

By analysis of the 5 significantly SHIP-induced genes, it is shown on Table IX that the *SELL/CD62L* gene was the only up-regulated among the signal transduction/plasma membrane group (+180%). This gene codes for a selectin L, which is integral to the plasma membrane. Three (3) from the five (5) significantly SHIP-induced transcripts corresponded to proteins involved in transcription, cell cycle and/or localized in nucleus (60%): *KLF2, BIN1, KCMF1.* The *KLF2* and *BIN1* mRNAs were confirmed to be SHIP-induced by both technologies, microarray analysis and quantitative real-time RT-PCR, whereas *KCMF1* mRNA was confirmed to be SHIP-induced after quantitative real-time RT-PCR analysis, as shown previously. In spite of the fact that the direction of the change for *KCMF1* obtained by quantitative real-time RT-PCR differed from that obtained by microarray analysis, in this group, the gene for *KCMF1* was the most significantly strong induced (+260%), followed by the *KLF2* gene (+220%) (Table IX). Considering the high magnitude of the significance from the SHIP-induced leading genes after validation by quantitative real-time RT-PCR, those for *KLF2* and *SELL/CD62L* were at the top, with *P* values lower than 0.001 (Table IX).

Similarly, by analysis of the 11 transcripts identified as significantly SHIP-reduced by quantitative real-time PCR, it is shown on Table X that all coincided with microarray analysis. Four SHIP-reduced genes are grouped in category signal transduction/plasma membrane (36.3%): *PAG, TRIB3, ARRDC3,* and *ARHGEF10.* In this category, the gene for *TRIB3* was the most strongly SHIP-repressed at the transcriptional level (-78%), followed by the genes for *ARHGEF10* (-66%), *ARRDC3* (-55%), and *PAG* (-50%), respectively. Five (5) out of the eleven (11) SHIP-repressed transcripts corresponded to proteins involved in transcription, cell cycle and/or localized in the nucleus (45.5%): *ATF5, TSC22, POLK, ZNF75,* and *DNAJB9.* Of these, the genes for *ATF5* and *ZNF75* were the most strongly repressed (-79%), followed by *DNAJB9* (-64%). One of the additional two SHIP-repressed transcripts corresponded to *IL26,* the only gene identified as significantly regulated that codes for an interleukin, and was strongly SHIP-repressed (-76%) in Jurkat-SHIP cells. The other one corresponded to *C6orf160* (-41%), which codes for a hypothetical protein.

Table IX. Validation of statistically significant SHIP-induced genes by quantitative real-time RT-PCR.

Comparison of the data obtained using the Affymetrix platform with the statistically significant results from quantitative real-time RT-PCR experiments for genes that were induced after the expression of SHIP in Jurkat T-cells (clone no.51). Affymetrix and quantitative real-time RT-PCR are shown as a fold change of the level of mRNA from Jurkat-SHIP cells (clone no.51) with the induction of SHIP expression with Doxycycline, relative to the level of that transcript in the same cell line without induction of SHIP expression.

Gene Symbol [*Homo sapiens*]	Title [*Homo sapiens*]	Fold change Affymetrix (+/-)	Fold change LightCycler (+/-)	Statistical significance [a]
Signal Transduction/Plasma membrane				
SHIP1 [c]	**SH2 containing inositol 5' phosphatase**	**18.4** [c]	**3.5** [c]	**(**)**
SELL / CD62L	**Selectin L, lymphocyte adhesion molecule 1/ CD62 antigen ligand**	**2.6**	**2.8**	**(***)**
Transcription/Cell cycle/Nucleus				
KLF2	**Krüppel-like factor 2 (lung)**	**3.0**	**3.2**	**(***)**
BIN1	**Bridging integrator 1**	**2.3**	**1.3**	**(*)**
KCMF1 [b]	**Potassium channel modulatory factor 1**	**-2.6**	**3.6**	**(*)**
Unknown function				
KIAA0117	**KIAA0117 protein**	**2.8**	**1.2**	**(*)**

[a] Statistical analysis was performed with a Student's t-test and the P-value is indicated by asterisks. (*): $P < 0.05$; (**): $P < 0.01$; (***): $P < 0.001$

[b] Validation by quantitative Real-Time RT-PCR showed that the gene was up-regulated after the expression of SHIP.

[c] Positive control. Increased expression of *SHIP* from the inducible expression vector. The endogenous *SHIP* expression did not change after the ectopic expression of SHIP from the vector (see 5.3.3)

Table X. Validation of statistically significant SHIP-repressed genes by quantitative real-time RT-PCR.

Comparison of the data obtained using the Affymetrix platform with the statistically significant results from quantitative real-time RT-PCR experiments for genes that were induced after the expression of SHIP in Jurkat T-cells (clone no. 51). Affymetrix and quantitative real-time RT-PCR are shown as a fold change of the level of mRNA from Jurkat T-cells (clone no. 51) with the induction of SHIP expression with Doxycycline, relative to the level of that transcript in the same cell line without induction of SHIP expression.

Gene Symbol [*Homo sapiens*]	Title [*Homo sapiens*]	Fold change Affymetrix (+/-)	Fold change LightCycler (+/-)	Statistical significance [a]
Signal transduction/Plasma membrane				
PAG	**Phosphoprotein associated with glycosphingolipid-enriched microdomains**	**-5.3**	**-2.0**	**(***)**
TRIB3	**Tribbles homolog 3 (*Drosophila*)**	**-3.7**	**-4.5**	**(*)**
ARRDC3	**Arresting domain containing 3**	**-3.5**	**-2.2**	**(***)**
ARHGEF10	**Rho guanine nucleotide exchange factor (GEF) 10**	**-2.1**	**-2.9**	**(*)**
Transcription/Cell cycle/Nucleus				
ATF5	**Activating transcription factor 5**	**-3.7**	**-4.8**	**(*)**
TSC22	**Transforming growth factor-beta-stimulated protein TSC22**	**-3.3**	**-1.3**	**(*)**
POLK	**Polymerase (DNA directed) kappa**	**-2.0**	**-1.7**	**(*)**
ZNF75	**Zinc finger protein 75 (D8C6)**	**-2.0**	**-4.7**	**(**)**
DNAJB9	**DnaJ (Hsp40) homolog, subfamily B, member 9/Microvascular endothelial differentiation gene 1**	**-3.3**	**-2.8**	**(**)**
Cell-cell signaling				
IL26	**Interleukin 26**	**-2.3**	**-4.1**	**(*)**
Unknown function				
C6ORF160 (LOC441164)	**Chromosome 6 open reading frame 160/ (LOC441164)**	**-2.0**	**-1.7**	**(*)**

[a] Statistical analysis was performed with a Student's t-test and the P-value is indicated by asterisks. (*): $P < 0.05$; (**): $P < 0.01$; (***): $P < 0.001$

Considering the high magnitude of the significance, it was shown that from the validated SHIP-repressed leading genes, those for *ARRDC3* and *PAG* were at the top of the SHIP-repressed genes, with *P* values lower than 0.001 (Table X).

By limiting the analysis to genes with at least two-fold significant change in the level of expression, 11 genes out of the 16 significantly SHIP-regulated were identified and selected (69%) (Tables XI and XII). Of these 11, three (3) of them were at least 2-fold significantly SHIP-induced (27%): *SELL/CD62L, KLF2, KCMF1,* and eight (8) were at least 2-fold significantly SHIP-repressed (73%): *PAG, TRIB3, ARRDC3, ARHGEF10, ATF5, ZNF75, DNAJB9, IL26* (Tables XI and XII). All of them showed high correlation to the microarray data, with the exception of *KCMF1*, whose transcript was demonstrated to be SHIP-induced. In the category signal transduction/plasma membrane, there is only one member, the transcript corresponding to *SELL/CD62L,* which was significantly 2.8-fold SHIP-induced (Table XI). In contrast, in the same category were confirmed the significant SHIP-mediated transcriptional repression (≥2-fold) of four genes, *TRIB3, ARHGEF10, ARRDC3*, and *PAG*, respectively (Table XII). In the category transcription/cell cycle/nucleus, two members, *KCMF1* and *KLF2* were shown to be significantly 3.6-fold and 3.2-fold SHIP-induced in Jurkat cells (Table XI). Similarly, in the same family the significant SHIP-mediated transcriptional repression (≥2-fold change) of three members, *ATF5, ZNF75,* and *DNAJB9,* respectively, was confirmed (Table XII). The only gene that codes for one interleukin that was confirmed as significantly SHIP-regulated was the *IL26* gene, whose transcript was strongly repressed (Table XII).

Accordingly, it was confirmed by quantitative real-time RT-PCR that SHIP regulated significantly at least 2-fold the transcriptional expression of 11 genes: 3 were significantly SHIP-induced (27%) and 8 significantly SHIP-repressed (73%) at the transcriptional level. The data indicate that SHIP is more implicated in the repression of genes. Additionally, SHIP has a specific effect in regulation of genes involved in signal transduction, transcription and cell cycle control. The regulation of only one interleukin indicates the high specificity of the SHIP effect on transcriptional regulation of genes included in this category. Considering the genes expressed in T cells, *SELL/CD62L, KLF2, PAG* and *IL26* were found.

Table XI. Validation of significantly SHIP-induced genes (≥ 2.0-fold) by quantitative real-time RT-PCR in Jurkat-SHIP cells [a].

Comparison of the data obtained using the Affymetrix platform with the statistically significant results from quantitative real-time RT-PCR experiments for genes that were at least 2-fold significantly induced after the expression of SHIP in Jurkat T-cells (clone no. 51). Affymetrix and quantitative real-time RT-PCR are shown as a fold change of the level of mRNA from Jurkat-SHIP cells (clone no. 51) with the induction of SHIP expression with Doxycycline, relative to the level of that transcript in the same cell line without induction of SHIP expression.

Gene Symbol [*Homo sapiens*]	Title [*Homo sapiens*]	Fold change Affymetrix (+/-)	Fold change LightCycler (+/-)	Description / Gene Ontology [b]
Signal Transduction/Plasma membrane				
SELL / CD62L	**Selectin L, lymphocyte adhesion molecule 1/ CD62 antigen ligand**	**2.6**	**2.8**	**L-selectin is expressed on naive T cells (Janeway *et al.*, 1999)/GO Biological Process: 7155:** cell adhesion (TAS)**; 6952:** defense response (IEA)**; 7157:** heterophilic cell adhesion (IEA)/ **GO Cellular Component: 5887**: integral to plasma membrane (TAS)/ **GO Molecular Function: 5194:** cell adhesion molecule activity (IEA); **42064:** cell adhesion receptor regulator (IEA);**8337:** selectin (TAS); **5529:** sugar binding (IEA)**/cDNA sources: AML, CLL.**
Transcription/Cell cycle/Nucleus				
KLF2/LKLF	**Krüppel-like factor 2 (lung)/ Lung Krüppel-like transcription factor**	**3.0**	**3.2**	**Expression of LKLF in Jurkat T cells is sufficient to program a quiescent phenotype (Buckley *et al*, 2001) /KLF2 inhibits Jurkat T leukemia cell growth via upregulation of cyclin-dependent kinase inhibitor p21WAF1/CIP1 (Wu and Lingrel, 2004) / GO Molecular Function: 3700:** transcription factor activity (NAS); **16563:** transcriptional activator activity (NAS)/ **GO Cellular Component: 5634:** nucleus (NAS).
KCMF1	**Potassium channel modulatory factor 1**	**-2.6[c]**	**3.6**	**Zinc finger, ZZ domain containing 1; differentially expressed in branching tubulogenesis 91; FGF-induced ubiquitin-protein ligase in gastric cancers/GO Molecular Function: 3676:** nucleic acid binding (IEA); **5216:** ion channel activity (IEA); **8270:** zinc ion binding (IEA)**/GO Cellular Component: 5634:** nucleus (IEA)**.**

[a] Induced genes (≥ 2.0-fold), compared by quantitative real-time RT-PCR and Affymetrix Microarray analyses.
[b] TAS: traceable author statement; IEA: inferred from electronic annotation; NAS: non-traceable author statement (Butler and Harris, 2000)
[c] Validation by quantitative real-time RT-PCR showed that the gene was up-regulated after the expression of SHIP.

Table XII. Validation of significantly SHIP-repressed genes (≥ 2.0-fold) by quantitative real-time RT-PCR in Jurkat-SHIP cells [a].

Comparison of the data obtained using the Affymetrix platform with the statistically significant results from quantitative real-time RT-PCR experiments for genes that were at least 2-fold significantly repressed after the expression of SHIP in Jurkat T-cells (clone no. 51). Affymetrix and quantitative real-time RT-PCR are shown as a fold change of the level of mRNA from Jurkat-SHIP cells (clone no. 51) with the induction of SHIP expression with Doxycycline, relative to the level of that transcript in the same cell line without induction of SHIP expression.

Gene Symbol [*Homo sapiens*]	Title [*Homo sapiens*]	Fold change Affymetrix (+/-)	Fold change LightCycler (+/-)	Description / Gene Ontology [b]
Signal transduction/Plasma membrane				
PAG	**Phosphoprotein associated with glycosphingolipid -enriched microdomains**	**-5.3**	**-2.0**	**The protein encoded by this gene is a type III transmembrane adaptor protein that binds to the tyrosine kinase csk protein. It is thought to be involved in the regulation of T cell activation** (Brdicka *et al,* 2000)./**GO Biological Process:7165:** signal transduction (experimental evidence)/**GO Molecular Function:5068:** transmembrane receptor protein tyrosine kinase adaptor protein activity (NR)/**GO Cellular Component:5887:** integral to plasma membrane (NR).
TRIB3	**Tribbles homolog 3 (*Drosophila*)**	**-3.7**	**-4.5**	**GO Biological Process:6468:** protein amino acid phosphorylation (IEA); **6915:** apoptosis (IEA)/**GO Molecular Function**:4672: protein kinase activity (IEA); **5524:** ATP binding (IEA)/ **GO Cellular Component: 5634:** nucleus (ISS)/**Protein Domains:** MAP kinase activated protein kinase 2, mapkap2 (scop);Protein kinase (InterPro);Serine/threonine protein kinase (InterPro).
ARRDC3	**Arresting domain containing 3**	**-3.5**	**-2.2**	**GO Biological Process:7165:** signal transduction (IEA); **7600:** sensory perception (IEA).
ARHGEF10	**Rho guanine nucleotide exchange factor (GEF) 10**	**-2.1**	**-2.9**	**ARHGEF10 is a member of the family of Rho guanine nucleotide exchange factors (GEFs), which are implicated in neural morphogenesis and connectivity and regulate the activity of small Rho GTPases by catalyzing the exchange of bound GDP by GTP (Verhoeven *et al.,* 2003)/GO Molecular Function: 5085:** guanyl-nucleotide exchange factor activity (IEA).

Gene Symbol [*Homo sapiens*]	Title [*Homo sapiens*]	Fold change Affymetrix (+/-)	Fold change LightCycler (+/-)	Description / Gene Ontology [b]
Transcription/Cell cycle/Nucleus				
ATF5	**Activating transcription factor 5**	**-3.7**	**-4.8**	**GO Biological Process:6357:** regulation of transcription from Pol II promoter (TAS);**74:** regulation of cell cycle (TAS)**/GO Molecular Function:3677:** DNA binding (IEA);**3714:** transcription co-repressor activity (TAS)**;3702:** RNA polymerase II transcription factor activity (TAS)**/GO Cellular Component: 5634:** nucleus (IEA).
ZNF75	**Zinc finger protein 75 (D8C6)**	**-2.0**	**-4.7**	**GO Biological Process:6355:** regulation of transcription, DNA-dependent (NAS)/ **GO Molecular Function:3677:** DNA binding (NAS); **8270:** zinc ion binding (NAS)/ **GO Cellular Component: 5634:** nucleus (NAS).
DNAJB9	**DnaJ (Hsp40) homolog, subfamily B, member 9**	**-3.3**	**-2.8**	**GO Biological Process: 6457:** protein folding (IEA)**/ GO Molecular Function: 3754:** chaperone activity (IEA)/**GO Cellular Component: 5634:** nucleus (IEA)**.**
Cell-cell signaling				
IL26	**Interleukin 26**	**-2.3**	**-4.1**	**Detected transcripts in a series of leukemia T-cell lines but not in B-cell lines; novel cellular homolog of IL-10 (Knappe *et al.,* 2000)/GO Biological Process:7267:**cell-cell signaling (TAS); **6955:** immune response (IEA)**/GO Molecular Function: 5125:** cytokine activity (IEA)**/ GO Cellular Component: 5625:** soluble fraction (TAS)**; 5615:** extracellular space (TAS).

[a] Repressed genes (≥ 2.0-fold), compared by quantitative real-time RT-PCR and Affymetrix Microarray analyses.
[b] NR: not recorded; IEA: inferred from electronic annotation; TAS: traceable author statement; NAS: non-traceable author statement; ISS: inferred from sequence or structural similarity (Butler and Harris, 2000).

KLF2 and *IL26* have been detected in leukemia T-cell lines (Tables XI and XII). Interestingly, *KLF2* expression is described to be sufficient to program a quiescent phenotype in Jurkat T cells (Buckley *et al,* 2001). This effect is analog to that shown before (Horn, 2003) on proliferation after the expression of SHIP. Therefore, KLF2 was chosen to be analyzed in association with the biology of Jurkat cells.

5.4. SHIP-mediated up-regulation of the T cell quiescent factor KLF2 in Jurkat T cells

Because KLF2 is involved in quiescence in naive T-cells and negative regulation on Jurkat T leukemia cell growth (Buckley *et al,* 2001; Wu and Lingrel, 2004), the SHIP-mediated up-regulation of the *KLF2* gene in Jurkat-SHIP cells (clone no. 51) was of particular interest. It has been shown in our laboratory that the expression of SHIP in Jurkat T-cells led to inhibition of proliferation (Horn *et al,* 2004). Therefore, it is possible that a relationship exists between the SHIP-mediated up-regulation of *KLF2* and the proliferation in Jurkat T-cells.

5.4.1 *KLF2* mRNA levels increased after the restoration of SHIP in Jurkat T cells

Microarray data revealed that *KLF2* was up-regulated 3.0-fold in Jurkat-SHIP cells after induction of SHIP expression (Table XI). In order to validate this result, the relative increase in mRNA was measured by quantitative real-time PCR using the LightCycler, following the protocols described in Material and Methods. It was confirmed that *KLF2* was up-regulated, 3.2-fold in Jurkat-SHIP cells after induction of SHIP expression (Table XI, Figures 15 and 16). As shown in Figure 15, the *KLF2* expression was increased after restoration of SHIP activity in comparison to the control gene (GAPDH), plotted as log of fluorescence versus cycle number (Garcia-Palma *et al,* 2005a). Following normalization with *GAPDH* and differential expression analysis, real-time quantitative RT-PCR of three independent experiments revealed a 3.2 ± 1.1-fold increase in SHIP-dependent *KLF2* mRNA expression that was statistically significant (Figure 16).

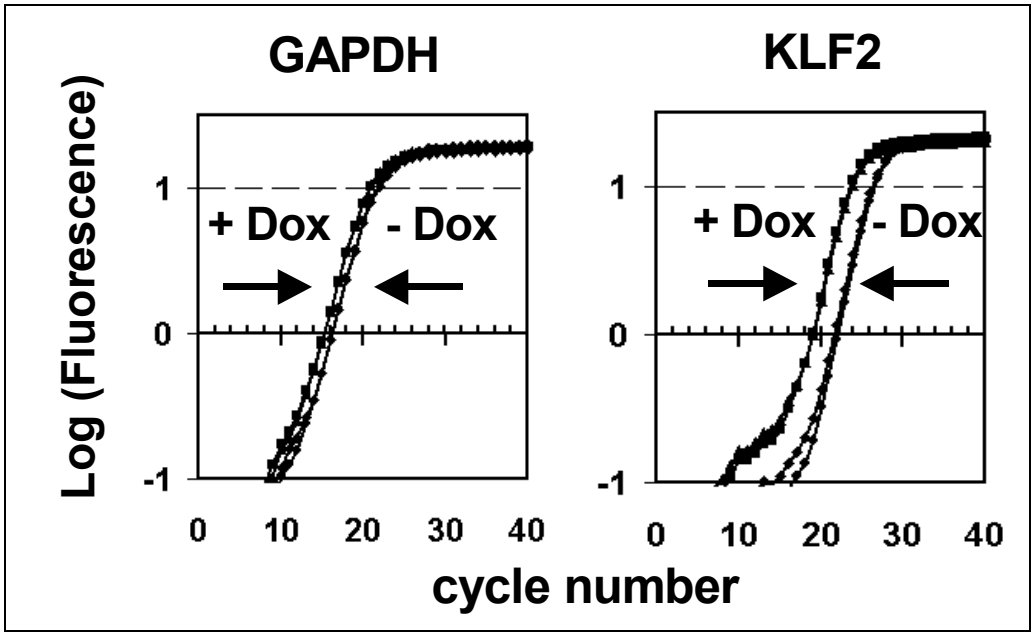

Figure 15. Inducible expression of SHIP in Jurkat cells up-regulates the expression of the *Krüppel-like factor 2* (*KLF2*).

Jurkat-SHIP cells (clone no. 51) were grown for 72 h either in medium containing 0.8 µg/ml doxycycline (Dox) to induce the expression of SHIP (+Dox) or in the same medium without doxycycline (-Dox). The results of one representative quantitative real-time polymerase chain reaction (RT-PCR) experiment run in duplicates after amplification of the house keeping gene *GAPDH* and the target gene *KLF2* from Jurkat-SHIP cells, which either express SHIP (+Dox) or do not express SHIP (-Dox), are shown as log of fluorescence vs. cycle number. (Modified from Garcia-Palma *et al,* 2005a).

5.4.2 Increase of KLF2 protein levels and reduction of phosphorylation on Akt after the restoration of SHIP in Jurkat T cells

To confirm changes at the protein level, the amount of KLF2 protein was analyzed by Western blotting using anti-KLF2 antibodies, and the chemiluminescence's signals were measured with an LAS3000 Imager using the AIDA software (Raytest/Fuji, Straubenhardt, Germany). Preliminary western blotting analyses were performed to confirm the differential regulation of KLF2 obtained by microarray and quantitative real-time PCR results at the protein level (Figure 17). Figure 17 shows the evidence that KLF2 protein levels are increased after the restoration of SHIP in Jurkat-SHIP cells (clone no. 51). Further western blot analyses were performed to study the relationship between KLF2, SHIP and the PI3K/Akt pathway. Therefore, the phosphorylation on Akt at residue serine 473 was in addition analyzed, as an indirect measurement of activity of this protein.

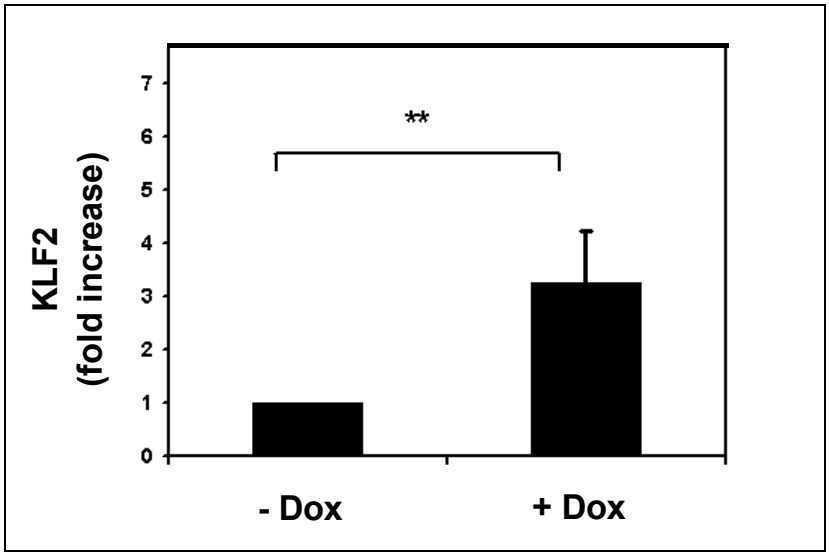

Figure 16. Quantification of the SHIP-induced *Krüppel-like factor 2* (*KLF2*) mRNA expression in Jurkat cells.

Jurkat-SHIP cells (clone no. 51) were grown as described in Figure 15. Quantification of the relative *KLF2* expression from three independent experiments in comparison with the housekeeping gene (*GAPDH*) revealed a relative 3.2-fold increase of *KLF2* cDNA after induction of SHIP expression. The value represents the mean ± SD of three independent experiments, normalized to the *GAPDH* expression levels. Each sample was performed in duplicate by quantitative real-time RT-PCR, at least two times. Statistical analysis was performed with a Student's *t*-test and the *P*-value is indicated by asterisks (**$P < 0.001$). (Modified from Garcia-Palma *et al,* 2005a).

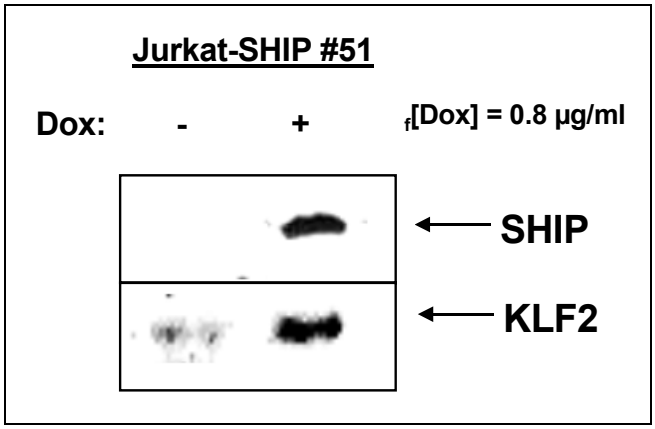

Figure 17. Validation of the increase of Krüppel-like factor 2 (KLF2) protein levels after the expression of SHIP in Jurkat cells.

Jurkat-SHIP cells (clone no. 51) were treated with or without doxycycline (Dox) as described in Figure 15. Cell lysates were prepared in NP40 Buffer and protein quantification analysis was performed. The lysates containing 100 µg of protein were separated in SDS-polyacrylamide gels. Preliminary Western blot analyses were performed with antibodies specific for SHIP and KLF2. In the representative experiment, the relative protein levels of KLF2 and SHIP are shown. The signals obtained with the antibodies specific for MAPK revealed that the levels of this protein were unchanged after the expression of SHIP (data not shown). $_f$[Dox]: final concentration of Doxycycline.

After induction of SHIP expression by the addition of doxycycline (Dox), the constitutive phosphorylation of Akt at serine residue 473 was strongly reduced to 20% (Figure 18). Simultaneously, the expression of KLF2 protein level was increased twofold relative to the expression of GAPDH protein level (Figure 18). It was also confirmed that GAPDH is neither regulated at the mRNA level nor protein level after the expression of SHIP in Jurkat cells (Figures 15 and 18).

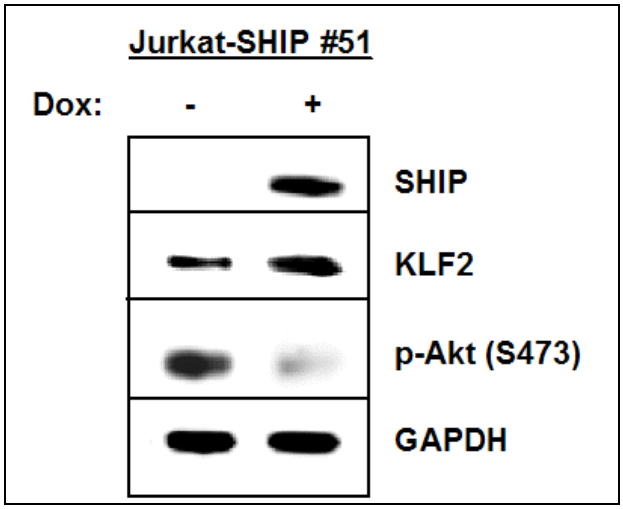

Figure 18. Krüppel-like factor 2 (KLF2) protein levels are increased after the expression of SHIP in Jurkat cells.

Jurkat-SHIP cells (clone no. 51) were grown and treated with or without doxycycline (Dox) as described in Figure 15. Cell lysates were prepared in NP40 Buffer, corresponding to three independent experiments (data not shown). Cell lysates containing 35 µg of protein were separated in 4%-12% Bis-Tris gradient gels. Western blot analyses were performed with antibodies specific for SHIP, KLF2, phosphorylated Akt (serine residue 473) and GAPDH. In the representative experiment, the quantification of protein levels and relative phosphorylation on Akt by the use of the AIDA Software is shown. Phosphorylation on Akt at residue serine 473 was reduced to 20%, whereas KLF2 protein levels were increased to 200%. The signals obtained with the antibodies specific for GAPDH showed that the levels of this protein were unchanged after the expression of SHIP. $_{f}$[Dox]: final concentration of Doxycycline. (Modified from Garcia-Palma *et al,* 2005a).

Parallel western blot analyses additionally confirmed that the amount of KLF2 increased similarly twofold relative to the amount of MAP-Kinase Erk2, and confirmed the reduction of the phosphorylation on Akt to 25% (Figure 19). In Figures 18 and 19 is shown that the constitutive phosphorylation at residue serine 473 of the protein kinase Akt in Jurkat T-cells is reduced after the restoration of SHIP. Simultaneously, the increase in the KLF2 protein levels, in comparison to the control, was confirmed.

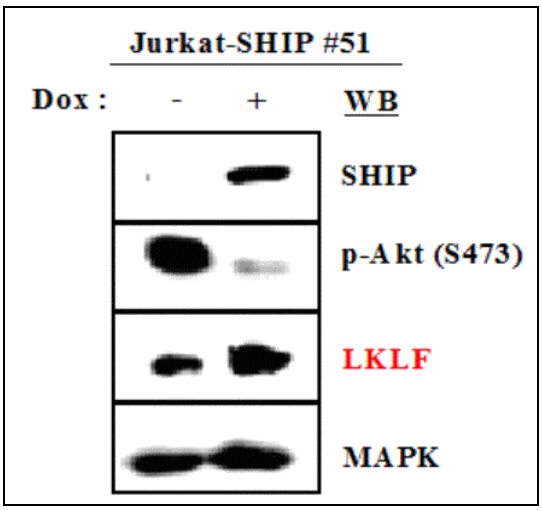

Figure 19. Western Blot analysis from the expression of KLF2 (LKLF) and phosphorylation of Akt (S473) in Jurkat-SHIP cells.

Cell lysates from Jurkat-SHIP cells (clone no. 51) were prepared in NP40 Buffer, as described in Figure 9. Cell lysates containing 100 µg of protein were separated in SDS-polyacrylamide gels and western blot analyses were performed with antibodies specific for SHIP, phosphorylated Akt (serine residue 473) and MAPK (Erk1 and Erk2). LKLF: KLF2. WB: western blot. Dox: Doxycycline.

5.5. Biological function of the T cell quiescent factor KLF2 in Jurkat-SHIP cells

After biochemical analysis of SHIP-mediated up-regulation of KLF2 in Jurkat T cells, and the examination of the PI3K/Akt signaling pathway and GAPDH and MAPK expressions, the biological function of KLF2 in Jurkat T-cells was researched, specifically the effect on proliferation. Additionally, it was analyzed the effect that both had on proliferation, the restoration of SHIP and the ectopic expression of KLF2, in vitro.

5.5.1. KLF2 has an inhibitory effect on proliferation in Jurkat T cells

In order to study the biological function of the T-cell quiescent factor 2 (KLF2) in Jurkat T cells, and the relationship with SHIP, proliferation analyses were performed in Jurkat T cells after the ectopic expression of KLF2, SHIP or both, KLF2 and SHIP. Proliferation assays were carried out by measuring BrdU incorporation into newly synthesized DNA in Jurkat-SHIP cells (clone no. 51) after transient transfection with the corresponding vector and

plasmid control, using FACS analysis. At least three independent experiments using sister cultures of Jurkat-SHIP cells (clone no. 51) were considered in each case.

5.5.2. Standardization of the transient transfection in Jurkat-SHIP cells

Firstly, the standardization of the transfection conditions by electroporation in Jurkat-SHIP cells (clone no. 51) was performed, with and without induction with Doxycycline (data not shown). The vector pEGFP-N1 (Clontech) was used as control for the optimization of the transfection conditions (data not shown). The parameters used in transfection after standardization are described in Materials and Methods. The vector pEGFP-N1 was used on every occasion in the performed transient transfections.

5.5.3. Standardization of the BrdU assay conditions in Jurkat-SHIP cells

BrdU (an analog of the DNA precursor thymidine) is incorporated into newly synthesized DNA by cells entering and progressing through the S (DNA synthesis) phase of the cell cycle (Gratzner and Leif, 1981; Miltenburger *et al,* 1987; Sasaki *et al,* 1989; Vanderlaan and Thomas, 1985). Prolonged exposures of cells to BrdU allows for the identification and analysis of actively cycling, as opposed to non-cycling, cell fractions. Pulse labeling of cells with BrdU at various time points, permits the determination of cell cycle kinetics. The bromodeoxyuridine (BrdU) incubation conditions were standardized for Jurkat-SHIP cells (clone no. 51). Thus, it was possible whit this high-resolution technique to determine the frequency of individual cells that have synthesized DNA. In order to achieve that, sister cultures were grown in the absence of doxycycline for 72h, changing the medium each 48h, followed by pulse labeling of cells with BrdU at various time points, in order to determine the cell cycle kinetics. The subsequently staining was performed with anti-BrdU-antibodies coupled to allophycocyanin (APC), according to the protocol of the manufacturer (BD Biosciences), with the corresponding controls. The BrdU-APC positive cells were analyzed by flow cytometry, in collaboration with Dr. Haag (Institute of Immunology, UKE). The percentage of BrdU incorporation was calculated for each population at each time point (Figure 20). Cells from the same population that were not BrdU-labeled were used as negative staining control for the assay (data not shown).

In Figure 20 are shown the percentages of cells that have incorporated BrdU in the time course study of BrdU pulsing. After pulse labelings of 1h 40min, 5h and 16h, the frequency of

cells that incorporated BrdU was 24%, 31% and 58%, respectively. It was determined that the optimal pulse labeling for subsequently proliferation experiments was a prolonged exposure of 15h of the cells to BrdU, which permitted identified approximately a 58% of actively synthesized DNA (BrdU incorporation).

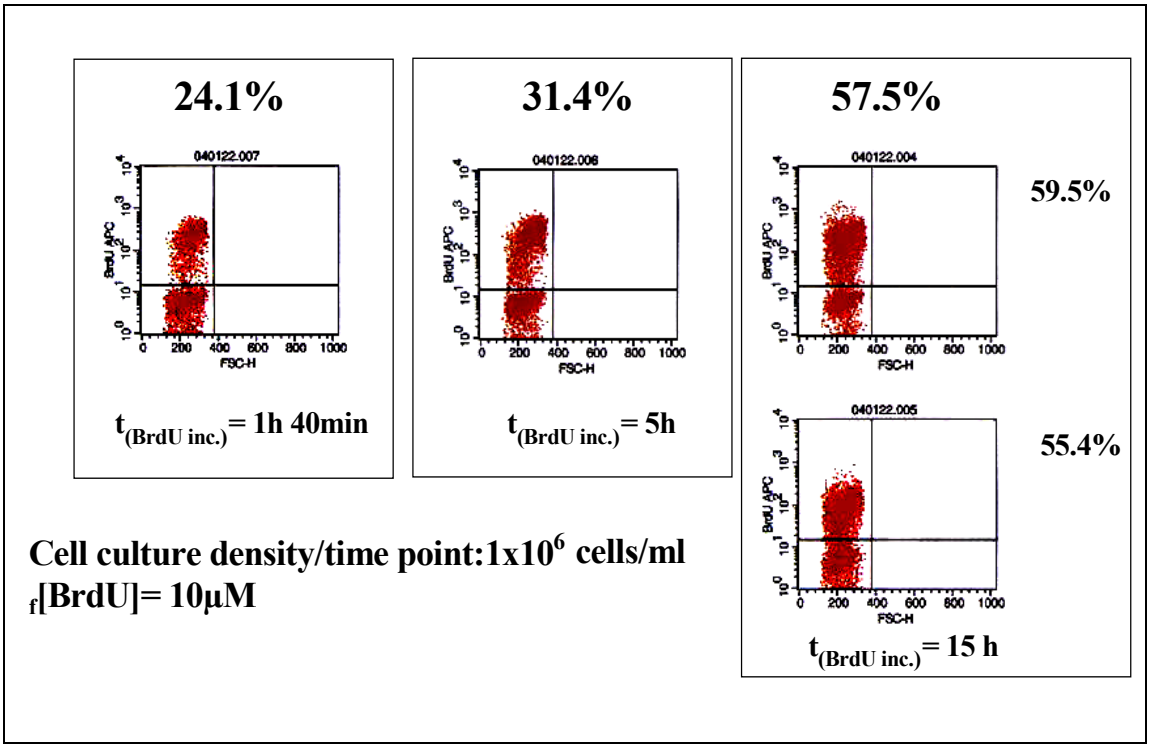

Figure 20. Flow cytometry analyses of Jurkat-SHIP cells for time course study of BrdU pulsing.

Jurkat-SHIP cells (clone no. 51) were grown in sister cultures for 72 h in the absence of doxycycline, followed by pulse labeling with 10µM BrdU at various time points. The cells were the harvested and staining with APC anti-BrdU, according to the protocol of the manufacturer (BD Biosciences). The BrdU-APC positive cells were analyzed by flow cytometry with a BD FACSCalibur. The percentage of BrdU incorporation was calculated for each population at each time point. Cell culture densities and final BrdU concentrations are indicated. The levels of cell-associated BrdU from representative experiments are shown as percentages. For $t_{(BrdU\ inc.)}$ = 15 h the percentages of two representative experiments are shown, and the mean value is shown above.

5.5.4. Analysis of the inhibitory effects of SHIP expression on the proliferation of Jurkat T cells

It has been reported that SHIP is a negative regulator of the proliferation (Horn, 2003). To confirm these results in Jurkat-SHIP cells clone no. 51, the expression of SHIP in these cells

was induced, and FACS analysis of newly synthesized DNA by BrdU incorporation were performed. Sister cultures of Jurkat-SHIP cells (clone no. 51) were grown in the presence or absence of doxycycline for 72h, changing the medium each 48h, followed by approx. 15h pulse labeling of cells with BrdU. The subsequently staining was performed as described on 5.5.3. The BrdU-APC positive cells were analyzed by flow cytometry. The percentage of BrdU incorporation was calculated for each population (Figure 21). Cells from the same population that were not BrdU-labeled were used as negative staining control for the assay.

Figure 21 shows the percentages of cells that have incorporated BrdU in two representative experiments in the presence or absence of SHIP expression in Jurkat-SHIP cells (clone no. 51), respectively. The frequency of cells that incorporated BrdU with SHIP expression was 47.7% and 46.4%, in comparison to 59.5% and 55.4% without SHIP expression, respectively. It was determined an approximately 10.4 % reduction of cells that were actively synthesizing DNA (BrdU incorporation) after the expression of SHIP in Jurkat T-cells.

5.5.5. Inhibitory effects of the Krüppel-like factor 2 (KLF2) and SHIP expression on the proliferation of Jurkat cells

The inhibitory effect of KLF2 on the proliferation of T cells, including Jurkat T cells has been demonstrated before (Buckley *et al,* 2001; Wu and Lingrel, 2004). To confirm these results in Jurkat-SHIP cells (clone no. 51) and to analyze whether the inhibitory effect of KLF2 on the proliferation of Jurkat cells could be increased by co-expression of SHIP, the KLF2 protein was expressed in Jurkat-SHIP cells grown either in the presence or absence of SHIP expression. The cells were stably transfected using the optimal electroporation conditions, and subsequently labeled with BrdU, as described in 5.5.2. and 5.5.3. The vectors used in the analysis were pKLF2-EGFP (EGFP: enhanced green fluorescent protein), kindly provided by Dr. Haag, from the Institute of Immunology (UKE, Hamburg) and the plasmid control pEGFP-N1 (Clontech) without insert. The vectors were amplified in *E. coli* host strains and plasmid preparations were performed. Validation control experiments were performed before the proliferation assays were carried out, as described in Material and Methods (data not shown).

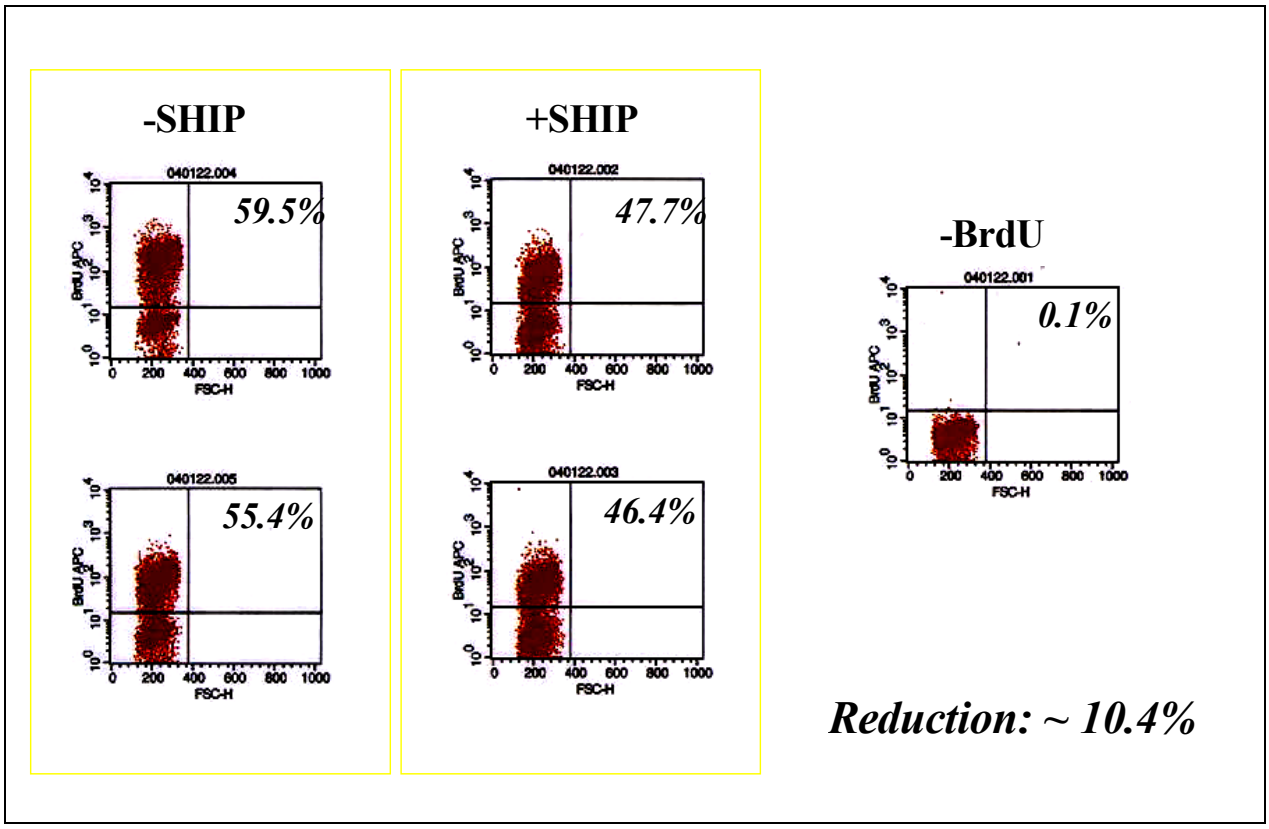

Figure 21. SHIP leads to a partial reduction of BrdU incorporation into newly synthesized DNA in Jurkat-SHIP cells.

Jurkat-SHIP cells (clone no. 51) were grown in sister cultures for 72 h in the presence of doxycycline, in order to induce the expression of SHIP (+ SHIP), and in the absence of doxycycline (-SHIP). After approx. 15h pulse labeling with 10µM BrdU, the cells were harvested and stained with APC anti-BrdU, according to the protocol of the manufacturer (BD Biosciences). The BrdU-APC positive cells were analyzed by flow cytometry with a BD FACSCalibur. The percentage of BrdU incorporation was calculated for each population. Cell culture densities and final BrdU concentrations were used as described on Figure 20. The levels of cell-associated BrdU from two representative experiments are shown as percentages. The approximate percentage of reduction of BrdU incorporation after the expression of SHIP in comparison to the control (-SHIP) is shown. The negative control used for the FACS analysis is shown (-BrdU).

Proliferation of the transfected cells was analyzed by measuring the bromodeoxyuridine (BrdU) incorporation and the percentage of BrdU-positive cells in the enhanced green fluorescent protein (EGFP)-gated population was determined by FACS analysis. The percentages of EGFP-positive cells that have incorporated BrdU in each population from four representative experiments are shown in Figure 22. The control cells, corresponding to the expression of the vector without insert (EGFP) and without induction of SHIP expression (-Dox), shown 24.1% incorporation of BrdU in the gated population. The sole expression of

SHIP led to a 9.1% incorporation of BrdU in the gated population. The frequency of cells that incorporated BrdU after the ectopic expression of KLF2 gated in M1 was 12.3%, without induction of SHIP expression, and 3.2% after SHIP expression, respectively.

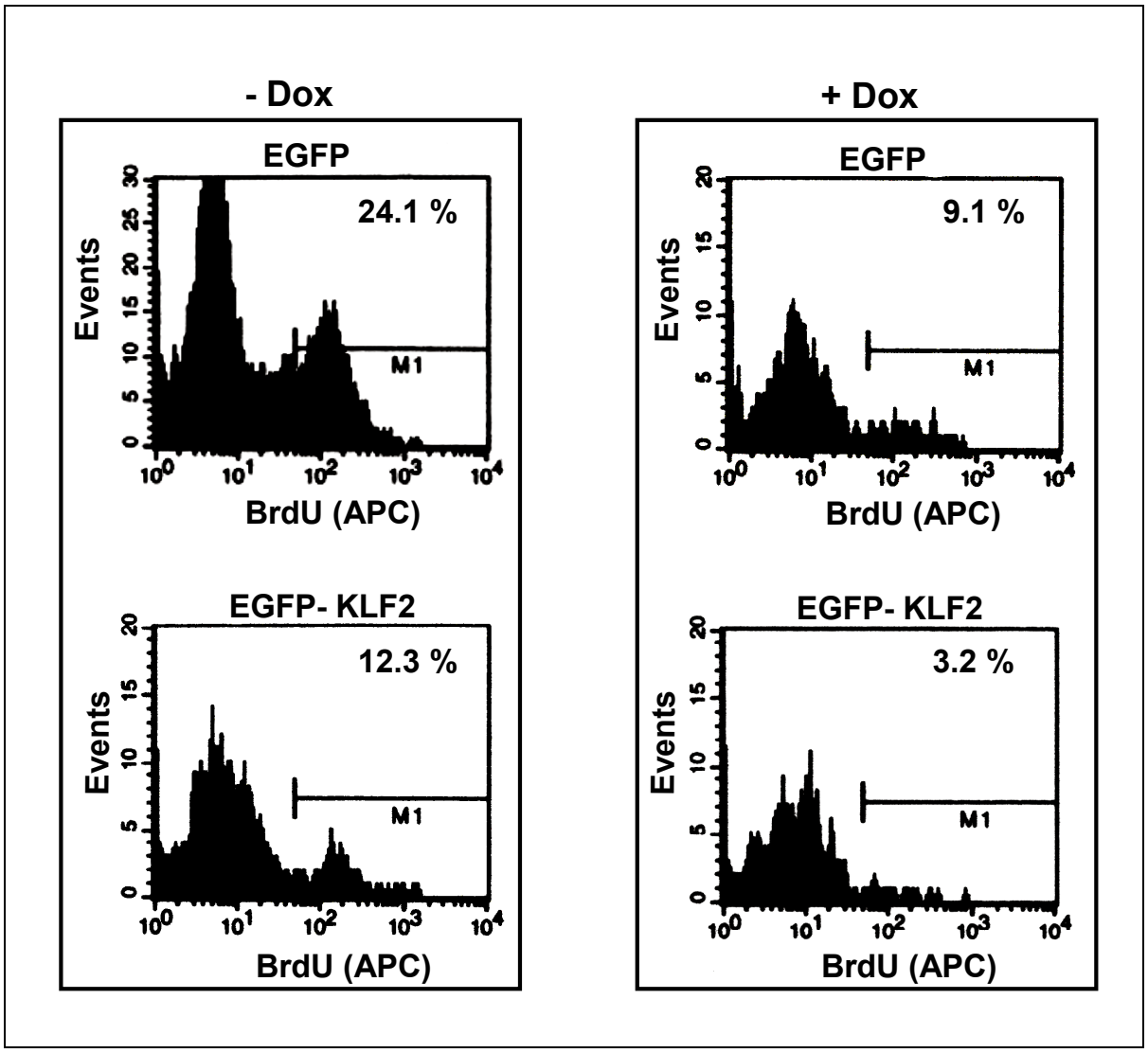

Figure 22. KLF2 has an inhibitory effect on the proliferation of Jurkat T cells.

Sister cultures of Jurkat-SHIP cells (clone no. 51) were grown for 48 h in the absence (-Dox) or presence (+Dox) of 0.8 µg/ml doxycycline. The cells were then stably transfected by electroporation procedures as described in Materials and Methods, either with 10µg of a vector containing EGFP or the EGFP-KLF2 vector. The cells were grown for additionally 24h before treatment with BrdU. After 15h labeling with 10 µM BrdU, the cells were stained with anti-BrdU antibodies coupled to the fluorochrome allophycocyanine (APC) and analyzed by flow cytometry. The BrdU-APC positive cells in the EGFP-gated population were measured. The percentages of BrdU-APC positive cells, determined by setting a gate (M1) on cells with a higher fluorescent intensity than the negative control (cells not labeled with BrdU), are shown for each representative experiment. (Modified from Garcia-Palma *et al,* 2005a).

Comparative analyses of the data shown in Figure 22 relative to the control (EGFP, -Dox) indicated that approximately 51% of the cells synthesized actively DNA (BrdU incorporation) after the ectopic expression of KLF2. Similarly, after expression of SHIP alone, 38% of cells actively synthesized DNA. When both, KLF2 and SHIP were expressed, 13% of cells synthesized actively DNA. Accordingly, it was shown that KLF2 has an inhibitory effect on the active synthesis of DNA, in a lower extent when compared to SHIP. Interestingly, when both KLF2 and SHIP are expressed in Jurkat T-cells, the inhibitory effect is further increased.

After proliferation analysis of at least three independent experiments, the inhibitory effect of KLF2 on the proliferation of Jurkat T-cells was confirmed. Mean values of three independent experiments with standard deviations are shown in Figure 23. The results indicate that the proliferation was reduced by 45.2% ± 5.1% in cells transfected with the KLF2-EGFP vector, relative to cells transfected with the parental EGFP vector. This was a similar reduction (60.3% ± 14.4%) in proliferation observed after expression of SHIP (+Dox). Co-expression of SHIP and KLF2 further reduced the proliferation significantly, i.e. by 83.7% ± 2.2% (P = 0.02), suggesting an additive effect of SHIP and KLF2 on the proliferation of Jurkat cells (Garcia-Palma *et al,* 2005a). As shown on Table XIII, FACS analysis of Jurkat T-cells after the induced expression of SHIP and ectopic expression of KLF2 revealed a partial reduction of incorporation of BrdU into newly synthesized DNA by cells entering and progressing through the S (DNA synthesis) phase of the cell cycle. The strong reduction of DNA synthesis after the expression of both, KLF2 and SHIP, revealed an additive effect of both in the negative regulation of proliferation in Jurkat T-cells.

5.5.6. Correlation between the protein expression levels of the Krüppel-like factor 2 (KLF2) and their inhibitory effect on newly synthesized DNA in Jurkat cells

The inhibitory effect of KLF2 on the proliferation of Jurkat T-cells was demonstrated, as shown in 5.5.5. To ascertain the correlation between the KLF2 protein levels and the inhibitory effect on newly synthesized DNA, the distribution of BrdU incorporation in function of the fluorescence intensity levels of expressed EGFP-KLF2 after the restoration of SHIP was measured, by using the populations analyzed by FACS (Figure 24).

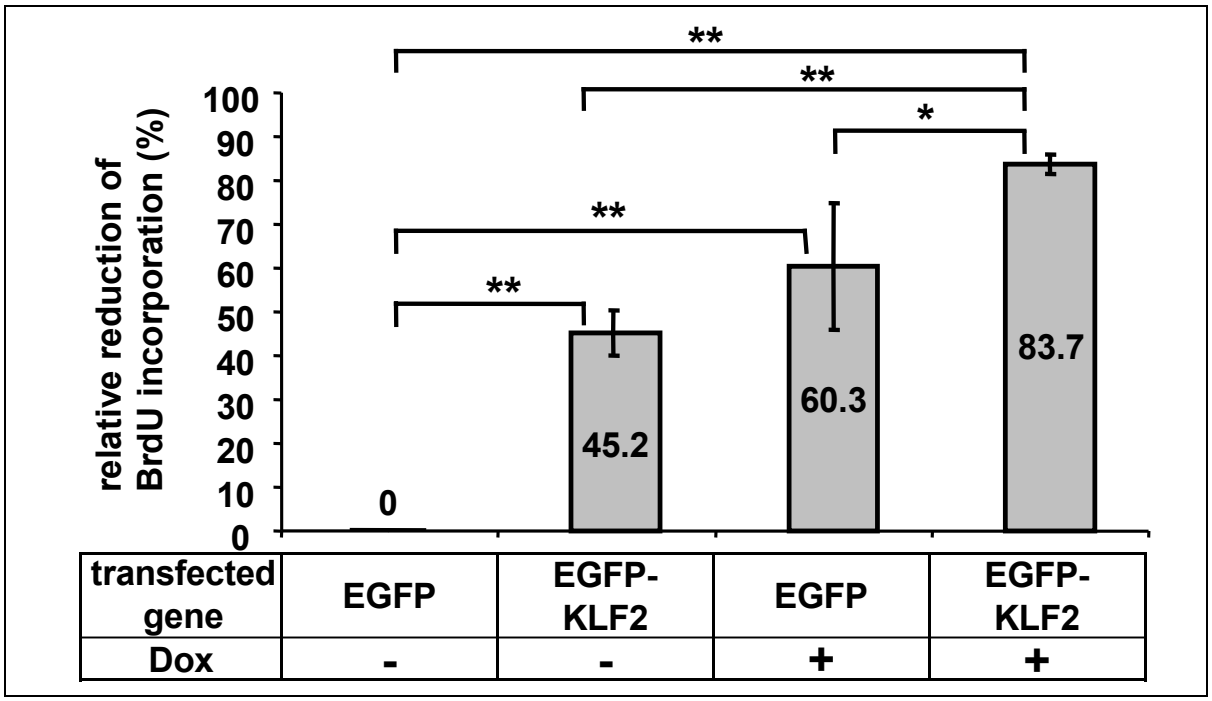

Figure 23. Inhibitory effects of SHIP and Krüppel-like factor 2 (KLF2) on the proliferation of Jurkat T cells.

Sister cultures of Jurkat-SHIP cells (clone no. 51) were grown for 48 h in the absence (-Dox) or presence (+Dox) of 0.8 µg/ml doxycycline. The cells were then stably transfected, labeled, stained with anti-BrdU antibodies coupled to the fluorochrome allophycocyanine (APC) and analyzed by flow cytometry as described in Material and Methods. The mean values of three independent experiments with the SDs of the relative reduction of BrdU incorporation in Jurkat-SHIP cells after ectopic expression of either KLF2 (KLF2-EGFP), SHIP (+Dox) or both, KLF2 and SHIP (KLF2-EGFP +Dox) in comparison with the vector transfected control cells (EGFP) are shown. Statistical analysis was performed with a Student's *t*-test and *P*-values are indicated by asterisks (*$P < 0.05$; **$P < 0.01$). (Modified from Garcia-Palma *et al,* 2005a).

Table XIII. KLF2 and SHIP lead to a strong reduction of BrdU incorporation into newly synthesized DNA in Jurkat T cells.

The expressions of SHIP and KLF2 in Jurkat T-cells have an additive effect on reduction of BrdU incorporation. BD FACSCalibur (BD Biosciences) confirmed 83.7% reduction of BrdU incorporation mediated by SHIP and LKLF in Jurkat T cells.

Induction/Expression	Relative Reduction of BrdU Incorporation
KLF2	45.2%
SHIP	60.3%
KLF2 + SHIP	83.7%

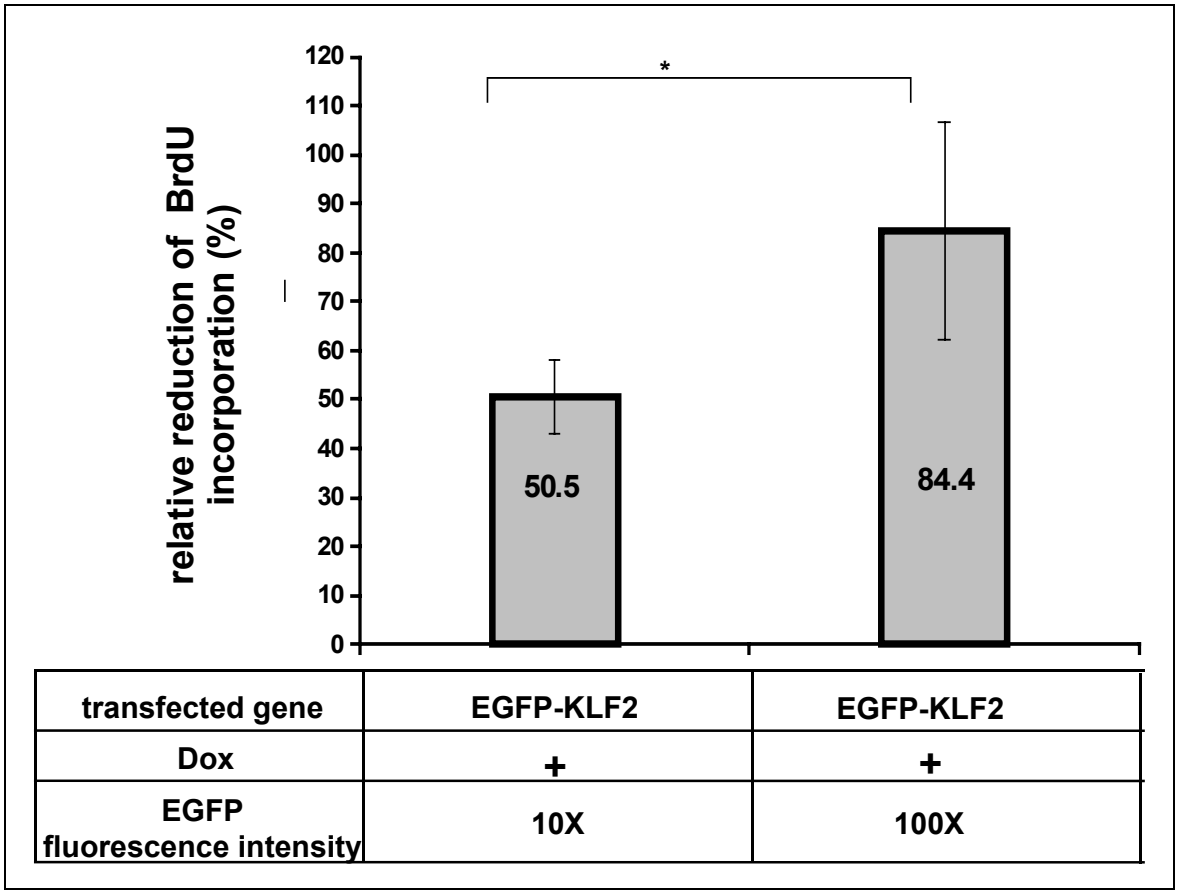

Figure 24. Inverse correlation between KLF2 protein expression levels and DNA synthesis in Jurkat cells after the expression of SHIP.

Sister cultures of Jurkat-SHIP cells (clone no. 51) were grown as described in Figure 23. The mean values of at least three independent experiments with the SDs of the relative reduction of BrdU incorporation vs. EGFP fluorescence intensity in Jurkat-SHIP cells after ectopic expression of KLF2 (KLF2-EGFP) and SHIP (+Dox) are shown. The values were calculated by comparison to the vector transfected control cells (EGFP). Statistical analysis was performed with a Student's *t*-test and the *P*-value is indicated by an asterisks (*$P < 0.05$).

As can been seen in Figure 24, the higher the fluorescence intensity of the EGFP-KLF2, the higher the reduction of BrdU incorporation. A 50.5% reduction of newly synthesized DNA correspond to the cell population that expressed 10-fold levels of EGFP-KLF2 fluorescence intensity, and 84.4% of reduction of newly synthesized DNA correspond to the cell population that expressed 100-fold levels of EGFP-KLF2 fluorescence intensity. These results suggest that the reduction of newly synthesized DNA is dependent on the level of the KLF2 protein in Jurkat T-cells after the expression of SHIP.

5.6. Effect of the inhibition of the PI3K/Akt signal transduction pathway on the expression of KLF2 in Jurkat T cells

KLF2 is down-regulated after T cell activation (Buckley *et al,* 2001). However, the signal transduction pathway mediating the regulation of KLF2 has not been reported. In this study, it has been demonstrated that KLF2 is up-regulated in Jurkat T-cells after the expression of SHIP (section 5.4.) and that leads to a reduction of proliferation (section 5.5.5). Because the activation of the T cell receptor results in stimulation of PI3-kinase, it was analyzed whether the PI3K/Akt pathway is involved in the regulation of KLF2. Inhibition of PI3-kinase with wortmannin and knockdown of the expression of Akt1 in Jurkat T-cells were carried out, in order to study the effect on the expression of KLF2.

5.6.1. Reduction of the Akt activity by PI3K inhibition with wortmannin leads to an increase of the expression of KLF2 in Jurkat T cells

The PI3K-kinase/Akt signal transduction pathway is constituvely activated in Jurkat T-cells (Horn, 2003) and has a positive effect on regulation of proliferation. Since there is a reduction of proliferation in Jurkat T-cells after treatment with the inhibitor wortmannin, it has been suggested that the proliferation in these cells is dependent on the constituvely activation of the PI3-kinase (Horn, 2003).

Purified PI3-kinase was shown to be a heterodimer consisting of a 85 kDa (p85) regulatory subunit and a 110 kDa (p110) catalytic subunit (Shibasaki *et al,* 1991). There are some references from diverse C-terminal truncated forms from the regulatory subunit of the PI3-kinase, which caused a constituvely activation of the protein. One of them is the P65-PI3K, found in the thymus lymphoma cell line CMN-5 (Jimenez *et al,* 1998). Furthermore, it has been described the p76α, identified in a Hodgkin's lymphoma-derive cell line (CO) (Jücker *et al,* 2002). It has been reported that in Jurkat T-cells the normal regulatory 85 kD subunit is present, and interacts with the catalytic subunit (Horn, 2003). Additionally, it has been shown that after treatment with wortmannin there is a reduction on the phosphorylation on Akt at residue serine 473. That means that the constituvely activation of Akt is dependent on the constituve activation of the PI3K (Horn ,2003).

Wortmannin is a pharmacological inhibitor of the PI3K catalytic subunit. Wortmannin was originally isolated from *Penicillium wortmannii (*Brian *et al,* 1957*)* and was subsequently shown to be an specific inhibitor of PI3K with a low nanomolar IC_{50} (Ui *et al,* 1995). Wortmannin is a competitive inhibitor of the ATP binding and binds more deeply in the ATP binding pocket than ATP. It binds in the ATP binding site so that one face of wortmannin packs against the N-terminal lobe (residues 831, 879, 881, and 882) and the other face packs against the C-terminal lobe (residues 950, 953, 961, 963, and 964). One edge of wortmannin is adjacent to residues 867 and 841, while the opposite edge is exposed to solvent along most of its length (Walker *et al,* 2000). The primary amine of active site Lys-833 attacks wortmannin at the furan ring (Wymann *et al,* 1996). The resulting covalent complex inhibits irreversibly the enzyme (Walker *et al,* 2000). Wortmannin covalently modifies PI3K by nucleophilic attack of Lys-833. This irreversible modification is an important determinant of the low nanomolar IC_{50} of wortmannin for PI3K (Walker *et al,* 2000).

In view of the fact that the phosphorylation on Akt at residue serine 473 is reduced after treatment with wortmannin in Jurkat T-cells, and that leads to a reduction in proliferation, inhibition of the PI3K with wortmannin was performed in Jurkat-SHIP cells (clone no. 51), in order to elucidate the likely association between the PI3K/Akt pathway and the induced expression of KLF2. In order to achieve that, sister cultures from at least three independent experiments were grown in the presence or absence of doxycycline (0.8 μg/ml) and wortmannin (100 nM) for 75h, respectively, changing the medium twice per day. The cells were subsequently harvested and cell lysates were prepared, according to the protocol described in Material and Methods. Western blot analyses were performed using antibodies specific for p-Akt (S473), KLF2, SHIP1 and MAPK. The chemiluminescence's signals were measured with an LAS3000 Imager using the AIDA software, as described in 5.4.2.

Figure 25 shows that the treatment of Jurkat-SHIP cells (clone no. 51) with wortmannin has a negative effect on the phosphorylation of Akt at residue serine 473, similar to the effect observed after the restoration of SHIP. The wortmannin-mediated inhibition on the phosphorylation on Akt shown in Figure 25 verified that the constituvely activation of Akt in Jurkat T-cells is inherent up-stream to the constituvely activation of PI3K. Consequently, an inhibition in the PI3K kinase leads to an inhibition of the activation of Akt. Interestingly, the inhibition of PI3K led to an increase in the protein level expression of KLF2, similar to that

observed after the restoration of SHIP. It was confirmed that the wortmannin-mediated inhibition of the PI3K/Akt signaling pathway in Jurkat-SHIP cells (clone 51) has an effect in the induction of the expression of KLF2.

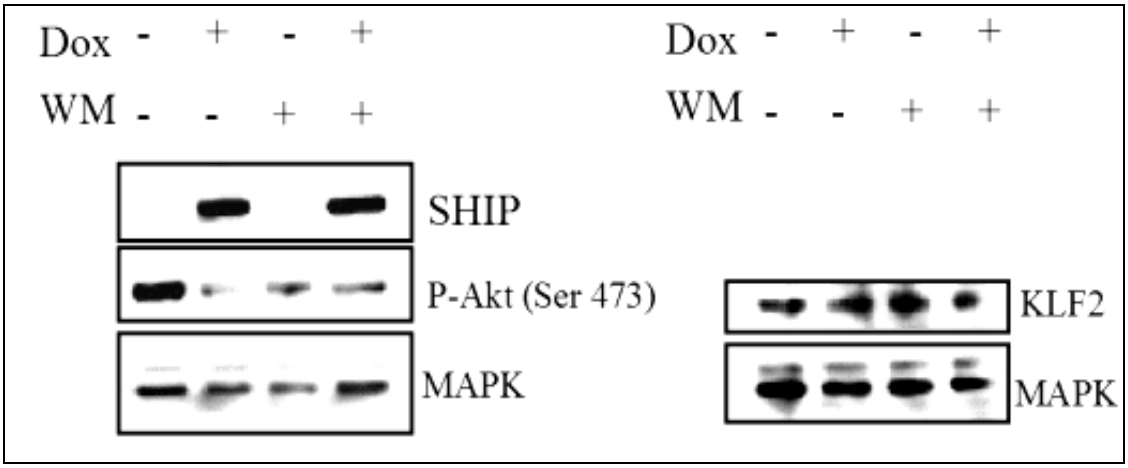

Figure 25. Reduced phosphorylation on Akt and increased Krüppel-like factor 2 (KLF2) protein levels after inhibition of PI3K with wortmannin in Jurkat-SHIP cells.

Jurkat-SHIP cells (clone no. 51) were incubated and grown with 100 nM wortmannin, and simultaneously induced or not induced with Doxycycline (0.8 µg/ml). The control cells were incubated with the same volume of DMSO or 70% EtOH, respectively. The culture medium was changed twice a day. After 75 h, the cells were harvested and cell lysates were prepared in NP40 buffer, corresponding to at least three independent experiments (data not shown). Cell lysates containing 30 µg of total protein were separated in 4%-12% Bis-Tris gradient gels. Western blot analyses were performed in duplicate membranes with antibodies specific for SHIP, KLF2, phosphorylated Akt (serine residue 473) and MAPK. The chemiluminescence signals and protein quantification were measured with an LAS3000 Imager and the AIDA software (Raytest/Fuji, Straubenhardt, Germany). Phosphorylation on Akt at residue serine 473 was reduced, whereas KLF2 protein levels were increased. Dox: Doxycycline; WM: Wortmannin.

In order to measure the changes in KLF2 protein expression that are the result of inactivation of Akt, because of the reduction on phosphorylation at residue Serine 473, and the level of this reduction itself, protein quantification analyses were carried out (Figure 26). In Figure 26 is shown that Akt has been reduced to 30% on its phosphorylation at residue serine 473 after the restoration of SHIP in Jurkat cells, which was similar by comparison to previous results. The reduction to 50% on phosphorylation on Akt (S 473) after treatment with wortmannin, as result of inactivation of the PI3-kinase was also verified. The data indicated that the simultaneous induction of SHIP expression and inactivation of the PI3-kinase with

wortmannin led to a reduction to 40% in phosphorylation on Akt at serine 473. These results agree with the previous results shown in this work and those reported before, concerning to the inactivation of Akt by inhibition of the PI3-kinase after treatment with wortmannin (Jücker *et al*, 2002).

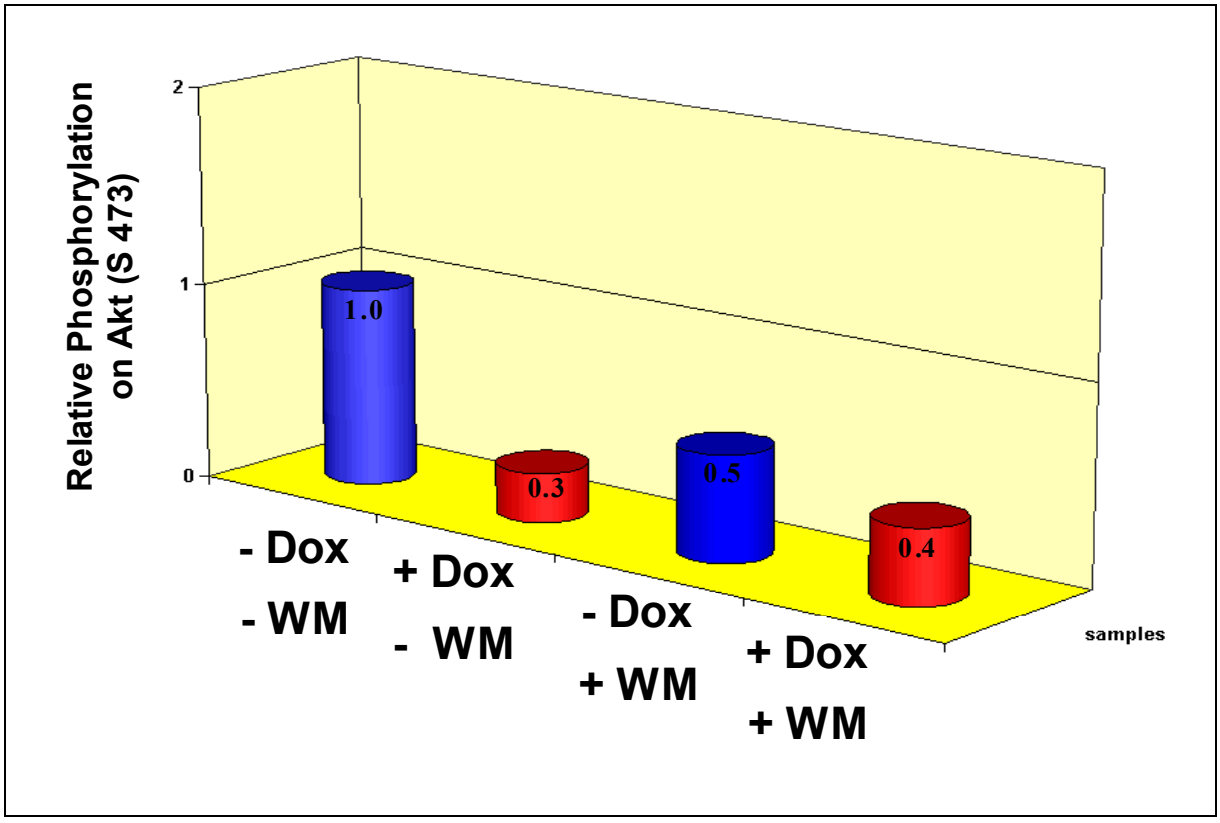

Figure 26. Relative reduction of phosphorylation on Akt (serine 473) after inhibition of PI3K with wortmannin in Jurkat-SHIP cells.

Jurkat-SHIP cells (clone no. 51) were incubated with wortmannin, and simultaneously induced with Doxycycline, as described in Figure 25. Cell lysates containing 30 µg of total protein were separated in 4%-12% Bis-Tris gradient gels. Western blot analyses were performed as described in Figure 25. In the representative experiments, the quantifications of the relative reduction of phosphorylation on Akt at residue serine 473 by the use of the AIDA Software are shown, represented as fold-changes relative to MAPK. +: with induction; - : without induction. Dox: Doxycycline. WM: Wortmannin.

It was confirmed that the inhibition of the PI3K/Akt pathway led to an increase in the expression of KLF2, analogous to the effect shown after the restoration of SHIP in Jurkat T-cells (Figures 25 and 27). After quantification analyses of the changes in the KLF2 protein level expression, the up-regulation of KLF2 after the restoration of SHIP was again verified (Figure 27). A very interesting and important result is the fact that the inhibition of the PI3K

with wortmannin in Jurkat T cells revealed a 2.4-fold increase in KLF2 protein levels, which represent an increment of 140%, in comparison to the control. Even after the restoration of SHIP and simultaneous inactivation of the PI3K/Akt pathway, there is an increment of 160% in the expression of the KLF2 protein in Jurkat T-cells.

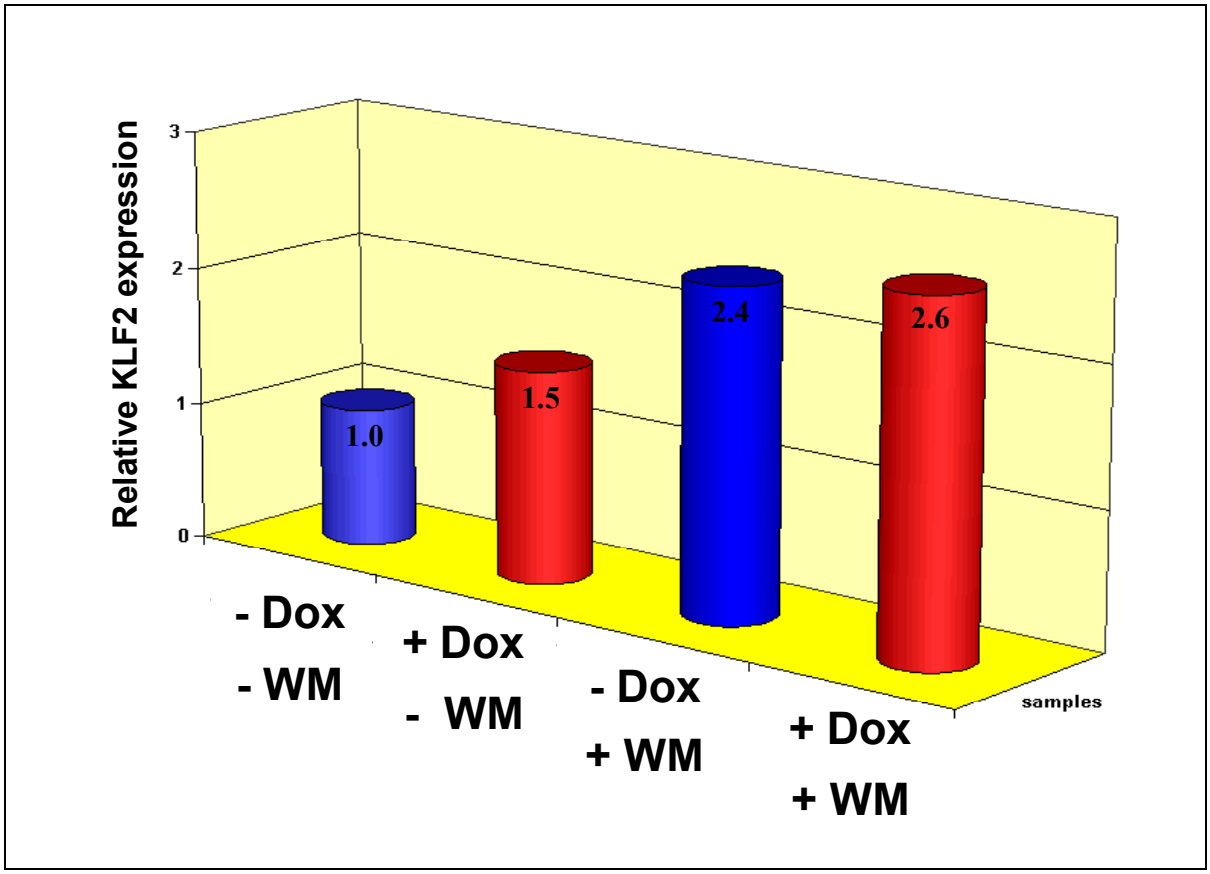

Figure 27. Relative increase on the expression of KLF2 protein levels after inhibition of the PI3K/Akt pathway with wortmannin in Jurkat-SHIP cells.

Jurkat-SHIP cells (clone no. 51) were incubated with wortmannin, and simultaneously induced with Doxycycline, as described in Figure 25. Cell lysates containing 30 µg of total protein were separated in 4%-12% Bis-Tris gradient gels. Western blot analyses were performed as described in Figure 25. In the representative experiments, the quantifications of the relative increase of KLF2 protein levels by the use of the AIDA Software are shown, represented as fold-changes relative to MAPK. +: with induction; - : without induction. Dox: Doxycycline. WM: Wortmannin.

The pharmacological inhibition of the PI3-kinase with wortmannin confirmed that the inactivation of the PI3K/Akt signaling pathways led to an increase in the expression of KLF2 in Jurkat T cells. The data suggest that the up-regulation of KLF2 in Jurkat cells is PI3K/Akt-dependent.

5.6.2. Silencing of Akt1 expression by RNAi leads to an increase in KLF2 expression in Jurkat cells

After elucidation of PI3K/Akt-mediated up-regulation of KLF2 by treatment with wortmannin in Jurkat-SHIP clone no. 51 cells, it was subsequently investigated whether knockdown of Akt1 is sufficient to induce the increase of KLF2 expression. In order to achieve that, the RNA interference technology was chosen to silencing specifically the Akt1 expression in Jurkat-SHIP cells (clone no. 51). The inhibition of the *Homo sapiens v-akt murine thymoma viral oncogene homolog 1* (Akt1; NM_005163.1) gene expression was achieved by the use of double stranded RNA, known as "AKT1 Validated Stealth™ RNAi DuoPak" (Invitrogen™). They consist of two non-overlapping duplexes per gene, consistent with the guidelines for publication –quality data. There are some advantages in the use of the Validated Stealth™ RNAi. The duplexes are already functionally tested and could be coupled to the Block-iT™ Fluorescent Oligo to provide a convenient control for transfection efficiency.

5.6.2.1. Control and optimization of RNAi transfection conditions in Jurkat-SHIP cells

Firstly, it was used a Fluorescent Oligo for Electroporation (Invitrogen™) in order to determine and optimize the efficiency of transfection. The Block-iT™ Fluorescent Oligo for Electroporation offers the following advantages:

•Easily detectable FITC signal indicating transfection efficiency.

•Proven correlation of transfection efficiency with Stealth™ RNAi.

Jurkat-SHIP cells (clone no. 51) were grown, induced or not with doxycycline and transfected by electroporation with the Block-iT™ Fluorescent Oligo for Electroporation, according to the basic protocol from the manufacturer for *Delivering Stealth™ RNAi or siRNA to Jurkat Cells by electroporation* (Invitrogen™). In the optimization procedure were tested some different parameters, such as Fluorescent Oligo concentration, electroporation conditions, transfection solutions and incubation times before fluorescent microscopy and FACS analysis. Figure 28 shows a qualitative analysis of the efficiency of transfection after fluorescent microscopic analysis. After induction of SHIP expression with Doxycycline and 24 h post-

transfection, the cells were qualitative analyzed by inverse fluorescence microscopy (Zeiss), in order to evaluate the Oligo uptake. The signal from the Block-iT™ Fluorescent Oligo for Electroporation was detected by the use of a standard FITC filter set.

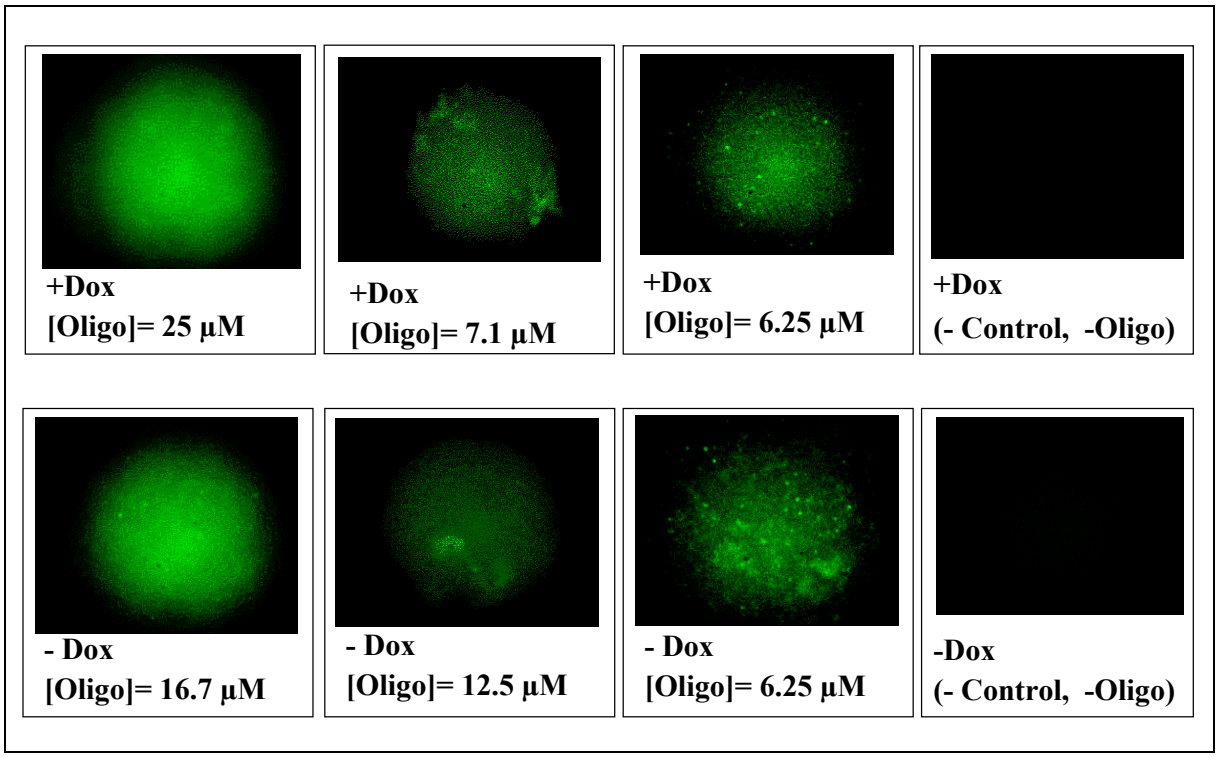

Figure 28. Qualitative analyses of transfection efficiencies performed in optimization assays by the use of the Block-iT™ Fluorescent Oligo for Electroporation in Jurkat-SHIP cells.

Sister cultures of Jurkat-SHIP cells (clone no. 51) were grown for 48 h in the absence (-Dox) or presence (+Dox) of 0.8 µg/ml doxycycline. The cells were then stably transfected by electroporation procedures with the Block-iT™ Fluorescent Oligo for Electroporation, following the instructions of the manufacturer (Invitrogen™), varying some parameters for the optimization. The cells were grown for additionally 24h in non-tissue culture 6-well plates before fluorescent microscopic analysis. The Oligo uptake was qualitatively assessed by observation of each well-plate, using an standard FITC filter set. The fluorescences of positive transfected cells are shown for each representative experiment, with respective controls. +: with induction; - : without induction. Dox: Doxycycline.

Figure 28 shows positive transfected cells after electroporation with different concentrations of the respective Fluorescent Oligo, from 6.25 µM to 25µM. Additionally, it was determined that the Fluorescent Oligo is stable 24h post-transfection. Therefore, at different concentrations of Block-iT™ Fluorescent Oligo for Electroporation, and 24h post-transfection, considerable amounts of positive transfected cells were observed. After qualitative analysis by fluorescent microscopy, the cells were grown for additionally 24h,

washed and harvested for FACS analysis, as described in Material and Methods, in order to quantify the efficiency of transfection with the different parameters used in the optimization of transfection of Jurkat-SHIP cells (clone no. 51) with the Block-iT™ Fluorescent Oligo for Electroporation (Figure 29). Furthermore, the stabilization of the Oligo 48h post-transfection was analyzed.

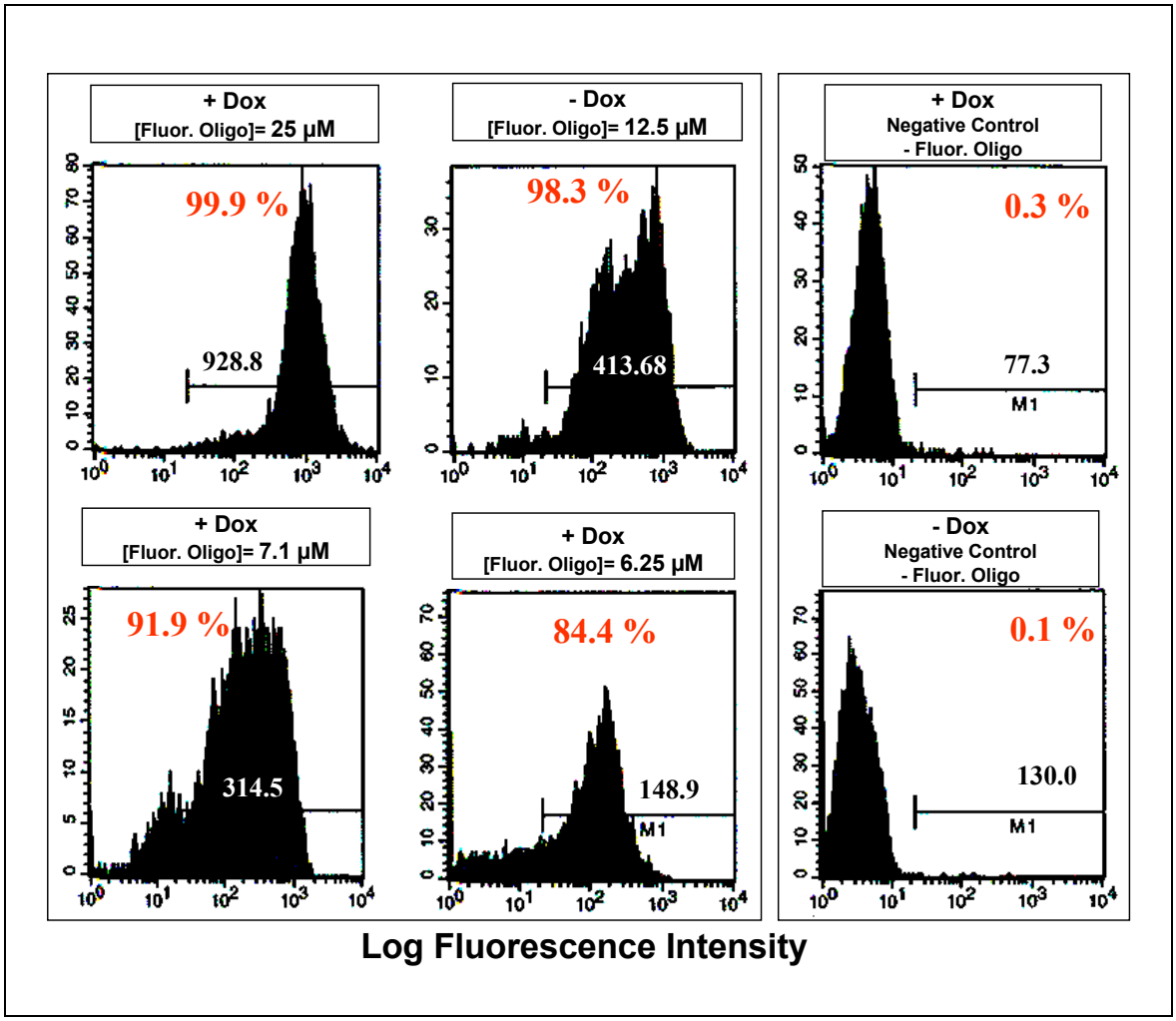

Figure 29. FACS analyses of transfection efficiencies, performed in optimization assays by the use of the Block-iT™ Fluorescent Oligo for Electroporation in Jurkat-SHIP cells (clone no. 51).

Sister cultures of Jurkat-SHIP cells (clone no. 51) were grown for 48 h in the absence (-Dox) or presence (+Dox) of 0.8 µg/ml doxycycline. The cells were then stably transfected by electroporation procedures with the Block-iT™ Fluorescent Oligo for Electroporation, following the instructions of the manufacturer (Invitrogen™), varying some parameters for the optimization. The cells were grown for additionally 48h in non-tissue culture 6-well plates, washed and harvested for FACS analysis. The efficiency of transfection was determined by analysis of positive transfected cells. The percentages of positive transfected cells, determined by setting a gate (M1) on cells with a higher fluorescent intensity than the negative control (cells transfected without Fluorescent Oligo), are shown for each representative experiment. The Mean Intensity values for the population gated in M1 are shown in each case. +: with induction; - : without induction. Dox: Doxycycline.

In Figure 29 are shown the percentages of positive transfected cells as a function of the fluorescence intensity, obtained from optimization assays of cell transfection with the Fluorescent Oligo. FACS analysis of Jurkat-SHIP cells (clone no. 51) revealed firstly, that the Block-iT™ Fluorescent Oligo for Electroporation is stable 48h post-transfection. Secondly, it was shown that the fluorescence intensity is proportional to the concentration of the Fluorescent Oligo used in the transfection procedures. At fluorescent oligo concentrations of 6.25 µM, a mean fluorescence intensity of 148.9 was measured. Increase in the concentration of electroporated fluorescent oligo resulted in increased mean fluorescence intensity values. The highest mean fluorescence intensity value was 928.8, corresponding to a Fluorescent Oligo final concentration of 25µM (Figure 29, upper panel, left). Thirdly, FACS analysis of the efficiency of transfection performed in the optimization assays by the use of the Block-iT™ Fluorescent Oligo for Electroporation revealed that the efficiency of transfection is furthermore proportional to the Fluorescent Oligo concentration. At lower Fluorescent Oligo concentrations, 6.25µM and 7.1 µM, the efficiencies of transfection obtained after 48h were 84.4% and 91.9%, respectively. The maximal efficiency of transfection obtained was 99.9%, corresponding to a concentration of 25µM of Fluorescent Oligo (Figure 29, upper panel, left).

As shown in Figure 29, the transfection of Jurkat-SHIP cells (clone no. 51) with the Block-iT™ Fluorescent Oligo for Electroporation was achieved and optimized, demonstrating that at least after 48h the Fluorescent Oligo is stable, generating high mean fluorescence intensities, proportional to the Oligo concentrations. Moreover, by optimization procedures a maximal efficiency of transfection of 99.9% was obtained, a high value that at the time of analysis was not reported for Jurkat T-cells from any other group or companies by electroporation procedures. The efficiency of transfection was determined on every occasion using 25µM Fluorescent Oligo, and the results were in each case reproducible (see 5.6.2.3).

5.6.2.2. *Akt1* is not regulated at the mRNA level after the restoration of SHIP in Jurkat cells

In order to identify changes in expression that are the result of inactivation of Akt1 by RNAi-mediated knock-down, validation by quantitative real-time PCR of the results already obtained by microarray analysis for *Akt1* was performed. Microarray analysis revealed that the *Akt1* mRNA is present in Jurkat-SHIP cells. Additionally, *Akt1* is not regulated at the

messenger RNA level after the restoration of SHIP in Jurkat cells (Table XIV). In this study, forward- and reverse-primers for the *Akt1* target sequence were designed, as described in 5.3.1. The specificity of the primer sequences was verified using *BLAST nucleotide-nucleotide* search analysis function (NCBI). The sequences for the primers obtained, their positions and the annealing Temperature used after optimization by conventional PCR and quantitative real-time RT-PCR are shown on Table XV. The primers shown on Table XV were tested at least once by conventional PCR and quantitative real-time RT-PCR (data not shown). The sequence from the housekeeping gene glyceraldehyde-3-phosphate-dehydrogenase (*GAPDH)* was used as normalization control for PCR and quantitative real-time RT-PCR, as described before. The calculation of fold-changes in the expression of *Akt1* was performed with the same programs used for the genes validated on section 5.3.4.

Following normalization with *GAPDH* and expression analysis relative to the control, real-time quantitative RT-PCR analysis from two independent experiments confirmed that *Akt1* mRNA expression is not regulated after the expression of SHIP in Jurkat cells (fold-change: 1.0 ± 0.1) (Table XVI). Table XVI shows the results that confirmed by microarray analysis and quantitative real-time PCR analysis that the mRNA level expression of *Akt1* is not regulated after the restoration of SHIP in Jurkat T-cells.

5.6.2.3. Akt1 knockdown leads to an increase in expression of KLF2 in Jurkat cells

The changes in Akt1 protein expression after knockdown by siRNA and the effect on KLF2 expression were analyzed. For that purpose, Jurkat-SHIP cells (clone 51) were grown and transfected with the Validated Stealth™ RNAi Duplexes against *Akt1* and the Block-iT™ Fluorescent Oligo for Electroporation as transfection control, using the conditions set in the optimization procedures previously described (5.6.2.1). 24h and 48h post-transfection, the control cells that were electroporated with the Fluorescent Oligo were washed, harvested and analyzed by FACS, in order to determine the efficiency of transfection (Figure 30). FACS analyses revealed efficiencies of transfection higher than 95%: 95.1% (-Dox) and 98.0% (+Dox), with mean intensity values of 615.3 and 697.8, respectively. These results indicate a high efficiency of transfection in the analysis.

Table XIV. *Akt1* mRNA expression identified on U133 microarrays after the expression of SHIP in Jurkat-SHIP cells [a]

Affymetrix Probe Set ID [b]	Gene Symbol [*Homo sapiens*]	Title [*Homo sapiens*]	RefSeq Transcript ID (GenBank Source)	Signal (-/+ Dox) [c]	Fold change (+/- Dox)
207163_s_at HG-U133A	*AKT1*	v-akt murine thymoma viral oncogene homolog 1	NM_005163.2	244.6P-271.9P	1.1 (NC) [d]

[a] Transcripts compared to untreated controls following doxycycline treatment for 82 h.
[b] Affymetrix GeneChip Human Genome U133 Array Set HG-U133A and HG-U133B Targets. ID: Identity.
[c] P: Present.
[d] NC: No change.

Table XV. Sequences of primers for the amplification of the *Akt1* target sequence, analyzed by quantitative real-time RT-PCR.

Gene Symbol [*Homo sapiens*]	RefSeq Transcript ID (GenBank Source)	Primer sequences (5'→3')	Primer				Product size (bp)	a.T (°C)
		(Forward and Reverse)	Length	Start	Tm (°C)	GC (%)		
AKT1	NM_005163.2	ACTAAGGCCGTGTCTCTGAGG	21	2509	60.82	57.14	275	57
		GTCGAAAAGGTCAAGTGCTACC	22	2783	60.17	50.00		

Table XVI. Validation of *Akt1* mRNA expression by quantitative real-Time RT-PCR.

Comparison of the data obtained using the Affymetrix platform (GeneChip Human Genome U133 Array Set HG-U133A and HG-U133B Targets) with the results from quantitative real-time RT-PCR experiments for *Akt1* after the expression of SHIP in Jurkat-SHIP cells (clone 51). Expression levels are shown as a fold change of the level of mRNA after the induction of SHIP expression with Doxycycline, relative to the level of that transcript without induction of SHIP expression.

Gene Symbol [Homo sapiens]	Title [Homo sapiens]	Fold change Affymetrix (+/-)	Fold change LightCycler (+/-)	Statistical significance [a]	Efficiency (E) [b]
AKT1	v-akt murine thymoma viral oncogene homolog 1	1.1	1.0	(NS)	1.6

[a] Statistical analysis was performed with a Student's t-test. NS: not significant.
[b] GAPDH-Target gene.

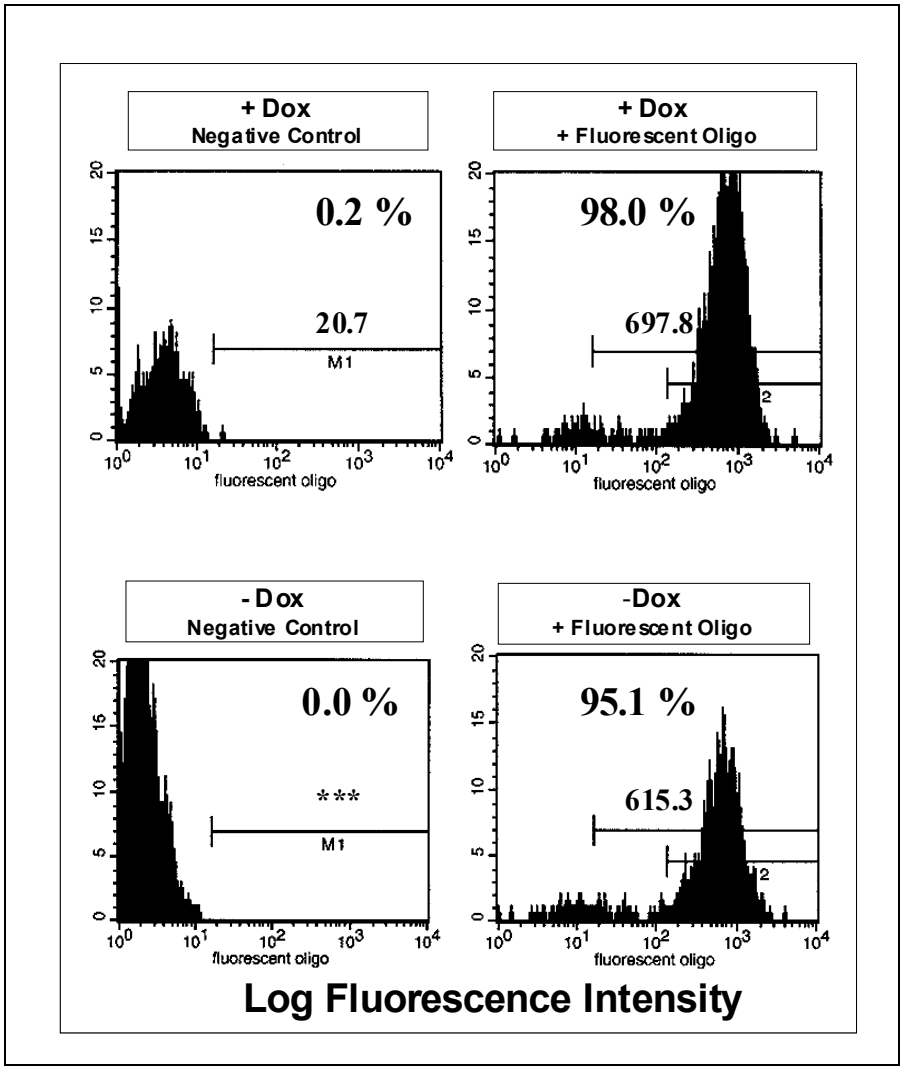

Figure 30. Quantitative analysis of efficiency of transfection, performed with the Block-iT™ Fluorescent Oligo for Electroporation in Jurkat-SHIP cells (clone no. 51) for siRNA analyses.

Sister cultures of Jurkat-SHIP cells (clone no. 51) were grown for 48 h in the absence (-Dox) or presence (+Dox) of 0.8 µg/ml doxycycline. The cells were then stably transfected by electroporation procedures with the Block-iT™ Fluorescent Oligo for Electroporation and Validated Stealth™ RNAi Duplexes against Akt1, respectively, following the instructions of the manufacturer and the parameters set by the optimization. The cells were grown for additionally 24h in non-tissue culture 6-well plates before FACS analysis. The efficiency of transfection was quantitatively determined by measure of the fluorescence intensity in the positive transfected population of cells. The percentages of fluorescence intensity are shown for each representative experiment, with their respective controls. +: with induction; - : without induction. Dox: Doxycycline.

After determination of efficiency of transfection, western blotting analyses were performed to verify the knockdown of Akt1 (Figure 31). Western blotting analyses after the knockdown of *Akt1* with Validated Stealth™ RNAi Duplexes revealed a reduction in the protein levels of Akt1, compared to the controls, and relative to MAPK. Moreover, the levels of KLF2 protein

increased proportional to the reduction of the Akt1 protein levels, as shown in the lanes corresponding to Duplex 1 and Duplex 2.

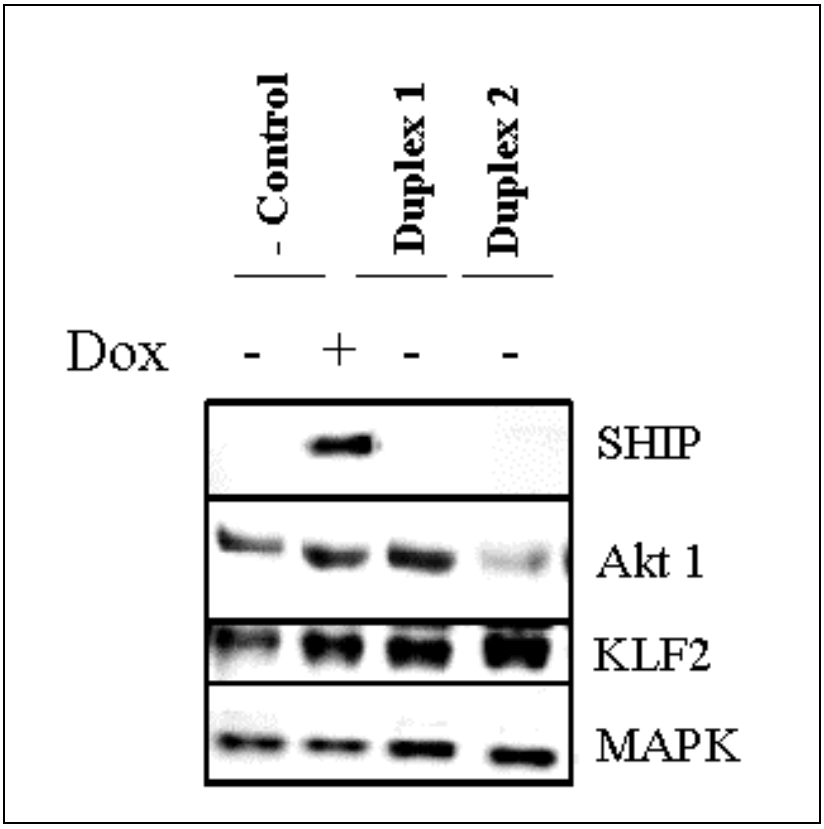

Figure 31. Knockdown of Akt1 leads to an increase of KLF2 protein levels in Jurkat-SHIP cells.

Sister cultures of Jurkat-SHIP cells (clone no. 51) were grown for 48 h in the absence (-Dox) or presence (+Dox) of 0.8 µg/ml doxycycline. The cells were then stably transfected by electroporation procedures with the Block-iT™ Fluorescent Oligo for Electroporation and Validated Stealth™ RNAi Duplexes against Akt1, respectively, following the instructions of the manufacturer and the parameters set by the optimization. The cells were grown for additionally 24h in non-tissue culture 6-well plates before FACS analysis for determination of efficiency of transfection, followed by harvesting of cells and preparation of cell lysates in NP40 buffer. Cell lysates were analyzed by 4%-12% Bis-Tris gradient gels and Western blotting analyses were performed with antibodies specific for SHIP, Akt1, KLF2 and MAPK. The chemiluminescence signals and protein quantification were measured with an LAS3000 Imager and the AIDA software (Raytest/Fuji, Straubenhardt, Germany). +: with induction; -: without induction. Dox: Doxycycline.

As depicted in Figure 31, increased levels of KLF2 protein were obtained with a considerable reduction of Akt1 expression achieved by the use of the Validated Stealth™ RNAi Duplex 2 against Akt1. The increase on KLF2 protein level after restoration of SHIP was again confirmed, as shown in the controls. The increased KLF2 protein level after knockdown of

Akt1 is similar to that obtained after the restoration of SHIP in Jurkat cells. In the analysis of quantification of the relative Akt1 protein knockdown, 37% reduction of Akt1 protein levels were achieved by the use of Duplex 1, and 51% relative Akt1 knockdown was attained by the use of the Duplex 2, respectively (Figure 32). Thus, the knockdown of Akt1 by the use of Validated Stealth™ RNAi Duplexes was shown to be effective. Moreover, the optimal silencing of Akt1 expression was achieved with the Duplex 2.

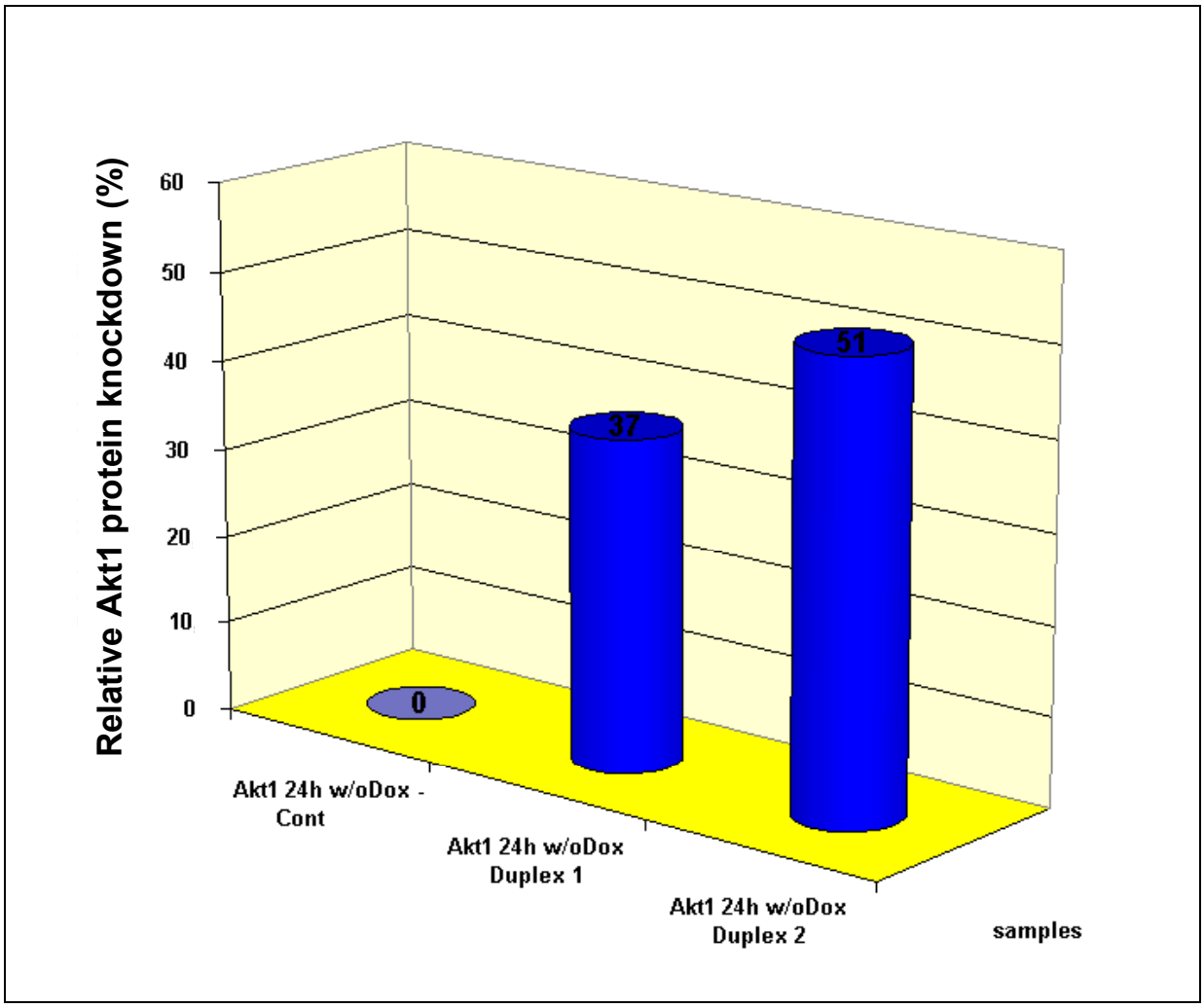

Figure 32. Quantification of the relative reduction of Akt1 protein levels after knockdown with Validated Stealth™ RNAi Duplexes in Jurkat-SHIP cells.

Jurkat-SHIP cells (clone no. 51) were grown and transfected with Validated Stealth™ RNAi Duplexes as described in Figure 31. Total cell lysates were prepared approximately 24 post-transfection and proteins were separated in 4%-12% Bis-Tris gradient gels. Western blotting analyses were performed as described in Figure 31. In the representative experiments, the quantifications of the relative reduction of Akt1 protein levels by the use of the AIDA Software are shown, represented as percentages correlated to MAPK. w/o : without induction. Dox: Doxycycline.

Correspondingly, the quantification analysis of the relative KLF2 protein expression after the Akt1 protein knockdown by RNA interference revealed that KLF2 protein levels increased relative to the reduction on the expression of Akt1 (Figure 33).

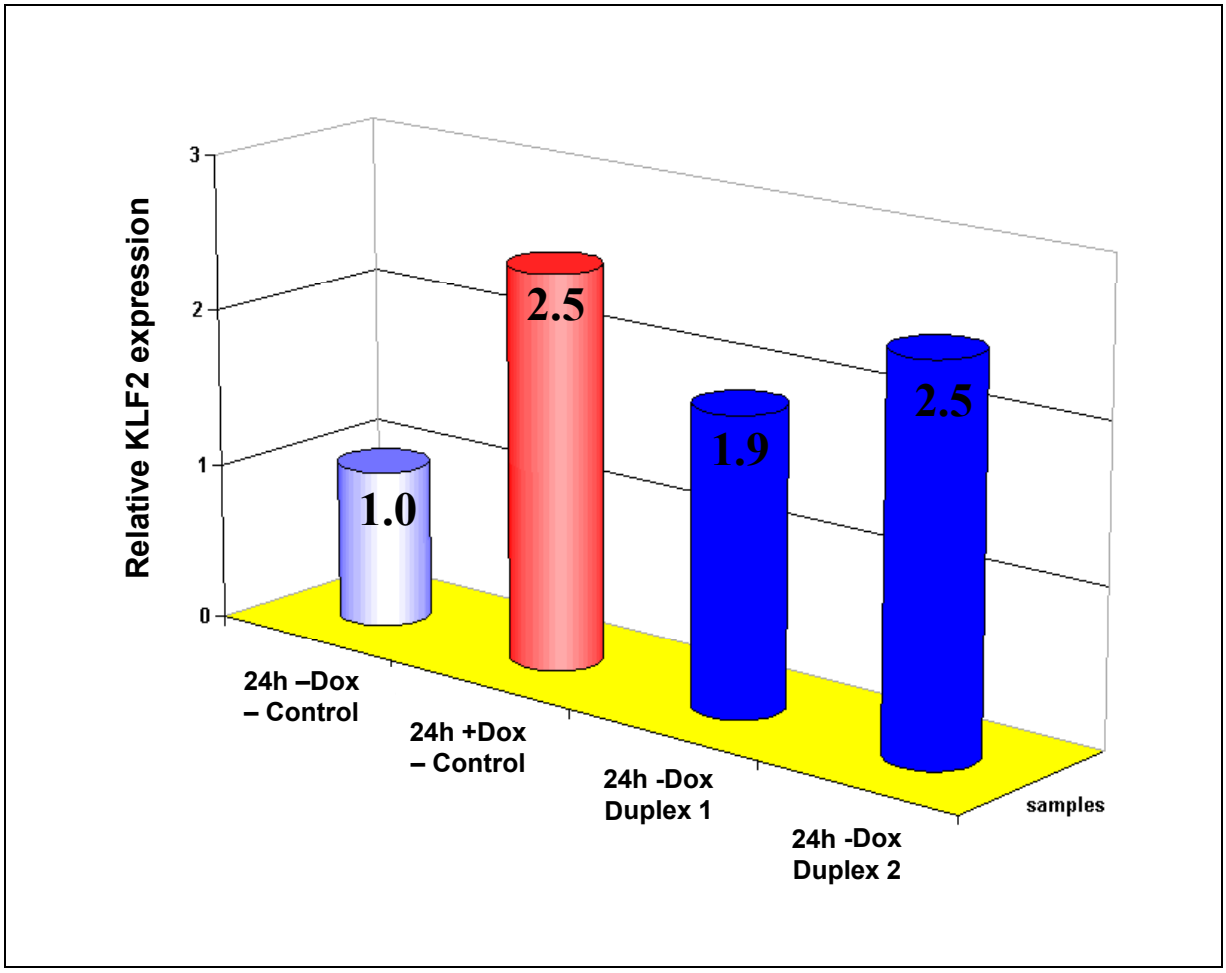

Figure 33. Quantification of the relative KLF2 protein expression after Akt1 knockdown with Validated Stealth™ RNAi Duplexes in Jurkat-SHIP cells.

Jurkat-SHIP cells (clone no. 51) were grown and transfected with Validated Stealth™ RNAi Duplexes as described in Figure 31. The total cell lysates were prepared approximately 24 post-transfection and proteins were separated in 4%-12% Bis-Tris gradient gels. Western blotting analyses were performed as described in Figure 31. In the representative experiments, the quantifications of the relative KLF2 protein expression after knockdown of Akt1 by the use of the AIDA Software are shown, represented as fold-changes correlated to MAPK. - : without induction. +: with induction. Dox: Doxycycline.

The knockdown of the expression of Akt 1 by RNAi led to a 1.9-fold increase (+ 90%) in the expression of KLF2 after 37% Akt1 knockdown, and a 2.5-fold increase (+150%) after 51%

knockdown, respectively (Figures 32 and 33). In addition, the expression of the inositol 5'-phosphatase SHIP led to 2.5-fold up-regulation of KLF2, as shown in Figure 33 with the negative control for the RNAi assay after the induction of SHIP expression.

5.7. Up-regulation of the T cell quiescence factor KLF2 occurs via the PI3K/Akt signaling pathway in Jurkat cells

The data obtained in section 5.6. indicated that the pharmacological inhibition of the PI3K/Akt signaling pathway, and the knockdown of Akt1 by the use of RNA interference, have a positive effect on the expression of KLF2 in Jurkat cells. Additionally, the positive effect of the restoration of SHIP expression on the up-regulation of KLF2 was confirmed. SHIP expression led to a reduction on phosphorylation on Akt at serine 473, resulting in the up-regulation of KLF2. These data are summarized on Table XVII.

Table XVII. Analyses of KLF2 protein expression after PI3K inhibition with wortmannin and Akt1 knockdown by RNAi in Jurkat cells.

Comparison of the data obtained using PI3K inhibition with wortmannin, with or without the restoration of SHIP, and Akt1 knockdown by RNA interference without restoration of SHIP, for KLF2 protein expression in Jurkat-SHIP cells (clone 51). Relative phosphorylation on Akt at residue serine 473 and relative expression of Akt1 protein after knockdown are shown as percentages, correlated to MAPK after protein quantification, in each case. Relative KLF2 protein levels are expressed as fold changes. WM: wortmannin.

Relative KLF2 Expression and P-Akt (Serine 473) phosphorylation after PI3K inhibition with Wortmannin				
	Control - SHIP -WM	+ SHIP - WM	- SHIP + WM	+ SHIP + WM
P-Akt (Serine 473)	100%	30%	50%	40%
KLF2	1.0	1.5	2.4	2.6
Relative Expression after Akt1 Knockdown with Stealth ™ RNAi DuoPak				
	Control - SHIP	Control + SHIP	Duplex 1	Duplex2
Akt 1	100%	100%	63%	49%
KLF2	1.0	2.5	1.9	2.5

The results confirmed the positive dependence of KLF2 expression on SHIP expression, since KLF2 protein levels increased 1.5-to 2.5-fold after restoration of SHIP expression. Moreover, the PI3K/Akt-mediated increase of KLF2 protein level was confirmed by inhibition of PI3K with wortmannin and silencing of Akt1 expression by siRNA. As shown on Table XVII, the expression of KLF2 protein increased after reduction of phosphorylation of Akt at serine 473, as consequence of the PI3K pharmacological inhibition with wortmannin. The 2.4-fold (+140%) KLF2 increase was achieved when the phosphorylation on Akt was 50%, and 2.6-fold (+160%) when 40%, respectively. Similar results were obtained after Akt1 knockdown by RNAi, as shown on the lower panel on Table XVII. The data indicate that the increase on KLF2 protein level is approximately inverse proportional to the reduction on Akt phosphorylation at serine 473 and the level of Akt1 knockdown. These data implicate the PI3K/Akt signaling pathway in the up-regulation of KLF2 in Jurkat cells.

6. Discussion

The SH2-containing Inositol 5-phosphatase SHIP has been described as a crucial component of signal transduction pathways that regulate cell growth and proliferation. The restoration of SHIP in Jurkat T cells leads to a reduction of proliferation, via inhibition of the PI3K/Akt pathway. In this study, changes in gene expression in Jurkat T cells after the restoration of SHIP were analyzed. The changes of the transcriptional profile induced by SHIP restoration in the human leukemic cell line Jurkat, their implication in the biology of these cells, functional analysis and the role of the PI3K/Akt pathway are described and will be discussed.

6.1. Microarray analysis revealed that SHIP regulates differentially transcriptional expression of 37 unique mRNAs in Jurkat cells

In order to investigate the differential expression of genes after the restoration of SHIP in the human T-cell leukemia cell line Jurkat, and their possible function in regulation of cell proliferation, microarray analyses were performed by screening of 39,000 transcripts of the human genome, using a Jurkat T cell line containing a doxycyline-inducible SHIP vector (Jurkat-SHIP cells (clone no. 51). The restoration of SHIP expression in this Jurkat T cell line, which does not express endogenous SHIP proteins, leads to the inactivation of the PI3K/Akt signal transduction pathway. Consequently, a partial inhibition of the proliferation of these cells has been observed.

In this study, microarray analysis of Jurkat-SHIP cells (clone no. 51) after the restoration of SHIP revealed a total of 35.0% (15,704 out of 44,928) probe sets identified as “present” in the human Chip Arrays HG-U133A and B (Affymetrix, Santa Clara, CA, USA). Additionally, 63.3% (28,441 out of 44,928) probe sets were identified as “absent”, and 1.7% (783 out of 44,928) as “marginal”. Further Significance Analysis of Microarrays resulted in 531 probe sets IDs (identities) that were significantly regulated after the expression of SHIP, based on the *p*-values ($P<0.05$) (Table II). The differential expression of those identities represented 1.2% (531/44,928) of the total population analyzed, and 3.4% (531/15,704) of the population

identified as “present”. Further analysis revealed that of the 531 probe set IDs, 41 probe set IDs were at least two-fold statistically significant regulated (7.7%). After analysis of the targets using different platforms, it was identified that one of the 41 probe set IDs represented the *SHIP* gene itself. Microarray analysis verified the induction of transcription of the *SHIP* gene expressed from the retroviral vector, cloned in Jurkat cells, since further experiments confirmed that the endogenous *SHIP* mRNA expression is not regulated in these cells (see 5.3.3). Accordingly, microarray analysis allowed the identification of 40 probe set IDs, which are significantly SHIP-regulated (≥ 2-fold) in Jurkat cells. Specifically, of those 40 probe sets, 16 were induced (40%) and 24 repressed (60%) by SHIP expression in Jurkat T cells (Tables III and IV). Subsequently, investigation of these 40 probe sets by using different platforms allowed the identification of 37 unique mRNAs, which correspond to known genes, ESTs and sequences that encode hypothetical proteins. The genes that were represented by two probe set IDs were *PAG*, *ATF* and the gene that codes for the hypothetical protein LOC284801. Of the 37 regulated mRNAs that exhibited at least 2.0-fold significant changes at the transcriptional level after the restoration of SHIP expression, 16 mRNAs were induced (43%), and 21 repressed (57%).

There are several studies that have used a cutoff of 1.5-fold (Haaland *et al,* 2005; Moreno *et al,* 2004; Schmalbach *et al,* 2004; Xin *et al,* 2003). The data seen at the 1.5-fold level included genes such as cyclin B, which has been confirmed at the protein level to be induced more than 1.5-fold (Moreno *et al,* 2004). Haaland *et al.* (2005) found 118 and 117 genes whose transcripts were induced and repressed, respectively, by using an initial cutoff of 1.5-fold with Affymetrix U133A human gene arrays in JL1.4 cells. They established a second cutoff of at least 2.5-fold in order to select genes to be further analyzed by real-time RT-PCR assays. Thus, their data revealed 27 and 22 genes whose transcripts were induced and repressed, respectively, by a cutoff of at least 2.5-fold. These results are similar to those obtained in this study by using a cutoff of 2.0-fold.

Of the 37 mRNAs identified here to be significantly SHIP-regulated (>2-fold), 24 correspond to known genes. Based upon Gene Ontology (GO) annotations (Gene Ontology) [http: //www.geneontology.org] of the 24 genes, 11 genes (46%) had GO annotations relating to nucleus, transcription or cell cycle, 7 genes (29%) encode proteins associated with intracellular signaling cascades and/or localization in the plasma membrane, and 1 gene (4%) codes for interleukin 26 (IL26) (Tables VII and VIII). Moreno *et al.* (2004) reported an

alteration of 39.8% genes involved in cell proliferation by SV40 small tumor antigen (ST), using microarray profiles. By analysis of the data reported here, SHIP appears to affect the expression of genes that are involved in transcription and cell cycle control.

In summary, the microarray analysis of significantly SHIP-regulated genes in Jurkat T cells allowed the identification of 37 unique mRNAs that were differentially expressed. They were chosen for confirmation by quantitative real-time RT-PCR.

6.2. Validation of the microarray analysis by quantitative real-time RT-PCR confirmed the effect of SHIP on differential gene expression in Jurkat T cells

Of the 37 significantly SHIP-regulated genes at the transcriptional level, 36 transcripts could be analyzed by quantitative real-time RT-PCR, in addition to *SHIP* itself. For one of the two ESTs identified, *AI820854,* no mRNA sequence was available at the time of the analysis (Table III). The quantitative real-time RT-PCR measurements of the 36 selected genes allowed the validation of 29 transcripts (81%), in addition to the overexpressed *SHIP* (Tables VII and VIII). The analysis demonstrated a good correlation between quantitative real-time PCR and the Affymetrix platform, with 26 out of 29 (90%) of the probes changing in the same direction by both methods. Validations by quantitative real-time RT-PCR indicate that the data obtained by microarray analysis identified consistently top regulated mRNAs, whose levels changed following induction of SHIP expression in Jurkat T cells. The high percentage of validation obtained here is consistent with observations reported before (Mao *et al,* 2005; Moreno *et al,* 2004). Moreno *et al*. (2004) confirmed also by QRT-PCR 90% of the microarray observations. These data confirm the high fidelity and reliability achieved from both techniques in the analysis of transcriptional regulation. Although the limitations of microarray and quantitative real-time RT-PCR analyses consist in the fact that changes at the mRNA levels are not always reflected at the protein level, both provides significant and useful information about transcriptional regulation profiles, that could be further confirmed by protein analysis. Further statistical analysis revealed that from the 29 transcripts validated by quantitative real-time RT-PCR, 16 were significantly regulated ($P< 0.05$) after the expression of SHIP in Jurkat cells (clone no. 51) (55%) (Tables IX and X). Among these genes, 5 were

significantly increased (31%) and 11 significantly decreased (69%). The data were subsequently analyzed by a cutoff of 2-fold in the expression changes. Thus, quantitative real-time RT-PCR confirmed and validated the significant transcriptional regulation (≥2-fold) of 11 genes by SHIP in Jurkat T cells (Tables XI and XII). Of these, 3 were significantly increased (27%): *CD62L*, *KLF2* and *KCMF1* and 8 significantly decreased (73%): *PAG, TRIB3, ARRDC3, ARHGEF10, ATF5, ZNF75, DNAJB9* and *IL26*.

Accordingly and in summary to this point, the quantitative real-time RT-PCR measurements for the 36 selected genes allowed the validation of 29 transcripts (81%), in addition to SHIP itself. The analysis demonstrated a good correlation between quantitative real-time PCR and the Affymetrix platform, with 90% of the probes changing in the same direction by both methods. By further analyses, quantitative real-time RT-PCR confirmed and validated the significant transcriptional regulation (≥2-fold) of 11 genes by SHIP in Jurkat T cells (Tables XI and XII). Of these, 3 were significantly increased (27%): *CD62L*, *KLF2* and *KCMF1* and 8 significantly decreased (73%): *PAG, TRIB3, ARRDC3, ARHGEF10, ATF5, ZNF75, DNAJB9* and *IL26*. The data indicate that SHIP is more implicated in the repression of genes (73%), which are involved in signal transduction, transcription control and cell cycle, in comparison to the induction of genes (27%).

6.2.1. SHIP regulates the transcription of genes coding for nuclear proteins, proteins integral to the membrane and one interleukin

Interestingly, 55% of the 11 genes identified (6/11), whose transcripts are at least 2-fold regulated by SHIP in Jurkat cells, code for proteins that are localized in the nucleus, according to GO annotations, i.e. *KLF2, KCMF1, TRIB3, ATF5, ZNF75,* and *DNAJ9.* Considering the proteins integral to membrane, the genes that code for CD62L and PAG were identified (18%). Additionally, the gene coding for IL26 was the only interleukin identified as significantly regulated (>2-fold). In comparison to the data reported in the literature, Haaland *et al.* (2005), found in Jurkat cells by microarray analysis that one-third of the mRNAs highly induced by the transcription factor KLF2 encode cell surface molecules, In this study, a high proportion of SHIP-regulated genes code for nuclear proteins including the transcription factor *KLF2*. The functional role of the up-regulation of *KLF2* in proliferation of Jurkat cells and the signaling pathway involved in the regulation of *KLF2* expression were analyzed in this study, and will be discussed in detail in further sections. SHIP appears to be a regulator of

transcription of nuclear proteins that could be involved in processes such as transcription, cell proliferation and apoptosis. The possible associations of the genes identified here with pathways involved in reduction of proliferation will be discussed in the next sections.

6.2.2. SHIP induces expression of genes involved in a quiescent phenotype and reduction of proliferation

The three genes which are up-regulated by SHIP encode the proteins SELL/CD62L (selectin L, lymphocyte adhesion molecule 1/ CD62 antigen ligand) (+180%), which is integral to the plasma membrane, and two proteins localized in the nucleus, the Krüppel-like transcription factor KLF2 (+220%) and the potassium channel modulatory factor 1, KCMF1 (+260). The *KCMF1* and *KLF2* genes were the highest SHIP-regulated at the transcriptional level, in spite of the fact that the *KCMF1* value by quantitative real-time RT-PCR differed from that obtained by microarray analysis. One possible explanation for this discrepancy between microarray analysis and quantitative real-time RT-PCR findings for *KCMF1* are the low signal intensity values obtained for the probe set identity (Table IV). Regardless, the significant SHIP-mediated regulation of KCMF1 was validated, and the direction of the quantitative real-time RT-PCR values was taken as a critical factor in the validation, since quantitative real-time RT-PCR is more accurate. Further protein analyses should be performed to verify the SHIP-mediated regulation of *KCMF1* at the protein level. The potassium channel modulatory factor 1, KCMF1 is a nuclear protein containing zinc finger. GO annotations associate this protein with signal transduction (Table XI). However, why SHIP should so markedly affect *KCMF1* expression remains unclear.

Of the three SHIP-induced genes validated by quantitative real-time RT-PCR (≥2-fold), the transcriptional regulation of *CD62L* and *KLF2* showed the highest statistical significance (P<0.001). It has been reported that CD62L and KLF2 are expressed in naïve T cells (Janeway *et al,* 1999; Buckley *et al*, 2001). The SHIP-mediated increase of both, CD62L and KLF2 observed in this study may be involved in programming a phenotype that resembles quiescence in Jurkat cells. The data suggest that the SHIP-mediated changes of transcription may establish a phenotype that resembles quiescence. Firstly, the function of CD62L will be considered. Selectins are specific for leukocyte-vascular cell interaction, and mediate extravasation. L-Selectin is distributed in naïve and some memory lymphocytes, neutrophils,

monocytes, macrophages and eosinophils. On naïve T cells, L-Selectin binds to sulfated carbohydrates on various proteins, such as the vascular addressins GlyCAM-1 and CD34. CD34 is expressed on endothelial cells in many tissues, but is properly glycosylated for L-Selectin binding only on the high endothelial venule cells of lymph nodes (Janeway *et al,* 1999). The interaction between L-selectin and the vascular addressins is responsible for the specific homing of naïve T cells to lymphoid organs. The crossing through the endothelial barrier into the lymphoid tissue is achieved when the integrins and molecules of the immunoglobulin superfamily are present. It has been reported that quiescent T cells are $CD62L^{+}$ (Abbas *et al,* 1994; Freitas and Rocha, 2000). Upon activation of the T cell, the expression of L-Selectin is lost. In view of the fact that SHIP leads to a reduction of proliferation in Jurkat T cells, it is possible that the SHIP-mediated up-regulation of *CD62L* in Jurkat T cells is a trait that contributes to this reduction of proliferation, similar to the phenotype of resting cells. Secondly, the inhibitory effect of KLF2 on the proliferation of T cells has been demonstrated before (Buckley *et al,* 2001; Wu and Lingrel, 2004). KLF2 is down-regulated after T cell activation (Buckley *et al,* 2001). However, the signal transduction pathway mediating the regulation of KLF2 has not been reported. Buckley *et al*. (2001) concluded that KLF2 inhibits the expression of c-myc. However, and in agreement with a study performed with the induction of KLF2 in Jurkat T-cells (Haaland *et al,* 2005), neither repression of c-myc mRNA by KLF2 nor SHIP was observed in the microarray analyses.

In summary to this point, the results presented here indicate that SHIP-mediated induction of transcriptional expression of *KLF2* and *CD62L* in Jurkat T cells appear to be involved in signaling pathways that may contribute to the maintenance of a state that resembles quiescence, and lead to reduction of proliferation.

6.2.3. SHIP inhibits the expression of genes involved in regulation of transcription and signal transduction

All of data from the 8 genes, whose transcripts were validated as significantly reduced by quantitative real-time RT-PCR coincided with the microarray analysis (Table XII). Four of them encode proteins implicated in initiating and propagating cellular signal cascades (50%). In this category, the mRNAs encoding *TRIB3* (Tribbles homolog 3 (*Drosophila*)) (-78%) was the most highly repressed transcript in Jurkat T cells after the restoration of SHIP, followed by *ARHGEF10* (-66%), *ARRDC3* (-55%), and *PAG* (-50%), respectively. It has been reported

that TRIB3 functions as a negative regulator of Akt (Du *et al,* 2003). TRIB3 expression is induced in liver under fasting conditions, and TRIB3 disrupts insulin signaling by binding directly to Akt and blocking its activation. They concluded that by interfering with Akt activation, TRIB3 contributes to insulin resistance in individuals with susceptibility to type 2 diabetes. The down-regulation of *TRIB3* shown here could indicate that in Jurkat T cells a similar mechanism in the interaction of Akt and TRIB3 may exist. Possibly, because of the constitutively activation of the PI3K/Akt pathway in Jurkat T cells, the negative effect of TRIB3 is masked, because the concentration of TRIB3 could not be enough to block Akt. After the restoration of SHIP, the PI3K/Akt pathway is inhibited because of the reduction of levels of $PI(3,4,5)P_3$ and reduced phosphorylation of Akt. It is possible that the concentration of TRIB3 is no longer necessary to block Akt, since it is already inhibited. Besides, a mechanism may exist that regulates the expression of TRIB3 when Akt is already inhibited. The exact mechanism of action remains to be elucidated.

The Rho guanine nucleotide exchange factor (GEF) 10 (ARHGEF10) encodes a guanine–nucleotide exchange factor for the Rho family of GTPase proteins (RhoGEFs) and contains a Dbl homology (DH) domain, a common feature for RhoGEFs (Verhoeven *et al,* 2003; Zheng, 2001). ARHGEF10 may form complex with G proteins and stimulate Rho-dependent signals. The SHIP-mediated repression of *ARHGEF10* observed in this study (-66%) (Table XII) suggests a reduction in the activation of some RhoGTPases, inhibiting their interaction with downstream effector proteins involved in cell–cycle progression and gene expression.

ARRDC3 codes for the arresting domain containing 3 protein. GO annotations associate this protein with signal transduction. However, why SHIP should so markedly affect *ARRDC3* expression remains elusive. PAG is a type III transmembrane adaptor protein that binds to the tyrosine kinase CSK, and it is thought that PAG is involved in the regulation of T cell activation (Brdicka *et al,* 2000). *In vitro* analyses have suggested that PAG can bind strongly to nearly all SH2 domain-containing proteins. However, only FYN and CSK associated with PAG in cells (Brdicka *et al,* 2000). PAG recruits CSK to the plasma membrane via phosphorylated Tyr-317 independent of FYN. It has been shown by western blot analysis that after T-cell activation PAG is dephosphorylated and the association with CSK, but not with FYN, markedly decreases. The authors concluded that the PAG-CSK complex increases the signaling threshold required for initiating an immune response, thus helping to keep lymphocytes in a resting state. Although SHIP-mediated down-regulation of *PAG* appears not

to contribute to a resting state, it could be possible that the repression in the expression of *PAG,* with subsequently reduction on the protein levels leads to a low concentration of protein that could be phosphorylated. Therefore, the association with CSK could diminish and in principle Src kinase could be active. It is known however, that CSK-dependent phosphorylation of Src kinase inactivates it, and has an effect on proliferation. Although high levels of PAG-CSK association help to maintain resting phenotype in lymphocytes, other mechanisms of signaling including down-regulation of *PAG* may contribute to reduction of proliferation of T cells. Maybe the association of some proteins with regulatory domains could neutralize or reduce the anti-resting effect in the absence of PAG-CSK-dependent inactivation of Src kinase. Other possibility could be that the down-regulation of *PAG* is involved in a signaling pathway that negatively regulates the proliferation of T cells, and which is until now unknown.

Three of the 8 genes, whose transcripts were significantly SHIP-reduced (>2-fold) coded for proteins involved in transcription, cell cycle and/or localized in the nucleus (37.5%). Of these, the genes for *ATF5* (-79%) and *ZNF75* (-79%) were the most strongly down-regulated, followed by *DNAJB9* (-64%).

ATF5 (activating transcription factor 5) is a member of the CREB/ATF factor family. ATFs bind to cAMP-inducible promoters and are involved in gene transcription. ATF5 is unique among the CREB/ATF family in that expression is strictly regulated with cell cycle and function is intimately linked with apoptosis (Forgacs *et al,* 2005). The known down-stream targets for ATF5 seem to be restricted to those genes that are involved in the regulation of apoptosis (Persengiev *et al,* 2002). ATF5 is an anti-apoptotic factor and its expression is down-regulated in a variety of cell lines undergoing apoptosis following growth factor deprivation. The action of ATF5 is thought to be conditionally related to apoptosis in that ATF5 levels must be reduced to allow apoptosis to proceed. It has been described that some transcription factors are regulated by Akt, among them the FoxO family of transcriptional regulators (Burgering and Kops, 2002), CREB and NF-κB. Akt phosphorylation of CREB increases binding to CBP and enhances CREB transcriptional activity (Pugazhenti *et al,* 1999). It was not observed by microarray analyses any significant changes in the mRNA expression of neither the FoxO family genes nor NF-κB or CREB. It could be possible that the repression of *ATF5* mRNA expression observed in this study is dependent on Akt inactivation. The SHIP-mediated inactivation of Akt in Jurkat-SHIP cells may involve an

indirect mechanism that does not require *de novo* protein synthesis dependent of ATF5. Thus, it is possible that the inactivation of Akt not only would have a direct effect of lack of phosphorylation on transcription factors, but also the inability to induce intermediate transcription factors that regulates gene expression. This model agrees in some extent with the results reported by Porstmann *et al.* (2005). They found by microarray analysis a number of transcriptional regulators among the genes modulated in response to Akt activation in human retinoic pigment epithelial (RPE) cells. One of them was the downregulation of the *CREBL1/ATF-6β* gene and up-regulation of sterol-regulatory element binding proteins (SREBP) genes, involved in fatty acid and cholesterol synthesis. Interestingly, ATF-6 inhibits SREBP-dependent transcription in response to glucose deprivation, and the authors try to find a possible association between the downregulation of ATF-6β and the Akt-dependent regulation of SREBPs. These data suggest that the SHIP-mediated inactivation of Akt has an effect on the repression of ATF5 expression, involved in reduction of proliferation in Jurkat T cells.

The *ZNF75* gene product, the Zinc finger protein 75 (D8C6) belongs also to the Krüppel C2H2-type zinc finger protein family (Villa *et al,* 1992). ZNF75 contains five C2H2-type zinc fingers and one KRAB (Krüppel-associated box) domain (UniProt (Swis-Prot/Tr EMBL). The function of ZNF75 and in general of KRAB-ZFPs is largely unknown. However, they appear to play important roles during cell differentiation and development. By analysis of function according to GO annotations, ZNF75 could be involved in DNA-dependent regulation of transcription (GO: 6355). The down-regulation of ZNF75 mRNA after the restoration of SHIP in Jurkat T-cells is presumably related to the repression of transcription of some genes involved in positive regulation of proliferation.

The *DNAJB9* gene (microvascular endothelial differentiation gene 1) codes for the DnaJ (Hsp40) homolog, subfamily B, member 9. Gene Ontology analysis (GO: 6457) involves DNAJB9 in protein folding. Probably DNAJB9 protein levels are reduced after signaling of low rate of protein synthesis in Jurkat cells after the expression of SHIP. It would be a mechanism of saving energy for the metabolism of the cell in conditions leading to a reduction in proliferation. In relation to the proliferation of leukemia, it would be a strategy to control in some extent the proliferation.

IL26 was the only interleukin that was SHIP-repressed in Jurkat cells (-76%). The presence of *IL26* transcripts in a series of leukemia T-cell lines has been already reported (Knappe *et al,* 2000). IL26 was identified as a novel cellular homolog of interleukin-10 by transformation of T lymphocytes with the herpes virus saimiri (HVS). The IL10- family is composed of six cellular cytokines (IL10, IL19, IL20, IL22, IL24, and IL26) and viral homologs (Dumoutier and Renauld, 2002). In this study, it was observed by analysis of the microarray data, that *IL10*, *IL19*, and *IL22* mRNAs were absent in Jurkat T cells. Additionally, mRNAs for the IL10 receptor (alpha) and IL20 receptor (alpha) were also absent. Notable is that in Jurkat T cells there is a lack of expression of a great variety of cytokines and their receptors, including IL1R2, interleukin l, beta (IL1B), IL2, IL2 receptors alpha and beta, IL3, IL4, IL4 receptor, IL5, IL7 (confirmed by PCR (data not shown)), IL8, IL9, IL11, IL13, IL15, IL17, IL18, IL21, among others. In contrast, mRNAs corresponding to interleukin enhancer binding factors were present, such as interleukin enhancer binding factor 1, 2, 3. Additionally, the presence of the mRNAs corresponding to IL6 (interferon, beta 2), IL16, IL17 receptor, and TF8 (repressor of IL2 expression) was observed. Nevertheless, their mRNA expression was not regulated by SHIP. *IL26* mRNA is expressed in activated NK cells and T cells with enhanced expression upon type 1 polarization. Additionally, IL26 is produced by activated memory but not by naïve $CD4^+$ T cells, independently of costimulation (Wolk *et al,* 2002), suggesting that IL26 may have an influence on the immune response. It has been described that the dimerization of the receptor units IL20R1 (CRF2-8) and IL10R2 (CRF2-4) generates a functional IL26R complex (Sheikh *et al,* 2004). IL26-mediated signaling through this receptor complex induced activation of two members of the STAT family, STAT1 and STAT3. In this study the mRNAs for *STAT1*, *STAT3* and *STAT6* are present and were not regulated after the expression of SHIP. However, the mRNAs for *STAT5A* and *STAT5B* are absent. This suggests that Jurkat T cells may include a signaling pathway involving IL26 and activation of STAT1 and STAT3 by phosphorylation of proteins.

Since the herpes virus saimiri-transformed T cells have been found to strongly over-express IL26, in contrasts to other T-cells lines and native peripheral blood cells, which transcribe IL26 at low levels. It has been proposed that IL26 is a good candidate to play a role in the autocrine growth stimulation, leading to spontaneous proliferation of T cells after (HVS) infection (Knappe *et al,* 2000). According to this, and taking in consideration the high level of the differential expression of *IL26* mRNA in Jurkat cells before and after the expression of SHIP, IL26 may play a role in the proliferation of Jurkat cells, via IL26 receptors and

activation of the Jak/STAT pathway, transmitting the signal from the membrane to the cell nucleus. Consequently, the SHIP-mediated repression of *IL26* may be involved in the reduced proliferation of these cells after expression of SHIP.

In summary, SHIP induces the expression of genes involved in a quiescent phenotype and represses the expression of genes involved in the regulation of transcription and signal transduction. Both effects, either alone or in combination may lead to the observed reduction of proliferation in Jurkat T cells after expression of SHIP.

There are some candidates for the study of biological functions. Considering the genes expressed in T cells, *CD62L, KLF2, PAG* and *IL26* were found. Among them, the most interesting are KLF2 from the increased genes and IL26 from the repressed ones, since both have been detected in leukemia T-cell lines (Tables XI and XII) (Buckley *et al,* 2001; Knappe *et al,* 2000) . The expression of KLF2 has been described to be sufficient to program a quiescent phenotype in Jurkat T cells (Buckley *et al,* 2001). This effect is analog to that shown before (Horn, 2003) on proliferation after the expression of SHIP. Therefore, KLF2 was chosen as the best candidate to be analyzed in association with the biology of Jurkat cells.

6.3. The up-regulation of the T cell quiescent factor KLF2 has an inhibitory effect on proliferation in Jurkat cells after the expression of SHIP

The Krüppel-like factor 2 (KLF2) is involved in quiescence in naive T-cells and its negative regulation on the cell growth of Jurkat T cells has been already shown (Buckley et al, 2001, Wu and Lingrel, 2004). Additionally, it has been shown in our laboratory that the expression of SHIP in Jurkat T-cells led to inhibition of proliferation (Horn *et al,* 2004). Therefore, the relationship between the SHIP-mediated up-regulation of *KLF2* and the proliferation in Jurkat T-cells was analyzed. The microarray data revealed that KLF2 was up-regulated 3.0-fold in Jurkat-SHIP cells after induction of SHIP expression. It was also confirmed by quantitative real-time RT-PCR a 3.2 ± 1.1-fold increase in SHIP-dependent *KLF2* mRNA expression that was statistically significant, in comparison to the house keeping gene *GAPDH* (Table XI, Figures 15 and 16). The changes at the KLF2 protein levels were also confirmed and quantified by western blot analysis. Additionally, the relationship between KLF2, SHIP and

the PI3K/Akt pathway was considered and investigated. After induction of SHIP expression by the addition of doxycycline (Dox), the constitutive phosphorylation of Akt at serine residue 473 was strongly reduced to 20%. Simultaneously, the expression of KLF2 protein level was increased twofold relative to the expression of GAPDH protein level. These results confirmed that SHIP induced not only the expression of KLF2 at the mRNA level, but also at the protein level, along with the inhibition of the phosphorylation of Akt, by reduction of phosphorylation at Serine 473. The results suggested that the gene functionality of KLF2 could be affected by the inactivation of Akt, and probably KLF2 is involved in reduction of proliferation in Jurkat T-cells after the expression of SHIP. To confirm these models in Jurkat-SHIP cells it was chosen at first the model of the effect of KLF2 on proliferation. The model of the Akt-mediated regulation of KLF2 was also analyzed and will be discussed later (See 6.5.).

The KLF2 protein was expressed by transient transfection in Jurkat-SHIP cells grown either in the presence or in absence of SHIP expression. Proliferation of the transfected cells, analyzed by bromodeoxyuridine (BrdU) incorporation in the enhanced green fluorescent protein (EGFP)-gated populations determined by FACS analysis revealed that proliferation was reduced by 45.2% ± 5.1% in cells transfected with the KLF2-EGFP vector relative to cells transfected with the parental EGFP vector. This was a similar reduction (60.3% ± 14.4%) in proliferation observed after the expression of SHIP (Garcia-Palma *et al,* 2005a). Co-expression of SHIP and KLF2 further reduced the proliferation significantly by 83.7% ± 2.2% (P = 0.02), suggesting an additive effect of SHIP and KLF2 on the proliferation of Jurkat cells (Garcia-Palma *et al,* 2005a). Firstly, the expression of KLF2 has an effect on the reduction of proliferation in Jurkat T-cells, confirming results reported by Buckley *et al.* (2001). Additionally, the negative effect of SHIP on proliferation as reported previously (Horn *et al,* 2004) was confirmed. Finally, a significant reduction on proliferation was observed after the co-expression of KLF2 and SHIP, indicating an additive negative effect of both proteins in the reduction of proliferation of Jurkat cells.

What may be the physiological function of the SHIP-mediated up-regulation of KLF2? KLF2 is a member of the family of Krüppel-like factors, which regulate the transcription of a variety of genes involved in physiological processes including growth and differentiation (Anderson *et al,* 1995; Kuo *et al,* 1997). Recent data indicate that KLF2 is down-regulated in human ovarian tumors and suggest a putative function of KLF2 as tumor suppressor gene (Wang *et*

al, 2005). It has been reported that KLF2 may exert its anti-proliferative effect either by transcriptional inhibition of the proteins that stimulate cell cycle progression, such as WEE1 or c-Myc (Buckley *et al*, 2001; Wang *et al*, 2005), or by up-regulation of proteins that inhibit cell proliferation, like the cyclin-dependent kinase inhibitor p21WAF1/CIP1 (Wu & Lingrel, 2004). However, involvement of WEE1, c-Myc or p21WAF1/CIP1 in the SHIP-mediated inhibition of proliferation is rather unlikely, because in this work changes in the expression of WEE1, c-Myc or p21WAF1/CIP1 were not detected after the induction of SHIP expression and the up-regulation of KLF2 (data not shown). Probably KLF2 exert its anti-proliferative effect in Jurkat-SHIP cells by transcriptional inhibition of other genes. As described in the previous section, ATF5 is an anti-apoptotic factor (Persengiev *et al,* 2002), and is believed that ATF5 levels must be reduced to allow apoptosis to proceed in some cell lines. Although SHIP expression leads to a reduction of proliferation in Jurkat cells, without affecting apoptosis, and ATF5 is an anti-apoptotic factor, it could be possible that ATF5 is involved in regulation of proliferation of these cells. A key goal in the elucidation of a possible correlation between KLF2 and ATF is therefore to determine whether the repression of *ATF5* is controlled by KLF2.. According to this model, it would result in a novel pathway that describes inhibition of transcription of genes that positively regulate cell proliferation, having as a result a reduction in cell proliferation or inhibition of transcription of genes involved in negative regulation of apoptosis, allowing the cells undergoing apoptosis.

A physiological process where KLF2 has been implicated is the development of T lymphocytes. Both KLF2 and SHIP are up-regulated during the step from immature double positive $CD4^+/CD8^+$ thymocytes to mature single-positive $CD4^+$ or $CD8^+$ T cells (Kuo *et al*, 1997; Liu *et al*, 1998). With respect to the observed up-regulation of KLF2 by SHIP reported here, it seems possible that SHIP is involved in the up-regulation of KLF2 during the development of single-positive $CD4^+$ or $CD8^+$ T cells. However, gene-targeting experiments in mice argue against this possibility. Whereas the number of mature peripheral T cells is reduced by 90% in KLF2-knock out mice, SHIP-knock out mice do not show changes in T-cell development (Kuo *et al,* 1997; Helgason *et al,* 1998). Another physiological process of T cells where KLF2 seems to be important is the regulation of T-cell quiescence (Kuo *et al,* 1997; Buckley *et al,* 2001). T cells circulate in the blood and lymphoid organs in a quiescent state until they become activated by the binding of an appropriate antigen to the T-cell receptor. Recent data suggest that T-cell quiescence is an active process and that KLF2 plays an important role in programming and maintaining single-positive $CD4^+$ or $CD8^+$ cells in their

quiescent state (Kuo *et al,* 1997; Buckley *et al,* 2001). KLF2 expression decreases rapidly upon T-cell receptor activation (Kuo *et al*, 1997; Schober *et al,* 1999). Nevertheless, the signaling pathways that intermediate between the T cell receptor and KLF2 are not known so far.

In summary, the data shown in this study clearly implicate KLF2 in the SHIP-mediated inhibition of proliferation of the human leukemic T cell line Jurkat, by reduction of newly synthesized DNA. This is the first study that associates KLF2 with SHIP. Additionally, the results revealed that the inhibitory effect of KLF2 on proliferation in Jurkat cells increased when co-expressed with SHIP. The inhibitory effects of Krüppel-like factor 2 (KLF2) and the correlation between KLF2 protein expression levels and DNA synthesis in Jurkat T-cells was demonstrated. The results of analysis of expression of KLF2 and reduction of newly synthesized DNA revealed that the reduction of newly synthesized DNA is dependent on the level of the KLF2 protein in Jurkat T-cells after the expression of SHIP. PI3K and SHIP are activated during T cell stimulation by the T cell receptor and the co-stimulatory molecule CD28 (reviewed in Ward & Cantrell, 2001). More information about the biology of Jurkat cells and signaling pathways are necessary to elucidate the mechanism of action of KLF2. Whether the up-regulation of KLF2 in Jurkat T cells is mediated by the PI3K/Akt pathway will be discussed in the following sections.

6.4. Akt1 is not regulated at the mRNA level by SHIP in Jurkat T cells

Microarray analyses showed that none of the three isoforms of Akt: Akt1, Akt2, Akt3 were regulated at the mRNA level after the expression of SHIP in Jurkat cells. Further validation by quantitative real-time RT-PCR for *Akt1* mRNA expression confirmed that SHIP has no effect on the regulation of the expression of the *Akt1* gene (Tables XIV, XVI). The data obtained here demonstrated that the SHIP-mediated inhibition of the activity of Akt occurs at the protein level, rather than at the transcriptional level.

6.5. Up-regulation of the T cell quiescence factor KLF2 occurs via the PI3K/Akt signaling pathway

KLF2 is down-regulated after T cell activation (Buckley *et al,* 2001) and here it was shown that KLF2 is up-regulated after the expression of SHIP in Jurkat T cells. Additionally, it was

demonstrated that the synthesis of new DNA is reduced after KLF2 expression, and this effect is increased when both KLF2 and SHIP are expressed. However, the signal transduction pathway mediating the regulation of KLF2 has not been reported. Because the activation of the T cell receptor results in stimulation of PI3-kinase, it was analyzed whether the PI3K/Akt pathway is involved in the regulation of KLF2. Inhibition of PI3-kinase with wortmannin and knockdown of the expression of Akt1 in Jurkat T-cells revealed the PI3K/Akt-mediated up-regulation of KLF2 in Jurkat cells. It has been suggested that the proliferation in Jurkat T cells is dependent on the constituve activation of the PI3-kinase (Horn, 2003). Additionally, it has been shown that the constitutively activated PI3K/Akt pathway is inhibited by the expression of SHIP, leading to a reduction of proliferation.

Because of PI3-kinase activation, Akt is translocated to the plasma membrane by binding to PI3-kinase-generated phosphoinositides, i.e. $PI(3,4,5)P_3$ and $PI(3,4)P_2$ through the Akt pleckstrin domain. Akt is subsequently activated by sequential phosphorylation of threonine 308 by phosphoinositide-dependent kinase (PDK) 1 and of serine 473 by protein kinase C βII (PKCβII) or DNA-dependent protein kinase (DNA-PK) (Chan *et al*, 1999; Feng *et al*, 2004; Kawakami *et al*., 2004).

6.5.1. The inhibition of the PI3K led to an increase of the expression of KLF2 in Jurkat T cells

In this study, it was shown that the pharmacological inhibition of the PI3K with wortmannin led to an inhibition of the activation of Akt in Jurkat cells. Interestingly, the inhibition of PI3K was associated with an increase in the protein levels of KLF2, similar to that observed when SHIP is expressed. The data obtained in this study revealed that the inhibition of PI3-kinase with wortmannin in Jurkat T-cells led to a reduction to 50% on Akt phosphorylation at residue serine 473 (Table XVII). Additionally, a 2.4-fold increase in KLF2 protein levels was observed, which represent an increase of 140%, in comparison to the control (Figures 25-27). The restoration of SHIP and simultaneous inhibition of PI3K, led to a reduction to 40% in phosphorylation on Akt and an increase of 160% in the expression of the KLF2 protein (Table XVII). The reduction on cell proliferation and induction of apoptosis by inhibition of the PI3K/Akt signaling pathway has been reported before (Jücker *et al,* 2002). It was analyzed whether the constitutive activation of PI3K/Akt signaling was involved in inhibition of apoptosis and stimulation of proliferation in a Hodgkin's lymphoma-derived cell line (CO).

Jücker *et al*. (2002) found an increased percentage of apoptotic cells after treatment with the inhibitors of the PI3K wortmannin and LY294002, and the cell proliferation was partly inhibited in a concentration-dependent manner. How is it possible that the up-regulation of KLF2 is SHIP-dependent and PI3K/Akt-dependent? The best two explanations point towards the levels of $PI(3,4,5)P_3$. The expression and activity of the inositol 5-phosphatase SHIP reduced the levels of $PI(3,4,5)P_3$ (Horn *et al*., 2004). Consequently, Akt could neither be recruited to the membrane nor phosphorylated, and becomes inactive. This might lead to the up-regulation of KLF2 down-stream in the signal cascade, among other events that lead to reduction of proliferation and arresting in the G1 phase. Similarly, wortmannin inhibits the PI3-kinase by binding to the PI3K catalytic domain. PI3K is no longer able to phosphorylate $PI(4,5)P_2$ to $PI(3,4,5)P_3$, resulting in the same effect described before at this point. Therefore, the effect of SHIP in the reduction of $PI(3,4,5)P_3$ levels is analog to that obtain after inhibition of PI3K in Jurkat cells. These arguments may explain how the levels of KLF2 are increased by SHIP or by inhibition of PI3K.

In conclusion, the pharmacological inhibition of the PI3-kinase with wortmannin demonstrated that the inactivation of the PI3K/Akt signaling pathways led to an increase in the expression of KLF2 in Jurkat T-cells. These data revealed that the KLF2 induction is PI3K-mediated in Jurkat cells. Thus, the inactivation of the PI3K/Akt pathway appears to be necessary for the induction of KLF2 expression, involved in the reduction of proliferation in Jurkat cells.

6.5.2. The knockdown of the Akt1 protein is sufficient to induce KLF2 in Jurkat T cells

After elucidation of PI3K/Akt-mediated up-regulation of KLF2 by treatment with wortmannin, it was subsequently investigated downstream in the signal pathway whether knockdown of Akt1 was sufficient to induce the increase of KLF2 expression. In order to achieve that, specific gene silencing by siRNA was used to downregulate selectively Akt1 expression. The Akt kinase is a crucial component of signal transduction pathways that regulate cell growth, proliferation and survival. It is activated in cells that have lost the tumor suppressor PTEN and is required for the oncogenic action of mutated Ras proteins (Porstmann *et al,* 2005). Although some of the substrates of Akt, such as Bad, are directly involved in the regulation of apoptosis, it has been recognized that regulation of transcription

by Akt may contribute to its prosurvival function (Brunet *et al,* 2001). Akt is also involved in promoting cell cycle progression by regulating cyclin D1 stability (Diehl *et al,* 1998) and modulating expression and subcellular localization of the cdk inhibitors p27Kip1 (Kops *et al,* 2002; Shin *et al,* 2002) and p21WAF1 (Zhou *et al,* 2001). In our laboratory an increase in the transit time of Jurkat cells through the G1 phase of the cell cycle has been observed after the restoration of SHIP, coupled to reduced levels of PtdIns(3,4,5)P_3, reduced activity of Akt and reduced phosphorylation of GSK-3β, a substrate of Akt, without affecting the constitutive dual phosphorylation of MAPK-kinases Erk1/Erk2 on T202/Y204 (Horn *et al,* 2004). In addition, a reduction in the phosphorylation of Rb at Ser-780 has been identified (Horn *et al,* 2004), involved in the transcription of genes necessary for G1/S transition, indicating that the SHIP-mediated downregulation of proliferation of Jurkat cells acts by increasing the transit time through the G1 phase of the cell cycle.

In this study, it was demonstrated by microarray analysis and quantitative real-time RT-PCR that the restoration of SHIP has no influence on changes at the transcriptional regulation of genes coding for p27Kip1 or p21WAF1 (data not shown). This agrees with the model proposed by Horn *et al.* (2004), who proposed that in SHIP-mediated reduction of proliferation in Jurkat cells, the control of p27Kip1 and p21WAF1 in the signal transduction pathways are concerned to other mechanisms, rather than regulation of their transcription by Akt. Although the transcription factors reported to be regulated by Akt were not found to be regulated in Jurkat cells after microarray analysis, it is likely that some of the transcription factors found in this work to be differentially expressed are novel targets for Akt regulation. In the previous section, it was demonstrated that the inhibition of PI3K led to an increase in KLF2 protein levels, involving reduction of phosphorylation on Akt. So, here is shown that knockdown of Akt by siRNA was sufficient to induce an increase of the KLF2 levels in Jurkat cells. Including high percentage of efficiency of transfection by electroporation in Jurkat cells (95.0-99.9%), not reported before for these cells, the silencing of Akt1 in Jurkat cells by western blot analyses and protein quantification was confirmed. The 37% silencing of the expression of Akt1 by RNAi led to a 1.9-fold increase (+ 90%) in the expression of KLF2, and 51% silencing of Akt1 expression led to 2.5-fold increase (+150%) in the expression of KLF2 in Jurkat cells, respectively (Figures 32 and 33). These results agree with those obtained after the expression of the inositol 5-phosphatase SHIP, leading to a reduction of the activity of Akt, resulting in the 2.5-fold up-regulation of KLF2 (Figure 33), in comparison to the negative control for the RNAi assay.

In summary, the data shown in this study revealed that the silencing of Akt is sufficient to induce the expression of KLF2 in Jurkat cells, and that the induction of KLF2 is dependant on the Akt1 protein levels. The changes observed in the induction of KLF2 after the pharmacological inhibition of the PI3-kinase and the silencing of Akt1 expression implicates the PI3K/Akt pathway in the induced expression of KLF2 in Jurkat cells. Because the expression of SHIP led to an inactivation of the PI3K/Akt pathway in Jurkat cells, resulting in a decrease in cell proliferation, it has been demonstrated that the up-regulation of KLF2 by SHIP is PI3K/Akt-dependent. That means that up-regulation of KLF2 occurs via inactivation of the PI3K/Akt signaling pathway in Jurkat cells.

How the PI3K/Akt signaling pathway regulates the induction of KLF2 remains to be elucidated. The most likely explanation is that the expression of KLF2 could be increased downstream in the signaling cascade, after reduction of phosphorylation of Rb. Rb inhibits progression from G1 to S phase of the cell cycle. It associates with a number of several proteins. However, many of the mechanisms involved and their role in cell cycle regulation are still unclear. It is known that Rb phosphorylated at Ser-780 can no longer bind to the transcription factor E2F. E2F is released from Rb and consequently induces the transcription of genes involved in the G1/S transition in the cell cycle. The known genes involved in G1/S transition were not shown by microarray analysis to be regulated at the transcription level after the expression of SHIP in Jurkat cells. Further studies are required to provide evidence of novel genes involved in the transition to the S-phase in Jurkat cells. The fact that the phosphorylation in Rb is reduced in Jurkat cells after the expression of SHIP via inactivation of the PI3K/Akt pathway, with increased transit time through the G1 phase (Horn *et al,* 2004), agrees with the hypothesis that Rb is a key player in the control of cell proliferation in these cells. It has been reported that the inactivation of Rb, either through mutations of the *Rb1* gene itself or through mutations that enhance Rb phosphorylation, has been widely observed in tumor cells (Sherr, 1996). Rb is constituvely phosphorylated in Jurkat cells (Horn, 2003), which inhibits its repressing function at the checkpoint in the cell-cycle control. The deregulation of the Rb pathway may represent one key event involved in the process of leukemogenesis.

7. Concluding remarks and perspectives

A model that summarizes the results obtained in this study including SHIP, KLF2, and the PI3K/Akt pathway, along with the previous reports for events occurring downstream in the signal cascade is shown in Figure 34.

The SHIP-mediated up-regulation of KLF2 may be mediated by the inhibition of transcriptional repressors of KLF2 during the G1/S transition in Jurkat cells. Probably, the transcription of these potential KLF2 repressors is activated by E2F, and when E2F is inhibited, the activation of these genes does not take place. Consequently, the transit time through the G1 phase is prolonged and the transcription of genes involved in a quiescent phenotype, such as KLF2, is simultaneously activated. Another possibility is that the inactivation of the PI3K/Akt pathway led to an activation of transcriptional activators of KLF2. Probably the reduction of phosphorylation on Rb, discussed before, leads to a transcriptional activation of genes that are activators of KLF2 and contribute to the prolonged time in the G1 phase.

In relation to the effect of KLF2 on proliferation, the increased activation of KLF2 could be also involved in the repression of transcription of S-phase genes, resulting in reduction of the rate of newly synthesized DNA in the population of Jurkat cells. Since the transcription of genes coding for p27Kip1 or p21WAF1 was not affected in Jurkat T cells after the expression of SHIP, it appears that the effect of KLF2 in regulation of cell proliferation, if associated with p27Kip1 or p21WAF1, takes place by other mechanisms rather than transcriptional regulation of those genes. A detailed elucidation of the signal pathways that regulate and deregulate cell proliferation involving SHIP, Akt, KLF2 and the cell cycle in Jurkat T cells needs to be further investigated.

The control of cell cycle and proliferation by transcriptional regulation include mechanisms that from the point of view of evolution give a selective advantage. The selection of traits that preserve “normal” cells capable to respond in an orchestrated way to diverse stimuli from the environment, including regulation and control of the proliferation, contribute to a high probability of survival of the organisms.

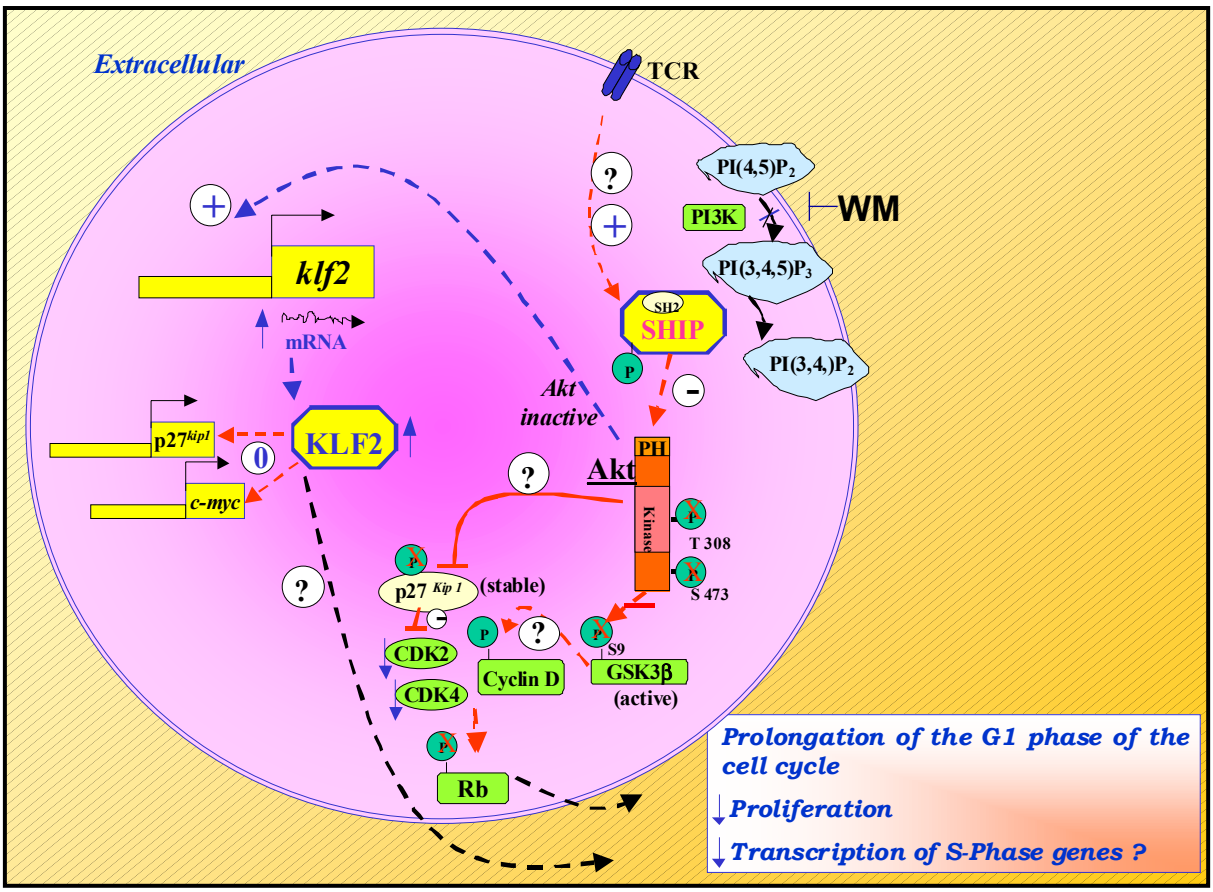

Figure 34. Up-regulation of the T cell quiescence factor KLF2 occurs via the Phosphatidylinositol 3-kinase/Akt signaling pathway.

After expression of SHIP in Jurkat T-cells, there is a reduction in the levels of PI(3,4,5)P_3 and inactivation of Akt by reduction of phosphorylation at residues Thr 308 and Ser 473. GSK3β is not phosphorylated at residue Ser 9, and becomes active; p27Kip1 is more stable, and the phosphorylation of Rb at Ser780 is reduced. Consequently, there is prolongation of the G1 phase of the cell cycle and reduction of proliferation. This also may implicate a reduction in the transcription of S-phase genes. A second event comprises the fact that the expression of KLF2 increases by the activity of SHIP. Additionally, inhibition of PI3-kinase with wortmannin and knockdown of the expression of Akt1 by RNAi led to an increase in the expression of KLF2. This implicates SHIP and the PI3-kinase/Akt signaling pathway in the up-regulation of KLF2 in Jurkat T cells. **PI3K:** Phosphoinositide 3-kinase. **Akt (PKB):** Protein kinase B. **GSK3β:** Glycogen synthase kinase-3b. **CDK:** Cyclin-dependent kinase. **RB:** Retinoblastoma tumor suppressor protein. **p27Kip1**: Cyclin-dependent kinase inhibitor 1B. **KLF2:** Krüppel-like factor 2. **PI(3,4,5)P_3:** phosphatidylinositol 3,4,5-trisphosphate. **TCR:** T cell receptor. **WM:** Wortmannin (From García-Palma *et al,* 2005b).

Mutation or deregulation of pathways that lead to unrestrained proliferation may represent a short-time success for the malignant cells, for example in cancer. However, such mutations contribute to a decrease in the expected rate of survival of the organisms. Currently many

studies try to identify not only the abnormalities that accompany the development of leukemia, but also the biology of such alterations.

With this study, the statistically significant differential expression (≥ 2-fold) of eleven genes (SHIP-induced: *KLF2, CD62L, KCMF1*; SHIP-repressed: *ATF5, ZNF75, DNAJB9, TRIB3, ARHGEF10, ARRDC3, PAG, IL26*) involved in transcription, signal transduction and cell proliferation was identified and verified in Jurkat cells by microarray and quantitative real-time RT-PCR analyses after the expression of SHIP, a negative regulator of proliferation. Further studies that elucidate possible associations of the genes identified in this study and their role in Jurkat cells need to be investigated. The SHIP-mediated induction of *KLF2* and its biological function on proliferation of Jurkat cells was demonstrated. Moreover, the additive effect of KLF2 co-expressed with SHIP in Jurkat cells was shown. The PI3K/Akt-mediated up-regulation of KLF2 was confirmed, and some possible mechanisms of regulation of the expression of KLF2 were considered.

Further microarray and quantitative real-time RT-PCR analyses of transcriptional profile of other leukemia T cells, i.e. from patients with T-ALL, should be carried out in order to identify the expression profiles of *KLF2* and the other 10 genes identified in these cells, and compared to expression of SHIP. Additionally, the analysis of PI3K/Akt signaling pathway activation should be also performed in these cells. The correlation between a constitutive PI3K/Akt signaling pathway and repression of KLF2 should be studied in those cells. Moreover, the performance of protein arrays might provide more information about the function of the remaining SHIP-regulated genes identified in this study, and their association with proliferation in Jurkat cells. This may contribute to the elucidation of their biological functions in leukemogenesis of T cells. All this might open an interesting new window that involves SHIP, PI3K/Akt and KLF2 as potential players for therapeutic intervention of some types of leukemia.

8. References

Abbas, A.K., Lichtman, A.H. & Pober, J.S. (1994) *Cellular and Molecular Immunology.* W.B. Saunders, London.

Affymetrix *(http://www.affymetrix.com/analysis/index.affx)*

Akashi, K., Traver, D., Miyamoto, T. & Weissman, I.L. (2000) A clonogenic common myeloid progenitor that gives rise to all myeloid lineages. *Nature* **404:** 193-197.

Amakawa, R., Fukuhara, S., Ohno, H., Matsuyama, F., Kato, I., Tanabe, S., Sideras, P., Mizuta, T.R., Honjo, T. & Okuma, M. (1991) Genomic organization of IgH gene compared with the expression of Bcl-2 gene in t(14;18)-positive lymphoma. *Blood* **77:** 1970-1976.

Anderson, K.P., Kern, C.B., Crable, S.C. & Lingrel, J.B. (1995) Isolation of a gene encoding a functional zinc finger protein homologous to erythroid Krüppel-like factor: identification of a new multigene family. *Mol. Cell. Biol.* **15:** 5957-5965.

Aoki, M., Batista, O., Bellicosa, A., Tsichlis, P. & Vogt, P.K. (1998) The Akt kinase: molecular determinants of oncogenicity. *Proc. Natl. Acad. Sci. USA* **95:** 14950-14955.

Bellacosa, A., Testa, J.R., Moore, R. & Larue, L. (2004) A portrait of AKT kinases: human cancer and animal models depict a family with strong individualities. *Cancer Biol. Ther.* **3:** 268-275.

Berridge, M.J. (1987) Inositol trisphosphate and diacylglycerol: two interacting second messengers. *Annu Rev Biochem* **56:** 159-193.

BLAST *(http://www.ncbi.nlm.nih.gov/BLAST/).*

Brdicka, T., Pavlistova, D., Leo, A., Bruyns, E., Korinek, V., Angelisova, P., Scherer, J., Shevchenko, A., Hilgert, I., Cerny, J., Drbal, K., Kuramitsu, Y., Kornacker, B., Horejsi, V. & Schraven, B. (2000) Phosphoprotein associated with glycosphingolipid-enriched microdomains (PAG), a novel ubiquitously expressed transmembrane adaptor protein, binds the protein tyrosine kinase Csk and is involved in regulation of T cell activation. *J. Exp. Med.* **191:** 1591-1604.

Brian, P.W., Curtis, P.J., Hemming, H.G. & Norris, G.L.F. (1957) Wortmannin, an antibiotic produced by *Penicillium wortmannii*. *Trans. Br. Mycol.* **40:** 365-368.

Brunet, A., Datta, S.R. & Greenberg, M.E. (2001) Transcription-dependent and -independent control of neuronal survival by the PI3K-Akt signaling pathway. *Curr. Opin. Neurobiol.* **11:** 297-305.

Buckley, A.F., Kuo, C.T. & Leiden, J.M. (2001) Transcription factor LKLF is sufficient to program T cell quiescence via a c-Myc-dependent pathway. *Nature Immunology* **2:** 698-704.

Burgering, B.M. & Kops, G.J. (2002) Cell cycle and death control: long live Forkheads. *Trends Biochem. Sci.* **27:** 352-360.

Butler, H. & Harris, M. (2000) *Guide to GO Evidence Codes.* Gene Ontology Consortium.

Chan, T.O., Rittenhouse, S.E. & Tsichlis, P.N. (1999) AKT/PKB and other D3 phosphoinositide-regulated kinases: kinase activation by phosphoinositide-dependent phosphorylation. *Annu. Rev. Biochem.* **68:** 965-1014.

Chiaramonte, R., Calzavarra, E., Basile, A., Comi, P. & Sherbert, G.V. (2002) Notch signal transduction is not regulated by SEL1L in leukaemia and lymphoma cells in culture. *Anticancer Res.* **22:** 4211-4214.

Chirgwin, J.M., Przybyla, A.E., MacDonald, R.J. & Rutter, W.J. (1979) Isolation of biologically active ribonucleic acid from sources enriched in ribonuclease. *Biochemistry* **18:** 5294-5299.

Cook, T., Gebelein, B., Mesa, K., Mladek, A. & Urrutia, R. (1998) Molecular cloning and characterization of TIEG2 reveals a new subfamily of transforming growth factor-β-inducible Sp1-like zinc finger-encoding genes involved in the regulation of cell growth. *J. Biol. Chem.* **273:** 25929-25936.

Crossley, M., Whitelaw, E., Perkins, A., Williams, G., Fujiwara, Y. & Orkin, S.H. (1996) Isolation and characterization of the cDNA encoding BKLF/TEF-2, a major CACCC-box-binding protein in erythroid cells and selected other cells. *Mol. Cell. Biol.* **16:** 1695-1705.

Cully, M., You, H., Levine, A.J. & Mak, T.W. (2006) Beyond PTEN mutations: the PI3K pathway as an integrator of multiple inputs during tumorigenesis. *Nat Rev Cancer* **6:** 184-192.

Davis, R.J. (1994) MAPKs: new JNK expands the group. *Trends Biochem. Sci.* **19:** 470-473.

Deutsches Kinderkrebsregister *http://www.kinderkrebsregister.de.*

Di Santo, J.P. (2001) Lung Krüppel-like factor: a quintessential player in T cell quiescence. *Nature Immunology* **2:** 667-668.

Diehl, J.A., Cheng, M., Roussel, M.F. & Sherr, C.J. (1998) Glycogen synthase kinase-3beta regulates cyclin D1 proteolysis and subcellular localization. *Genes & Dev.* **12:** 3499-3511.

Diehn, M., Alizadeh, A.A., Rando, O.J., Liu, C.L., Stankunas, K., Botstein, D., Crabtree, G.R. & Brown, P.O. (2002) Genomic expression programs and the integration of the CD28 costimulatory signal in T cell activation. *Proc Natl Acad Sci U.S.A.* **99:** 11796-11801.

Dive, C., Evans, C.A. & Whetton, A.D. (1992) Induction of apoptosis-new targets for cancer chemotherapy. *Semin Cancer Biol* **3:** 417-427.

Du, K., Herzig, S., Kulkarni, R.N. & Montminy, M. (2003) TRB3: a tribbles homolog that inhibits Akt/PKB activation by insulin by liver. *Science* **300:** 1574-1577.

Dumoutier, L. & Renauld, J.C. (2002) Viral and cellular interleukin-10 (IL-10)-related cytokines: from structures to functions. *Eur. Cytokine Network* **13**.

Entrez Gene *http://www.ncbi.nlm.nih.gov.*

Etienne, W., Meyer, M., Peppers, J. & Meyer Jr., R. (2004) Comparison of mRNA expression by RT-PCR and DNA microarray. *BIotechniques* **36:** 618-626.

Feng, J., Park, J., Cron, P., Hess, D. & Hemmings, B.A. (2004) Identification of a PKB/Akt hydrophobic motif Ser-473 kinase as DNA-dependent protein kinase. *J. Biol. Chem.* **279:** 41189-41196.

Feng, W.C., Southwood, C.M. & Bieker, J.J. (1994) Analyses of beta-thalassemia mutant DNA interactions with erythroid Krüppel-like factor (EKLF), an erythroid cell-specific transcription factor. *J. Biol. Chem.* **269:** 1493-1500.

Ferrando, A. & Look, T. (2002) *Gene signature identifies leukemia patients who should avoid transplants.* In: News & Publications. Press Releases. Dana-Farber Cancer Institute.

Finco, T.S., Kadlecek, T., Zhang, W., Samelson, L.E. & Weiss, A. (1998) LAT is required for TCR-mediated activation of PLCgamma1 and the Ras pathway. *Immunity* **9:** 617-626.

Forgacs, E., Gupta, S.K., Kerry, J.A. & Semmes, O.J. (2005) The bZIP Transcription Factor ATFx Binds Human T-cell Leukemia Virus Type 1 (HTLV-1) Tax and Represses HTLV-1 Long Terminal Repeat-Mediated Transcription. *J. Virol.* **79:** 6932-6939.

Foucar, K., McKenna, R., Bloomfield, C., Bowers, T. & Brunning, R. (1979) Therapy-related leukemia. *Cancer* **43:** 1285-1296.

Freitas, A.A. & Rocha, B. (2000) Population biology of lymphocytes: the flight for survival. *Ann. Rev. Immunol.* **18:** 83-111.

Garcia-Palma, L., Horn, S., Haag, F., Diessenbacher, P., Streichert, T., Mayr, G.W. & Jucker, M. (2005a) Up-regulation of the T cell quiescence factor KLF2 in a leukaemic T-cell line after expression of the inositol 5'-phosphatase SHIP-1. *British Journal of Haematology* **131:** 628-631.

García-Palma, L., Horn, S., Haag, F., Streichert, T., Diessenbacher, P., Mayr, G.W. & Jücker, M. (2005b) *Up-regulation of the T cell quiescence factor KLF2 occurs via the Phosphatidylinositol 3-kinase/Akt signaling pathway.* In: 9th Joint Meeting of the Signal Transduction Society (STS). Weimar, Germany.

Garofalo, R.S., Orena, S.J., Rafidi, K., Torchia, A.J., Stock, J.L., Hildebrandt, A.L., Coskran, T., Black, S.C., Brees, D.J., Wicks, J.R., McNeish, J.D. & Coleman, K.G. (2003) Severe diabetes, age-dependent loss of adipose tissue, and mild growth deficiency in mice lacking Akt2/PKBβ. *J. Clin. Invest.* **112:** 197-208.

Geier, S.J., Algate, P.A., Carlberg, K., Flowers, D., Friedman, C., Trask, B. & Rohrschneider, L.R. (1997) The human SHIP gene is differentially expressed in cell lineages of the bone marrow and blood. *Blood* **89:** 1876-1885.

Gene Ontology [http: //www.geneontology.org].

GeneAnnot (http://genecards.weizmann.ac.il/geneannot/).

GeneBank (http://www.ncbi.nlm.nih.gov/entrez/query.fgci?db=Nucleotide).

Gilliland, D.G. (2002) Molecular genetics of human leukemias: New insights into therapy. *Semin Hematol* **39:** 6-11.

Golub, T.R., Barker, G.F., Bohlander, S.K., Hiebert, S.W., Ward, D.C., Bray-Ward, P., Morgan, E., Raimondi, S.C., Rowley, J.D. & Gilliland, D.G. (1995) Fusion of the *TEL* gene on 12p13 to the *AML1* gene on 21q22 in acute lymphoblastic leukemia. *Proc. Natl. Acad. Sci. U.S.A* **92:** 4917-4921.

Graeler, M. & Goetzl, E.J. (2002) Activation-regulated expression and chemotactic function of sphingosine 1-phosphate receptors in mouse splenic T cells. *FASEB J.* **16:** 1874-1878.

Graf, T. (2002) Differentiation plasticity of hematopoietic cells. *Blood* **99:** 3089-3101.

Gratzner, H.G. & Leif, R.C. (1981) An immunofluorescence method for monitoring DNA synthesis by flow cytometry. *Cytometry* **1:** 385-393.

Haaland, R.E., Yu, W. & Rice, A.P. (2005) Identification of LKLF-regulated genes in quiescent $CD4^+$ T lymphocytes. *Molecular Immunology* **42:** 627-641.

Hagen, G., Müller, S., Beato, M. & Suske, G. (1992) Cloning by recognition site screening of two novel GT box binding proteins: a family of Sp1 related genes. *Nucleic Acids Res.* **20:** 5519-5525.

Hannun, Y.A. (1997) Apoptosis and the dilemma of cancer chemotherapy. *Blood* **89:** 1845-1853.

Helgason, C.D., Damen, J.E., Rosten, P., Grewal, R., Sorenson, P., Chappel, S.M., Borowski, A., Jirik, F., Krystal, G. & Humphries, R.K. (1998) Targeted disruption of SHIP leads to hemopoietic perturbations, lung pathology, and a shortened life span. *Genes & Dev.* **12:** 1610-1620.

Hellenbrecht, A., Messerer, D. & Gökbuget, N. (2003) *Häufigkeit von Leukämien bei Erwachsenen in Deutschland.* Kompetenztnetz Leukämien.

Horn, S. (2003) *Funktion der Inositolpolyphosphat-5'-Phosphatase SHIP in der Signaltransduktion hämatopoetischer Zellen und ihre Bedeutung für die humane Leukämogenese.* In: zelluläre Signaltransduction, Vol. Dr. rer. nat., p. 152. Universität Hamburg, Hamburg.

Horn, S., Endl, E., Fehse, B., Weck, M., Mayr, G.W. & Jücker, M. (2004) Restoration of SHIP activity in a human leukemia cell line downregulates constitutively activated phosphatidylinositol 3-kinase/Akt/GSK-3beta signaling and leads to an increased transit time through the G1 phase of the cell cycle. *Leukemia* **18:** 1839-1849.

Horn, S., Meyer, J., Heukeshove, J., Fehse, B., Schulze, C., Li, S., Frey, J., Poll, S., Stocking, C. & Jücker, M. (2001) The inositol 5-phosphatase SHIP is expressed as 145 and 135 kDa protein in blood and bone marrow cells in vivo, whereas carboxyl-truncated forms of SHIP are generated by proteolytic cleavage in vitro. *Leukemia* **15:** 112-120.

Jäger, U., Böcskör, S., Le, T., Mitterbauer, G., Bolz, I., Chott, A., Kneba, M., Manhalter, C. & Nadel, B. (2000) Follicular lymphomas' BCL-2/IgH junctions contain templated nucleotide insertions: novel insights into the mechanism of t(14;18) translocation. *Blood* **95:** 3520-3529.

Jamieson, C., Ailles, L., Dylla, S., Muijtjens, M., Jones, C., Gotlib, J., Li, K., Manz, M.G., Keating, A., Sawyers, C.L. & Weissman, I.L. (2004) Granulocyte-macrophage progenitors as candidate leukemic stem cells in blast-crisis CML. *N Engl J Med* **351:** 657-667.

Janeway, C.A., Travers, P., Walport, M. & Capra, J.D. (1999) *Immunobiology: the immune system in health and disease.* Elsevier Science Ltd/Garland Publishing, New York.

Jimenez, C., Jones, D.R., Rodríguez-Viciana, P., Gonzalez-Garcia, A., Leonardo, E., Wennström, S., von Kobbe, C., Toran, J.L., R.-Borlado, L., Calvo, V., Copin, S.G., Albar, J.P., Gaspar, M.L., Diez, E., Marcos, M.A.R., Downward, J., Martinez-A, M.I. & Carrera, A.C. (1998) Identification and characterization of a new oncogene derived from the regulatory subunit of phosphoinositide 3-kinase. *EMBO J.* **17:** 743-753.

Jücker, M., Schiffer, C.A. & Feldman, R.A. (1997) A tyrosine-phosphorylated protein of 140 kD is constitutively associated with the phosphotyrosine binding domain of Shc and the SH3 domains of Grb2 in acute myeloid leukemia cells. *Blood* **89:** 2024-2035.

Jücker, M., Südel, K., Horn, S., Sickel, M., Wegner, W. & Feldman, R.A. (2002) Expression of a mutated form of the p85alpha regulatory subunit of phosphatidylinositol 3-kinase in a Hodgkin's lymphoma-derived cell line (CO). *Leukemia* **16:** 894-901.

Kaczynski, J., Cook, T. & Urrutia, R. (2003) Sp1-and Kruppel-like transcription factors. *Genome Biol.* **4:** 206.

Kadonaga, J.T., Carner, K.R., Masiarz, F.R. & Tjian, R. (1987) Isolation of cDNA encoding transcription factor Sp1 and functional analysis of the DNA binding domain. *Cell* **51:** 1079-1090.

Katso, R., Okkenhaug, K., Ahmadi, K., White, S., Timms, J. & Waterfield, M.D. (2001) Cellular function of phosphoinositide 3-kinases: implications for development, homeostasis, and cancer. *Annu Rev Cell Dev Biol* **17:** 615-675.

Kawakami, Y., Nishimoto, H., Kitaura, J., Maeda-Yamamoto, M., Kato, R.M., Littman, D.R., Rawling, D.J. & Kawakami, T. (2004) Protein kinase CβII regulates Akt phosphorylation on Ser-473 in a cell type-and stimulus-specific fashion. *J. Biol. Chem.* **279:** 47720-47725.

Knappe, A., Hor, S., Wittman, S. & Fickenscher, H. (2000) Induction of a novel cellular homolog of interleukin-10, AK155, by transformation of T lymphocytes with herpesvirus saimiri. *J. Virol.* **74:** 3881-3887.

Kondo, M., Weissman, I.L. & Akashi, K. (1997) Identification of clonogenic common lymphoid progenitors in mouse bone marrow. *Cell* **91:** 661-672.

Kops, G.J., Medema, R.H., Glassford, J., Essers, M.A., Dijkers, P.F., Coffer, P.J., Lam, E.W. & Burgering, B.M. (2002) Control of cell cycle exit and entry by protein kinase B-regulated forkhead transcription factors. *Mol. Cell. Biol.* **22:** 2025-2036.

Kozyrev, S.V., Hansen, L.L., Poltaraus, A.B., Domninsky, D.A. & Kisselev, L.L. (1999) Structure of the human CpG-island-containing lung Kruppel-like factor (LKLF) gene and its location in chromosome 19p13.11-13 locus. *FEBS Lett.* **448:** 149-152.

Kuo, C.T., Veselits, M.L. & Leiden, J.M. (1997) LKLF: a transcriptional regulator of single-positive T cell quiescence and survival. *Science* **277:** 1986-1990.

Kyriakis, J.M. & Avruch, J. (2001) Mammalian mitogen-activated protein kinase signal transduction pathways activated by stress and inflammation. *Physiol Rev* **81:** 807-869.

Lee, J.W., Soung, Y.H., Kim, S.Y., Lee, H.W., Park, W.S., Nam, S.W., Kim, S.H., Lee, J.Y., Yoo, N.J. & Lee, S.H. (2005) *PIK3CA* gene is frequently mutated in breast carcinomas and hepatocellular carcinomas. *Oncogene* **24:** 1477-1480.

Leung, R.K. & Whittaker, P.A. (2005) RNA interference: from gene silencing to gene-specific therapeutics. *Pharmacol. Ther.* **107:** 222-239.

Li, E., Bestor, T.H. & Jaenisch, R. (1992) Targeted mutations of the DNA methyltransferase gene results in embryonic lethality. *Cell* **69:** 915-926.

Lichter, P., Bray, P., Ried, T., Dawid, I.B. & Ward, D.C. (1992) Clustering of C2-H2 zinc finger motif sequences within telomeric and fragile site regions of human chromosomes. *Genomics* **13:** 999-1007.

Lin, J. & Weiss, A. (2001) T cell receptor signalling. *J Cell Sci* **114:** 243-244.

Lin, Y.-W. & Aplan, P.D. (2004) Leukemic transformation. *Cancer Biology & Therapy* **3:** 13-20.

Lioubin, M.N., Algate, P.A., Schickwann, T., Carlberg, K., Aebersold, R. & Rohrschneider, L.R. (1996) $p150^{SHIP}$, a signal transduction molecule with inositol polyphosphate-5-phosphatase activity. *Genes & Dev.* **10:** 1084-1095.

Liu, Q., Shalaby, F., Jones, J., Bouchard, D. & Dumont, D.J. (1998) The SH2-containing inositol polyphosphate 5-phosphatase, SHIP, is expressed during hematopoiesis and spermatogenesis. *Blood* **91:** 2753-2759.

Liu, Y., Wei, S.H., Ho, A.S., de Waal, M.R. & Moore, K.W. (1994) Expression cloning and characterization of a human IL-10 receptor. *J. Immunol.* **152:** 1821-1829.

Livak, K.J. & Schmittgen, T.D. (2001) Analysis of relative gene expression data using real time quantitative PCR and the $2^{-\Delta\Delta C}{}_T$ method. *Methods* **25:** 402-408.

Lucas, D.M. & Rohrschneider, L.R. (1999) A novel spliced form of SH2-containing inositol phosphatase is expressed during myeloid development. *Blood* **93:** 1922-1933.

Luo, J.-M., Liu, Z.-L., Hao, H.-L., Wang, F.-X., Dong, Z.-R. & Ohno, R. (2004) Mutation Analysis of SHIP Gene in Acute Leukemia. *J. Exp. Hematology.* **12:** 420-426.

Luo, J.-M., Yoshida, H., Komura, S., Ohishi, N., Pan, L., Shigeno, K., Hanamura, I., Miura, K., Iida, S., Ueda, R., Naoe, T., Akao, Y., Ohno, R. & Ohnishi, K. (2003) Possible dominant-negativ mutation of the SHIP gene in acute myeloid leukemia. *Leukemia* **17:** 1-8.

Makover, D., Cuddy, M., Yum, S., Bradley, K., Alpers, J., Sukhatme, V. & Reed, J.C. (1991) Phorbol ester-mediated inhibition of growth and regulation of proto-oncogene expression in the human T cell leukemia line JURKAT. *Oncogene* **6:** 455-460.

Mao, R., Wang, X., Spitznagel Jr, E.L., Frelin, L.P., Ting, J.C., Ding, H., Kim, J.-w., Ruczinski, I., Downey, T.J. & Pevsner, J. (2005) Primary and secondary transcriptional effects in the developing human Down syndrome brain and heart. *Genome Biol.* **6:** R107.

March, M.E. & Ravichandran, K. (2002) Regulation of the immune response by SHIP. *Semin. Immunol.* **14:** 37-47.

Mateyak, M.K., Obaya, A.J. & Sedivy, J.M. (1999) c-Myc regulates cyclin D-Cdk4 and -cdk6 activity but affects cell cycle progression at multiple independent points. *Mol. Cell. Biol.* **19:** 4672-4683.

Matsumoto, N., Laub, F., Aldabe, R., Zhang, W., Ramirez, F., Yoshida, T. & Terada, M. (1998) Cloning the cDNA for a new human zinc finger protein defines a group of closely related Krüppel-like transcription factors. *J. Biol. Chem.* **273:** 28229-28237.

McLean, T.W., Ringold, S., Neuberg, D., Stegmaier, K., Tantravahi, R., Ritz, J., Koeffler, H.P., Takeuchi, S., Jansenn, J.W., Seriu, T., Bartram, C.R., Sallan, S.E., Gilliland, D.G. & Golub, T.R. (1996) TEL/AML-1 dimerizes and is associated with a favorable outcome in childhood acute lymphoblastic leukemia. *Blood* **88:** 4252-4258.

Meijerink, J.P., Mensink, E.J., Wang, K., Sedlak, T.W., Sloetjes, A.W., de Witte, T., Waksman, G. & Korsmeyer, S.J. (1998) Hematopoietic malignancies demonstrate loss-of-function mutations of BAX. *Blood* **91:** 2991-2997.

Merck & Co. Inc. (2002) The Merck Manual-Home Edition, Sec. 14, Ch. 157, Leukemias. (http://www.merck.com/pubs/mmanual_home/sec14/).

Miller, I.J. & Bieker, J.J. (1993) A novel, erythroid cell-specific murine transcription factor that binds to the CACCC element and is related to the Kruppel family of nuclear proteins. *Mol. Cell. Biol.* **13:** 2776-2786.

Miller, J., McLachlan, A.D. & Klug, A. (1985) Repetitive zinc-binding domains in the protein transcription factor IIIA from Xenopus oocytes. *EMBO J.* **4:** 1609-1614.

Miltenburger, H.G., Sachse, G. & Schliermann, M. (1987) S-phase cell detection with a monoclonal antibody. *Dev. Biol. Stand.* **66:** 91-99.

Min, Y.H., Eom, J.I., Cheong, J.W., Maeng, H.O., Kim, J.Y., Jeung, H.K., Lee, S.T., Lee, M.H., Hahn, J.S. & Ko, Y.W. (2003) Constitutive phosphorylation of Akt/PKB protein in acute myeloid leukemia: its significance as a prognostic variable. *Leukemia* **17:** 995-997.

Moreno, C.S., Ramachandran, S., Ashby, D.G., Laycock, N., Plattner, C.A., Chen, W., Hahn, W.C. & Pallas, D.C. (2004) Signaling and transcriptional changes critical for transformation of Human cells by Simian Virus 40 small tumor antigen or protein phosphatase 2A B56γ knockdown. *Cancer Research* **64:** 6978-6988.

NCBI: National Center for Biotechnology Information (*http://www.ncbi.nlm.nih.gov).*

Ng, C., Koyama, K., Okamura, S., Kondoh, H., Takei, Y. & Nakamura, Y. (1999) Isolation and characterization of a novel TP53-inducible gene, TP53TG3. *Genes Chromosomes Cancer* **26:** 329-335.

Nishizuka, Y. (1988) The molecular heretogeneity of protein kinase C and its implication for cellular regulation. *Nature* **334:** 661-665.

OMIM™: Online Mendelian Inheritance in Man™ (http://www.ncbi.nlm.nih.gov). *Johns Hopkins University*

Ono, M., Bolland, S., Tempst, P. & Ravetch, J.V. (1996) Role of the inositol phosphatase SHIP in negative regulation of the immune system by the receptor FcgRIIb. *Nature Immunology* **383:** 263-266.

Passegue, E., Jamieson, C., Ailles, L. & Weissman, I. (2003) Normal and leukemic hematopoiesis: Are leukemias a stem cell disorder or a reacquisition of stem cell characteristics? *Proc Natl Acad Sci U S A* **100:** 11842-11849.

Pavletich, N.P. & Pabo, C.O. (1991) Zinc finger-DNA recognition: crystal structure of a Zif268-DNA complex at 2.1 Å. *Science* **252:** 809-817.

Persengiev, S.P., Devireddy, L.R. & Green, M.R. (2002) Inhibition of apoptosis by ATFx: a novel role for a member of the ATF/CREB family of mammalian bZIP transcription factors. *Genes & Dev.* **16:** 1806-1814.

Philipsen, S. & Suske, G. (1999) A tale of three fingers: the family of mammalian Sp/XKLF transcription factors. *Nucleic Acids Res.* **27:** 2991-3000.

Porstmann, T., Griffiths, B., Chung, Y.-L., Delpuech, O., Griffiths, J.R., Downward, J. & Schulze, A. (2005) PKB/Akt induces transcription of enzymes involved in cholesterol and fatty acid biosynthesis via activation of SREBP. *Oncogene* **24:** 6465-6481.

Pugazhenthi, S., Boras, T., O'Connor, D., Meintzer, M.K., Heidenreich, K.A. & Reusch, J.E. (1999) Insulin-like growth factor I-mediated activation of the transcription factor cAMP response element-binding protein in PC12 cells. Involvement of p38 mitogen-activated protein kinase-mediated pathway. *J. Biol. Chem.* **274:** 2829-2837.

Ramakers, C., Ruitjer, J.M., Deprez, R. & Moorman, A.F. (2003) Assumption-free analysis of quantitative real-time polymerase chain reaction (PCR) data. *Neurosciences Letters* **339:** 62-66.

Roberts, C.W., Shutter, J.R. & Korsmeyer, S.J. (1994) Hox11 controls the genesis of the spleen. *Nature* **368:** 747-749.

Rohrschneider, L.R., Fuller, J.F., Wolf, I., Liu, Y. & Lucas, D.M. (2000) Structure, function, and biology of SHIP proteins. *Genes & Dev.* **14:** 505-520.

Romana, S.P., Poirel, H., Leconiat, M., Flexor, M.A., Mauchauffe, M., Jonveaux, P., Macintyre, E.A., Berger, R. & Bernard, O.A. (1995) High frequency of t(12;21) in childhood B-lineage acute lymphoblastic leukemia. *Blood* **86:** 4263-4269.

Rowley, J.D. (1973) Identification of a translocation with quinacrine fluorescence in a patient with acute leukemia. *Ann. Genet.* **16:** 109-112.

Sasaki, K., Murakami, T. & Takahashi, M. (1989) Flow cytometric analysis of cell proliferation kinetics using the anti-BrdUrd antibody. *Gan To Kagaku Ryoho* **16:** 2338-2344.

Sattler, M., Mohi, M.G., Pride, Y.B., Quinnan, L.R., Malou, f.N.A., Podar, K., Gesbert, F., Iwasaki, H., Li, S., Van Etten, R.A., Gu, H., Griffin, J.D. & Neel, B.G. (2002) Critical role for Gab2 in transformation by BCR-ABL. *Cancer Cell* **1:** 479-492.

Sattler, M., Verma, S., Byrne, C.H., Shrikhande, G., Winkler, T., Algate, P.A., Rohrschneider, L.R. & Griffin, J.D. (1999) BCR/ABL directly inhibits expression of SHIP, an SH2-containing polyinositol-5-phosphatase involved in the regulation of hematopoiesis. *Mol. Cell. Biol.* **19:** 7473-7480.

Schaffhausen, B. (1995) SH2 domain structure and function. *Biochim. Biophys. Acta* **1242:** 61-75.

Schmalbach, C.E., Chepeha, D.B., Giordano, T.J., Rubin, M.A., Teknos, T.N., Bradford, C.R., Wolf, G.T., Kuick, R., Misek, D.E., Trask, D.K. & Hanash, S. (2004) Molecular profiling and the identification of genes associated with metastatic oral cavity/pharynx squamous cell carcinoma. *Arch Otolaryngol Head Neck Surg* **130:** 295-302.

Schneider, U., Schwenk, H.U. & Bornkamm, G. (1977) Characterization of EBV-genome negative "null" and "T" cell lines derived from children with acute lymphoblastic leukemia and leukemic transformed non-Hodgkin lymphoma. *Int. J. Cancer* **19:** 621-626.

Schober, S.L., Kuo, C.T., Schluns, K.S., Lefrancois, L., Leiden, J.M. & Jameson, S.C. (1999) Expression of the transcription factor Lung Krüppel-Like Factor is regulated by cytokines and correlates with survival of memory T cells *in vitro* and *in vivo*. *J. Immunol.* **163:** 3662-3667.

SenBanerjee, S., Lin, Z., Atkins, G.B., M.Greif, D., Rao, R.M., Kumar, A., Feinberg, M.W., Chen, Z., Simon, D.I., Luscinskas, E.W., Michel, T.M., Gimbrone Jr., M.A., García-Cardeña, G. & Jain, M.K. (2004) KLF2 Is a Novel Transcriptional Regulator of Endothelial Proinflammatory Activation. *J. Exp. Med.* **199:** 1305-1315.

Sheikh, F., Baurin, V.V., Lewis-Antes, A., Shah, N.K., Smirnov, S.V., Anantha, S., Dickensheets, H., Dumoutier, L., Renauld, J.-C., Zdanov, A., Donelly, R.P. & Kotenko, S.V. (2004) Cutting Edge: IL-26 Signals through a Novel Receptor Complex Composed of IL-20 Receptor 1 and IL-10 Receptor 2. *J. Immunol.* **172:** 2006-2010.

Sherr, C. (1996) Cancer cell cycles. *Science* **274:** 1672-1677.

Shibasaki, F., Homma, Y. & Takenawa, T. (1991) Monomer and heterodimer forms of phosphatidylinositol-3-kinase. *J. Biol. Chem.* **266:** 8108-8114.

Shields, J.M. & Yang, V.W. (1998) Identification of the DNA sequence that interacts with the gut-enriched Krüppel-like factor. *Nucleic Acids Res.* **26:** 796-802.

Shin, I., Yakes, F.M., Rojo, F., Shin, N.Y., Bakin, A.V., Baselga, J. & Arteaga, C.L. (2002) PKB/Akt mediates cell-cycle progression by phosphorylation of p27(Kip1) at threonine 157 and modulation of its cellular localization. *Nat. Med.* **8:** 1145-1152.

Shurtleff, S.A., Buijs, A., Behm, F.G., Rubnitz, J.E., Raimondi, S.C., Hancock, M.L., Chang, G.C., Pui, C.H., Grosveld, G. & Downing, J.R. (1995) TEL/AML1 fusion resulting from a cryptic t(12;21) is the most common genetic lesion in pedriatic ALL and defines a subgroup of patients with an excellent prognosis. *Leukemia* **9:** 1985-1989.

Skorski, T., Bellacosa, A., Nieborowska-Skorska, M., Majewski, M., Martinez, R., Choi, J.K., Trotta, R., Wlodarski, P., Perrotti, D., Chan, T.O., Wasik, M.A., Tsichlis, P.N. & Calabretta, B. (1997) Transformation of hematopoietic cells by BCR/ABL requires activation of a PI-3k/Akt-depent pathway. *EMBO J.* **16:** 6151-6161.

Sogawa, K., Kikuchi, Y., Imataka, H. & Fujii-Kuriyama, Y. (1993) Comparison of DNA-binding properties between BTEB and Sp1. *J. Biochem. (Tokyo)* **114:** 605-609.

Southwood, C.M., Downs, K.M. & Bieker, J.J. (1996) Erythroid Krüppel-like factor exhibits an early and sequentially localized pattern of expression during mammalian erythroid ontogeny. *Dev. Dyn.* **206:** 248-259.

Spangrude, G.J., Heimfeld, S. & Weissman, I.L. (1988) Purification and characterization of mouse hematopoietic stem cells. *Science* **241:** 58-62.

Sprent, J. & Surh, C.D. (2001) Generation and maintenance of memory T cells. *Curr. Opin. Immunol.* **13:** 248-254.

Stephens, L.R., Jackson, T.R. & Hawkins, P.T. (1993) Agonist-stimulated synthesis of phosphatidylinositol 3,4,5-trisphosphate: a new intracellular signalling system? *Biochim. Biophys. Acta* **1179:** 27-75.

Stiles, B., Gilman, V., Khanzenzon, N., Lesche, R., Li, A., Qiao, R., Liu, X. & Wu, H. (2002) Essential role of AKT-1/protein kinase B in PTEN-controlled tumorigenesis. *Mol. Cell. Biol.* **22:** 3842-3851.

Straus, D.B. & Weiss, A. (1993) The CD3 chains of the T cell antigen receptor associate with the ZAP70 tyrosine kinase and are tyrosine phosphorylated after receptor stimulation. *J. Exp. Med.* **178:** 1523-1530.

Thiesen, H.J. & Bach, C. (1990) Target detection assay (TDA): a versatile procedure to determine DNA binding sites as demonstrated on SP1 protein. *Nucleic Acids Res.* **18:** 3203-3209.

Thompson, J.D., Higgins, D.G. & Gibson, T.J. (1994) CLUSTAL W: improving the sensitivity of progressive multiple sequence alignment through sequence weighting, position-specific gap penalties and weight matrix choice. *Nucleic Acids Res.* **22:** 4673-4680.

Tschopp, O., Yang, Z.Z., Brodbeck, D., Dummler, B.A., Hemmings-Mieszczak, M., Watanabe, T., Michaelis, T., Frahm, J. & Hemmings, B.A. (2005) Essential role of protein kinase B γ(PKBγ/Akt3) in postnatal brain development but not in glucose homeostasis. *Development* **132:** 2943-2954.

Turner, J. & Crossley, M. (1999) Mammalian Kruppel-like transcription factors: more than just a pretty finger. *Trends Biochem. Sci.* **24:** 236-240.

Tzachanis, D., Freeman, G.J., Hirano, N., van Puijenbroek, A.A., Delfs, M.W., Berezovskaya, A., Nadler, L.M. & Boussiotis, V.A. (2001) Tob is a negative regulator of activation that is expressed in anergic and quiescent T cells. *Nat. Immunol.* **2:** 1174-1182.

Ui, M., Okada, T., Hazeki, K. & Hazeki, O. (1995) Wortmannin as a unique probe for an intracellular signaling protein, phosphoinositide 3-kinase. *Trends. Biochem. Sci.* **20:** 303-307.

UniGene (http://www.ncbi.nlm.nih.gov/entrez/query.fcgi?db=unigene&cmd=search&term=).

van Ree, J.H., Roskrow, M.A., Becher, A.M., McNall, R., Valentine, V.A., Jane, S.M. & Cunningham, J.M. (1997) The human erythroid-specific transcription factor EKLF localizes to chromosome 19p13.12-p13.13. *Genomics* **39:** 393-395.

Vanderlaan, M. & Thomas, C.B. (1985) Characterization of monoclonal antibodies to bromodeoxyuridine. *Cytometry* **6:** 501-505.

Vanhaesebroeck, B. & Alessi, D.R. (2000) The PI3K-PDK1 connection: more than just a road to PKB. *Biochem. J.* **346:** 561-576.

Vanhaesebroeck, B., Leevers, S.J., Ahmadi, K., Timms, J., Katso, R., Driscoll, P.C., Woscholski, R., Parker, P.J. & Waterfield, M.D. (2001) Synthesis and function of 3-phosphorylated inositol lipids. *Annu Rev Biochem* **70:** 535-602.

Verhoeven, K., De Jonghe, P., Van de Putte, T., Nelis, E., Zwijsen, A., Verpoorten, N., De Vriendt, E., Jacobs, A., Van Gerwen, V., Francis, A., Ceuterick, C., Huylebroeck, D. & Timmerman, V. (2003) Slowed conduction and thin myelination of peripheral nerves associated with mutant Rho guanine-nucleotide exchange factor 10. *Am. J. Hum. Genet.* **73:** 926-932.

Villa, A., Patrosso, C., Biunno, I., Frattini, A., M., R., Mostardini, M., Evans, G., Susani, L., Strina, D., Redolfi, E., Lazzari, B., Pellegrini, M. & Vezzoni, P. (1992) Isolation of a zinc finger motif (ZNF75) mapping on chromosome Xq26. *Genomics* **13:** 1231-1236.

Walker, E.H., Pacold, M.E., Perisic, O., Stephens, L., Hawkins, P.T., Wymann, M.P. & Williams, R.L. (2000) Structural determinants of Phosphoinositide 3-kinase inhibition by wortmannin, LY294002, quercetin, myricetin, and staurosporine. *Molecular Cell* **6:** 909-919.

Wang, F., Zhu, Y., Huang, Y., McAvoy, S., Johnson, W.B., Cheung, T.H., Chung, T.K., Lo, K.W., Yim, S.F., Yu, M.M., Ngan, H.Y., Wong, Y.F. & Smith, D.I. (2005) Transcriptional repression of WEE1 by Kruppel-like factor 2 is involved in DNA damage-induced apoptosis. *Oncogene* **24:** 3875-3885.

Wani, M.A., Conkright, M.D., Jeffries, S., Hughes, M.J. & Lingrel, J.B. (1999a) cDNA isolation, genomic structure, regulation, and chromosomal localization of human lung Kruppel-like factor. *Genomics* **60:** 78-86.

Wani, M.A., Wert, S.E. & Lingrel, J.B. (1999b) Lung Kruppel-like factor, a zinc finger transcription factor, is essential for normal lung development. *J. Biol. Chem.* **274:** 21180-21185.

Ward, S.G. & Cantrell, D.A. (2001) Phosphoinositide 3-kinases in T lymphocyte activation. *Curr. Opin. Immunol.* **13:** 332-338.

Weiss, A. & Littman, D.R. (1994) Signal transduction by lymphocyte antigen receptors. *Cell* **76:** 263-274.

Wen, S.T. & Van Etten, R.A. (1997) The PAG gene product, a stress-induced protein with antioxidant properties, is an Abl SH3-binding protein and a physiological inhibitor of c-Abl tyrosine kinase activity. *Genes Dev.* **11:** 2456-2467.

Whitehead Institute for Biomedical Research (http://frodo.wi.mit.edu/cgi-bin/primer3/primer3_www.cgi) *Primer 3.*

Wolk, K., Kunz, S., Asadullah, K. & Sabat, R. (2002) Cutting edge: immune cells as sources and targets of the IL-10 family members? *J. Immunol.* **168:** 5397.

Wu, J. & Lingrel, J.B. (2004) KLF2 inhibits Jurkat T leukemia cell growth via upregulation of cyclin-dependent kinase inhibitor p21WAF1/CIP1. *Oncogene* **23:** 8088-8096.

Wymann, M.P., Bulgarelli-Leva, G., Zvelebil, M.J., Pirola, L., Vanhaesebroeck, B., Waterfield, M.D. & Panayotou, G. (1996) Wortmannin inactivates phosphoinositide 3-kinase by covalent modification of Lys-802, a residue involved in the phosphate transfer reaction. *Mol. Cell. Biol.* **16:** 1722-1733.

Xin, W., Rhodes, D.R., Ingold, C., Chinnaiyan, A.M. & Rubin, M.A. (2003) Dysregulation of the annexin family protein family is associated with prostate cancer progression. *Am J Pathol. Jan;162(1):* **162:** 255-261.

Yamaguchi, F., Tokuda, M., Hatase, O. & Brenner, S. (1996) Molecular cloning of the novel human G protein-coupled receptor (GPCR) gene mapped on chromosome 9. *Biochem. Biophys. Res. Commun.* **227:** 608-614.

Yusuf, I. & Fruman, D.A. (2003) Regulation of quiescence in lymphocytes. *Trends Immunol* **24:** 380-386.

Zhang, W., Sloan-Lancaster, J., Kitchen, J., Trible, R.P. & Samelson, L.E. (1998) LAT: the ZAP-70 tyrosine kinase substrate that links T cell receptor to cellular activation. *Cell* **92:** 83-92.

Zheng, Y. (2001) Dbl family guanine nucleotide exchange factors. *Trends Biochem. Sci.* **26:** 724-732.

Zhou, B.P., Liao, Y., Xia, W., Spohn, B., Lee, M.H. & Hung, M.C. (2001) Cytoplasmic localization of p21Cip1/WAF1 by Akt-induced phosphorylation in HER-2/neu-overexpressing cells. *Nat. Cell. Biol.* **3:** 245-252.

9. Appendix

List of Abbreviations

Akt	Protein kinase B
ALL	acute lymphocytic leukemia
AML	acute myeloid leukemia
bp	base pair
CDK	cyclin dependent kinase
cDNA	complementary deoxyribonucleic acid
CLL	chronic lymphocytic leukemia
CLP	common lymphoid progenitors
CML	chronic myeloid leukemia
CMP	common myeloid progenitor
DNA	deoxyribonucleic acid
Dox	Doxycycline
DEPC	diethylpyrocarbonate
dNTP	deoxyribonucleic triphosphate
E	efficiency of quantitative real-time RT-PCR amplification
EDTA	ethylenediamine-tetraacetic acid
EGFP	enhanced green fluorescent protein
EST	expressed sequence tag
FACS	fluorescence activated cell sorter
FCS	fetal calf serum
FITC	Fluoresceine isothiocyanate
Grb2	growth factor receptor-bound protein 2
h	hours
IC_{50}	half of maximal inhibitory concentration
Ig	immunoglobulin
IL	interleukin
$Ins(1,3,4)P_3$	Inositol-1,3,4-trisphosphate
IκB	inhibitor of NFκB
kDa	kilodalton
KLF2	Krüppel-like factor 2 (lung)
LTR	long-terminal repeat

MAPK	mitogen-activated protein kinase
µg	microgram
mg	milligram
min	minute
mM	millimolar
mRNA	messenger ribonucleic acid
NCBI	National Center for Biotechnology Information
NFκB	nuclear factor κB
ORF	open reading frame
PI3K	phosphoinositide 3-kinase
PBS	phosphate buffered saline solution
PCR	polymerase chain reaction
PDK	phosphoinositide-dependent protein kinase
PTB-Domain	phosphotyrosine binding domain
PtdIns(3,4)P_2	Phosphatidylinositol-(3,4)-bisphosphate
PtdIns(4,5)P_2	Phosphatidylinositol-(4,5)-bisphosphate
PtdIns(3,4,5)P_3	Phosphatidylinositol-(3,4,5)-trisphosphate
PTEN	phosphatase and tensin homologue deleted on chromosome ten
RB	retinoblastoma tumor suppressor protein
rtTA	reverse tetracycline-controlled transactivator
SD	standard deviation
SDS	sodium dodecyl sulfate
Shc	SH2-containing collagen-related protein
SH-Domain	Src homology domain
SHIP	SH2-containing inositol 5'-Phosphatase
TRE	Tetracycline-response element
TCR	T-cell receptor
U	unit
UV	ultraviolet
v/v	volume per volume
WB	Western Blot
WM	Wortmannin
w/v	weight per volume

Acknowledgements

Firstly, I would like to express my deep gratitude to PD Dr. Manfred Jücker for giving me the opportunity to work on my doctoral thesis in the department of cellular signal transduction, Institute of Biochemistry and Molecular Biology I, Center of Experimental Medicine (UKE, Hamburg) and for his excellent guidance. He greatly supported my way into the leukemia research. Thank you for sharing your expertise and your important comments and suggestions. I thank Prof. Dr. G.W. Mayr for his support, expert opinion and valuable cooperation in consenting to be my PhD supervisor. My very special thanks to DAAD/FUNDAYACUCHO, for the support with a doctoral fellowship. Special thanks go to Prof. Dr. Udo Wienand (Biocenter Klein Flottbek, University of Hamburg), for being a referee of my doctoral thesis and for his excellent comments. I really appreciated the excellent collaboration of Prof. F. Haag (Institute of Immunology, UKE, Hamburg), for his outstanding assistance in the FACS measurements and for providing kindly the human KLF2 vector. My thanks to Dr. T. Streichert (Institute of Clinical Chemistry, UKE), for the collaboration with the Microarray assays. I really appreciated the speedy and outstanding help of Dr. S. Horn. I would like to thank Dr. J. Weitzel and Dr. K. Sultan for their valuable comments, and W. Wegner, M. Kröger and B. Henkel for excellent technical assistance. I really appreciated the friendly, speedy and excellent help of Prof. Dr. Carol Stocking-Harbers (HPI, Hamburg) for the English language evaluation of my doctoral thesis. I am grateful to Prof. Dr. M. Böttger (Biocenter Klein Flottbek, University of Hamburg) for his excellent comments. I thank PD Dr. H. Quader (Biocenter Klein Flottbek, University of Hamburg) for not hesitating to agree when I asked him to be a referee in my thesis' defense. I would like to thank all the referees in my thesis' defense from UKE, from the Department of Biology, and from HPI. I thank Ms. A. Sült-Wüpping (Department of Biology, University of Hamburg) for her valuable cooperation. I am deeply grateful to my parents, Bernardo and Elvia, my brothers, Stefan Winkelmann, and all my friends. To all the staff of the Institute of Biochemistry and Molecular Biology I, for being very helpful and cooperative.